Assessment of Precision Technologies for Accurate Delivery of Crop Inputs

by

Tyrel Lee Harbuck

A dissertation submitted to the Graduate Faculty of
Auburn University
in partial fulfillment of the
requirements for the Degree of
Doctor of Philosophy

Auburn, Alabama
August 9, 2010

Keywords: precision agriculture, autoguidance, GPS, subsurface-drip irrigation

Approved by

John Fulton, Co-chair, Associate Professor of Biosystems Engineering
Donald Eakes, Co-chair, Professor of Horticulture
Mark Dougherty, Assistant Professor of Biosystems Engineering
Jeff Sibley, Professor of Horticulture
Steven Taylor, Professor of Biosystems Engineering

Abstract

At the Tennessee Valley Research and Extension Center (TVREC), Belle Mina, Alabama, Global Positioning System (GPS)-assisted machine guidance and subsurface-drip irrigation (SDI) have been implemented to study precision agriculture practices. Crop yield can be adversely affected if 1) not planted optimally relative to SDI product placement, or 2) the SDI system performance has degraded. Recent evidence of guidance-system drift and soil moisture variability after irrigation at TVREC prompted performance evaluations of both systems. Use of an optical total station was investigated to quantify positioning error in a GPS-based autoguidance system when using different correction-signal services. Also developed was an assessment technique for *in-situ* pressure-compensating SDI application uniformity at variable operating pressures or slopes.

The total station provided an absolute frame of reference for comparing accuracy and repeatability of Wide-Area Augmentation System (WAAS), John Deere® SF1 and SF2, and Real-Time Kinematic (RTK) correction signals. Recommended techniques for proper correction-signal testing were to perform site calibration, establish semi-permanent reference monuments, conduct guidance tests in northward/southward or eastward/westward path orientations, and account for tracking-prism tilt. Measured cross-track error (XTE) was influenced by drive-path orientation for RTK, SF2, and WAAS; SF1 performance was consistent regardless of orientation. XTE for SF1 and

WAAS were more representative of manufacturer's claims. Unsigned 95% short-term and long-term error probability was preferred to describe guidance performance over signed pass-to-pass (P2P) and year-to-year (Y2Y) errors, respectively.

A field-testing apparatus was fabricated to interface with the *in-situ* SDI product to deliver water over a range of operating pressures (48, 83, 117, and 138 kPa) while measuring sample discharge. Apparatus discharge rates agreed to within a half-percent of per-emitter laboratory discharge rates. Lowest discharge was observed for the irrigated SDI product operating at 48-kPa. Discharges from the non-irrigated and irrigated SDI treatments at 83 and 117 kPa were not different (α=0.05).

In summary, water delivery is dictated by SDI placement and functionality; as a consequence, other farming practices have to be conducted with a high level of spatial accuracy in relation to the SDI system in order to maximize crop yield, like the RTK correction signal. Techniques and equipment developed in this study provide autoguidance and SDI researchers with innovative approaches to evaluate long-term performance of these precision-agriculture systems.

Acknowledgments

I would like to express my sincere gratitude to all of those in the Biosystems Engineering Department that contributed not only to my research program, but also to the betterment of myself from a teaching, extension, and personal point of view. Special thanks are extended to Bobby Norris, David Harkins, Brad Durham, and the other station personnel at the Tennessee Valley Research and Extension Center for assistance with field work. I would like to thank Anora Brooks, Daniel Mullenix, Corey Kichler, Christian Brodbeck, Seth Basinger, and Ajay Sharda for helping to facilitate this research effort. And, of course, I would like to thank those who served on my committee: Dr. Mark Dougherty, Dr. Steven Taylor, Dr. Jeff Sibley, Dr. Joe Eakes for serving as the co-chair of this project, and certainly Dr. John Fulton for advising me these many years. Lastly, I would like to thank Dr. Delos Hughes for his patronage, advice, and his assurances that everything "will be fine," my parents, and the rest of my family and friends for love and support that they have shown me throughout my lifetime of academic endeavors.

Table of Contents

List of Tables

List of Figures

List of Abbreviations

CEP	Circular Error Probable
CV	Coefficient of Variation
DEM	Digital Elevation Model
DGPS	Differential GPS
DOP	Dilution of Precision
EDM	Electronic Distance Measurement
GNSS	Global Navigation Satellite System
GPS	Global Positioning System
ID	Interior Diameter
IQR	Inter-Quartile Range
NMEA	National Marine Electronic Association
P2P	Pass-to-Pass error/accuracy
PND	Personal Navigation Device
RMS/RMSE	Root Mean Square Error
RTK	Real-Time Kinematic
SD	Standard Deviation
SDI	Subsurface Drip Irrigation
SEP	Spherical Error Probable
TCM	Terrain Compensation Module
TPS	Terrestrial Positioning System
TVREC	Tennessee Valley Research and Extension Center
U.S. DoD	United States Department of Defense
UTM	Universal Transverse Mercator
WAAS	Wide-Area Augmentation System
XTE	Cross-Track Error
Y2Y	Year-to-Year error/accuracy

CHAPTER ONE

INTRODUCTION

1.1 PREFACE

The concept of Precision Agriculture can best be described by an almost literal interpretation of the term---applying practices and technologies to agriculture to better capture and understand the precise interactions between the crop and the land. Precision Agriculture enhances current farming techniques not only by improving crop yields, but also to endorse a better stewardship with the environment at large by demonstrating how tillage, fertilizers, pesticides, and even water usage can be minimized on a commercial scale. As a consequence, farmers can experiment with new and innovative ways of growing, maintaining, and harvesting their crops in order to maximize production and profits.

One of the obvious relationships between the crop and the land is their physical proximity to one another. But, the physical position of the farm equipment in relation to the crop and to the land is just as important. For instance, vehicle and implement control is necessary so as not to destroy the crop by inadvertent damage from moving equipment. Likewise, if a farmer knows that a certain area within a field tends to produce less than other areas, the farmer can either avoid the area altogether or develop a site-specific management strategy to address this inherent variability. With these applications in

mind, knowing the spatial relationships between the crop, the land, and the equipment are crucial for implementing most precision-agriculture practices.

In the state of Alabama, an increasing number of farmers and producers are adapting their farming practices to advance the application of Precision Agriculture. At the Tennessee Valley Research and Extension Center (TVREC, Belle Mina, Alabama), most of the agronomic crops research relates in some way to Precision Agriculture---either directly by testing different crop management strategies, or indirectly by utilizing precision-agriculture technologies and strategies in daily operations. While several plots exist at this facility, one particular plot of approximately 6 ha has been used in an experimental capacity since fall of 2003; the research objectives for this extended-year study involve evaluating cotton (*Gossypium hirsutum* L.) lint yields in response to accumulated biomass from cover-crops and supplemental irrigation optimized for crop yield. For this experiment, two particular precision-agriculture strategies are employed throughout the study-GPS/GNSS-based machine guidance, to aid in the precise placement of the cotton crop, and subsurface-drip irrigation (SDI), to provide water within the rooting system of the crop. When SDI and/or controlled traffic practices are coupled with a high-accuracy guidance system, farming practices exhibit higher profits, according to Gan-Mor and Clark (2001); therefore, a reliable relationship between machine guidance and SDI is desired.

In order for the long-term experiment to remain valid from year to year, a new season's cotton crop has to be planted in a precise spatial relationship with the irrigation product underground; also, the irrigation has to perform as anticipated to minimize yield variability within plots but also to maximize overall yield. Anecdotal reports from the

TVREC staff have suggested that the seed placement for each season's cotton crop in relation to the estimated position of the SDI tape has not been consistent from one year to the next. According to the machine operators, the GPS-assisted guidance software on-board the field equipment performed as anticipated, in that no conspicuous errors were evident at the time of seed placement. No discernible bias of the software or the equipment could be determined through routine equipment maintenance checks; also, this effect tended to be better or worse depending on the GPS correction signal being used to assist with navigation during field procedures.

Cotton lint yield data exhibited variability across the study site from previous seasons and especially within individual plots that received supplemental watering via SDI. Typically, the TVREC staff monitors seasonal water usage for irrigated plots via flow meters installed at the head of the field. However, yield variability did not appear to be evenly dispersed throughout the plots. Flow-meter readings could offer at best an average measure of irrigation performance for the entire experiment plot, instead of focusing on the specific areas within the field that exhibited the variability.

1.2 JUSTIFICATION

1.2.1 MACHINE GUIDANCE

In order to better describe the study topic of guidance system accuracy, some background information regarding satellite navigation is required. The Global Positioning System (GPS) is an array of about 24 navigation satellites, maintained by the U.S. Department of Defense (DoD), and placed in precise orbits at an altitude of approximately 20,000 km. Unlike geostationary satellites, these navigation satellites are

revolving around the planet in six orbital planes (relative to the Equator), four satellites per orbital plane. Despite the fact that these satellites are in constant motion, their positions relative to one another are essentially "fixed" by careful monitoring from the U.S. DoD. Essentially, each GPS satellite serves as a radio "beacon" upon which anyone on Earth with a compatible GPS receiver can "receive the GPS" information from satellites in view. The software in the receiver can compute the approximate distance to each satellite in view, and by a geometric process of trilateration (similar to triangulation, except distances are used in the solution, not angles), the receiver can determine its position on Earth if at least four satellites are visible.

This raw, or autonomous, position solution could be several meters from the true geographical location. Several conditions relating to the quality of the GPS receiver, the amount of signal interference, and even local environmental conditions may accumulate this error. However, several of these conditions can be managed to a large extent allowing the error to be mitigated. Several manufacturers offer "correction signals" that serve to enhance the real-time positioning of GPS/GNSS receivers; autoguidance systems almost exclusively require some form of correction signal to operate at a performance level acceptable to most users.

Several GPS correction signals are available, and these signals typically can be ranked according to their accuracies. Consequently, the higher-accuracy correction signals require more of a financial investment for the farmer in order to optimize farm equipment and/or field operations. Manufacturers and commercial providers of correction-signal services advertise these accuracies in order to attract customers; however, as there are currently no established procedures or guidelines in the agricultural

or engineering community to evaluate the dynamic accuracy of GPS-assisted guidance systems, it is believed that the information provided by manufacturers may not be presented in clear context relative to their competitors.

As shown by the positioning-error phenomenon witnessed at TVREC, variability in GPS correction-signal accuracy may not be readily apparent if the vehicle operator relies solely upon the solution generated by the guidance-system software. However, the vehicle operator may notice during a guidance maneuver that the vehicle is not tracking on a repeatable drive path or that proper seed placement relative to an SDI system did not occur. In terms of guidance-system testing, utilizing an absolute or terrestrial frame of reference would be equivalent to having an operator witness any positioning discrepancies independent of the guidance system. Furthermore, if positioning error is being propagated through the GPS solutions themselves, then a terrestrial or non-GPS-based testing procedure may provide a clear insight into investigating dynamic guidance-system performance. Developing a procedure that relies upon an absolute frame of reference would also allow for guidance-system performance testing over extended periods of time, in order to quantify system accuracies from a long-term point of view.

1.2.2 SDI Application Uniformity

While a great deal of research has been conducted regarding the benefits of SDI, literature is limited in evaluating the longevity or the application uniformity of a typical SDI system under field conditions. Engineering standards and procedures exist that allow academic/industry researchers to evaluate and quantify SDI performance statistics, but the current standard (ASAE S553, 2008) is more suited to a laboratory situation. It is

believed that a field procedure can be developed to quantify SDI product performance in much the same way as the current standards allow in a laboratory setting.

If an SDI system is malfunctioning at the field level, then a producer would likely be able to identify such a problem easily through observation by an overall decline in crop growth throughout the season or by witnessing a catastrophic failure related to water flow in the system. However, not all SDI malfunctions are easy to observe; a crimped lateral line, clogged emitters, or miniscule holes in the lateral line caused by abrasion from sub-soil rocks or rodents may go unnoticed for several seasons. It is believed that a field-based testing methodology should be able to diagnose SDI product samples in a more site-specific manner as opposed to a field level.

Pressure-compensating SDI provides a consistent and uniform water application method in spite of dynamic pressure changes created by the SDI pumping system or by static pressure changes created by elevation differences between emitters. Pressure-compensating SDI is a relatively new product in the marketplace, so little research has been reported on testing the reliability of this product over an extended period of time. It is believed that a field-based testing methodology should provide for evaluation of an SDI product with respect to typical operating-system pressures and static pressure forces to determine if the pressure-compensating features of such an SDI product are maintained over time.

1.3 OBJECTIVES

The overall goal of this research is to evaluate guidance-system accuracy and *in-situ* SDI application uniformity, as both of these precision-agriculture technologies are related to one another. The objectives of this research are to:

1. Evaluate techniques for using an optical total station to provide terrestrial-based, dynamic accuracy testing of an autoguidance system when using different GPS-based correction services.
2. Compare short-term and long-term accuracies of an autoguidance system when using different GPS-based correction services.
3. Develop and validate *in-situ* testing techniques to assess application uniformity of SDI products.
4. Evaluate if variable operating pressure or terrain slope impacted application uniformity of a pressure-compensating SDI product.

1.4 ORGANIZATION OF DISSERTATION

This dissertation is presented in manuscript format. Chapter 1 provides introductory statements justifying the emphasis that was put toward this research followed by the main objectives. Chapter 2 is an extensive literature review supplying information on the characteristics of guidance-system and SDI operation. Each of the Chapters 3 through 5 represents an individual manuscript that focuses on different portions of this research. Chapter 3 documents the formulation of guidance-system testing techniques utilizing an optical total station. Chapter 4 characterizes long-term absolute accuracies and short-term relative accuracies of four GPS correction signals

commonly utilized by guidance-system operators. Chapter 5 documents the formulation of in-field SDI testing techniques as well as SDI uniformity results conducted at the TVREC. Chapter 6 summarizes this research project, presents overall conclusions, and includes future research suggestions. At the end of the dissertation, a Reference section and Appendices were developed, documenting hardware and software specifications for all equipment utilized throughout the project as well as supplemental guidance and SDI-application data.

CHAPTER TWO

LITERATURE REVIEW

With the rise in popularity of Precision Agriculture, guidance system innovations and irrigation innovations have developed quickly over the last decade. Several publications from industry and academia were reviewed to gain knowledge on the operating principles behind static GPS testing, guidance systems, GPS correction signals, dynamic GPS testing, and total stations. Other manuscripts pertaining to overview of SDI and evaluating SDI performance were reviewed.

2.1 OVERVIEW OF STATIC GPS

The infrastructure behind GPS operation is based on three components: the *space segment*, the *control segment*, and the *user segment*. The *space segment* consists of the navigational satellite array, or constellation, located in precisely-known and closely-monitored orbits surrounding Earth. The *control segment* consists of monitoring stations located around the world that track the "health" of the satellites, compare their actual positions with their predicted positions, and are able to change the status of the constellation when necessary. Both the *space segment* and the *control segment* are maintained by different organizations in the U.S. Government, so civilian intervention or manipulation is improbable. The *user segment* refers to the general public that can utilize

the positioning or timing capabilities from the satellites, provided they have a compatible receiver and software program that can process the satellite signals (Hurn, 1989).

2.1.1 PRINCIPLES OF OPERATION

In simple terms, the GPS satellites broadcast continuous independent radio signals to Earth, containing specialized data messages describing each satellite's identity, operational health, predicted position, and a timestamp. Based on the physical equation $D=RT$, where D=distance traveled, R=rate of travel, and T=time of travel, a GPS receiver can calculate how far away multiple satellites are based on the amount of time needed to receive each satellite's data message. This is possible because the satellites are in precise orbits (approximately 20,000 km from Earth) and because radio waves in the vacuum of space travel at the speed of light (approximately 300,000 km s^{-1}). Due to the assumption that the GPS satellites are in fixed orbits, with Earth at the center of those orbits, a geometric coordinate system can be derived to locate any point within the interior sphere of the constellation; this geometric coordinate system can then be converted into a geodetic coordinate system, consisting of latitude, longitude, and height. A GPS receiver must process the signals from a minimum of four GPS satellites before the receiver can accurately derive its location within the coordinate system, but the architecture of the satellite constellation is designed such that at least six satellites should be available to the user at any time of day throughout the world (except for the polar regions) (Hurn, 1989).

2.1.2 MEASURES OF ACCURACY AND PRECISION

Several factors can influence positioning accuracy: satellite clock errors, satellite orbital errors, errors in the GPS receiver, signal distortion caused by the atmosphere, and

signal multipath (Upadhyaya *et al*., 2003). Errors related to the navigational satellites can be predicted to a high order through careful monitoring by the U.S. DoD. Receiver errors can often be related to the quality of the hardware components present in the receiver, such as the on-board clock and the radio-frequency microchip that receives the signals from space. Atmospheric errors are created by the hindrance of the satellite radio signals through different levels of the atmosphere; in addition, satellites that are located closer to the horizon tend to output radio signals that are more susceptible to atmospheric distortion due to the increased signal travel distance (Srivastava *et al*., 1993) . Positioning errors are often the greatest for this category, but atmospheric modeling can greatly reduce the error. Multipath is a term that refers to localized radio-signal disturbance, often affected by nearby reflective surfaces, buildings, or vegetation; these errors are site-specific and can be mitigated through careful placement of the GPS receiver or antenna.

The term *accuracy* refers to how well the GPS receiver calculates its position relative to an accepted "true" position (Buick, 2002; Upadhyaya *et al.,* 2003). *Static accuracy*, or the accuracy of a receiver that has not been moved during testing, is often quantified in statistical terms of circular error probable (CEP), spherical error probable (SEP), and root mean square error (RMS error, RMSE). CEP is described as the radius of a circle in which 50 percent of the GPS receiver's calculated two-dimensional coordinates are contained within some extended window of time. SEP is conceptually the same as CEP, except that three-dimensional coordinates are evaluated. RMS error can be used to evaluate accuracy with the following equation:

$$\sqrt{\frac{\sum_{i=1}^{n} \boldsymbol{d_i^2}}{\boldsymbol{n}}},$$

$$where\ d_i^2 = (X_i - X_o)^2 + (Y_i - Y_o)^2,$$

$$(X_i, Y_i) refers\ to\ sample\ coordinates\ and$$

$$(X_o, Y_o) refers\ to\ accepted\ true\ coordinates$$

The term *precision* refers to how closely the receiver repeatedly calculates its current position relative to the previous calculated position. RMS error can also be used to evaluate precision with the following equation:

$$\sqrt{\frac{\sum_{i=1}^{n} \boldsymbol{e_i^2}}{\boldsymbol{n}}},$$

$$where\ e_i^2 = (X_i - \bar{X})^2 + (Y_i - \bar{Y})^2,$$

$$\bar{X} = \sum_{i=1}^{n} (X_i) and\ \bar{Y} = \sum_{i=1}^{n} (Y_i)$$

(Upadhyaya *et al.*, 2003).

An additional source of positioning error comes from the satellite geometry available at the time of data acquisition. The term that is used to quantify the geometry of the overhead satellites is Dilution of Precision (DOP). While a minimum of four satellites are typically required for a receiver to determine its position, having those satellites clustered in one part of the sky is functionally not as robust as having the same satellites distributed evenly overhead. A DOP value is reported as a unitless number that inversely relates relative to the distribution of the satellites---more spatial dispersion of overhead satellites means a smaller DOP, while a more clustered satellite picture means a larger DOP. Because a DOP value is a function of the satellite geometry, this value can

also be used indirectly to determine potential accuracy and precision of positioning data (Stombaugh *et al*., 2005).

2.2 GUIDANCE SYSTEMS

Machine guidance refers to the utilization of extra-sensory devices relaying information to a central computer controller to aid in the navigation of farming equipment. Such controllers (and the peripheral devices that accompany them) are generally referred to as "guidance systems"; while some guidance systems provide visual or audible cues to instruct the vehicle operator where to go, more advanced systems have the capabilities of automatically steering the vehicle as it travels over terrain. Such systems are often referred to as "autoguidance," in order to distinguish from "manual guidance" systems requiring an operator to steer the vehicle.

Machine guidance requires some form of navigational aid in order to direct the vehicle over terrain. As mentioned previously, the most commonly-available navigational aid for machine guidance is satellite navigation. A GPS receiver can determine a position relative to the orbiting satellites and derive coordinates for its physical location as they correspond to a standard recognized navigational format, such as latitude and longitude. Machine-guidance systems equipped with GPS receivers utilize the positioning information in order to associate the vehicle's current position and velocity with navigational cues, such as a digital map or an assigned route; for farming applications, the assigned route may simply correspond to the orientation and layout of the crop rows in the field.

2.2.1 USES AND BENEFITS

Producers and vehicle operators spend many hours behind steering wheels performing routine operations, such as preparing seed beds, applying fertilizers and pesticides, or planting and harvesting crops. The repetitive nature of these activities over the course of the work day will often contribute to operator fatigue, leading to row skips or overlap. Yields can be impacted by this, but now farmers have the ability to drive crop rows with greater accuracy over row counting or using foam markers to indicate prior passes. Also, with an increased emphasis on stewardship of the farmland through more efficient farming, a farmer can collect site-specific field information that allows for less wasteful (and more profitable) farming operations that serve to maximize a crop yield.

One important benefit of incorporating a guidance system into agricultural machinery is that new and innovative production practices can be developed. For instance, researchers have utilized guidance systems and other navigational enhancements to develop a rice transplanter (Nagasaka *et al.*, 2002), an agricultural "field robot" (Noguchi *et al*., 2002) that performed tillage and planting tasks better than skilled labor, and a self-propelled sprayer (Giles and Downey, 2003). Also, because many guidance systems are designed to "stream" the real-time GPS positioning data to other software applications, everyday farming operations are being re-invented through GPS availability. Supplemental GPS data contribute to mapping weeds in the field (Downey *et al.*, 2003; Tian, 2002), conducting real-time soil-characteristic surveys (Freeland *et al*., 2002), and even measuring field topographic changes (Westphalen *et al*., 2003).

2.2.2 TYPICAL COMPONENTS

Essentially, a guidance system is comprised of an **antenna** that receives position information from navigational satellites, a **receiver** that processes this information, a **computer** that interprets information from the vehicle and/or receiver, and an **input/output device** for the driver (Figure 2.1). All of these components can be modified and enhanced for a farmer's specific needs and farm operations. Some optional features include a receiver that receives multiple position signals for increased accuracy, a computer with data–logging capability for recording field attributes or application rates, or a user-friendly interface with audible cues and graphical displays for the driver. Other equipment or vehicle enhancements may be required depending on the status of the vehicle, such as incorporation of an electrohydraulic steering system, addition of mechanical "feelers" to sense the crop's presence, or other such sensors (Reid *et al.*, 2000).

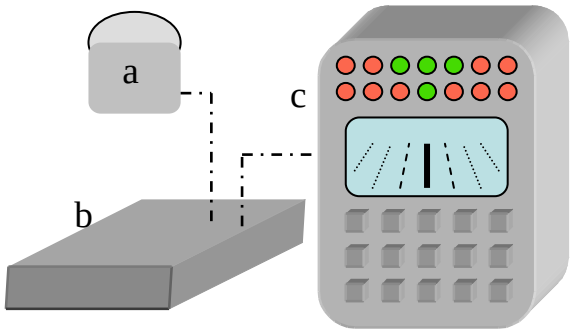

Figure 2.1. Example guidance-system setup. Typical guidance system components include a GPS antenna/receiver (a), a computer module (b), and an input/output device (c).

2.3 GPS CORRECTION

Positions derived from "raw" or autonomous GPS-satellite observations are typically not accurate enough for most precision-agriculture-related field operations; if a receiver were to calculate a location using only the positioning information from the GPS satellites, the location would be accurate within approximately 9 m. Enhancements have been developed over the last twenty years by governmental and civilian interests to reduce the positioning errors inherent in the GPS system. Depending on which "correction signal" one utilizes will often determine the general accuracy one may expect from a GPS position and, consequently, from the performance of a guidance system. Because certain field operations require differing levels of positioning accuracy, guidance-system operators must understand what range of accuracies are associated with which correction signal.

2.3.1 CHARACTERISTICS OF GPS CORRECTION

Certain errors are inherent in GPS positioning. Most errors can be accounted for in a real-time sense, and when these adjustments are included in the processing, position accuracy increases. A GPS receiver that is capable of making use of these enhancements is referred to as Differentially-corrected GPS (DGPS). A DGPS receiver may be further classified as single-frequency or dual-frequency, referring to the receiver's capabilities to collect additional position information from the satellites. With a DGPS receiver, it is possible to refine positional accuracy to a few inches, as opposed to several feet (Hurn, 1993). There are three categories of DGPS receiver, each with its own inherent accuracies, based on the type of differential correction used by a receiver; in addition,

several differential-correction signals are available by commercial means, differing in operational costs and advertised accuracies for each, so users have options for obtaining differentially-corrected positioning based on application demands and budget.

2.3.2 WIDE-AREA AUGMENTATION SYSTEM (WAAS)

Practically all GPS receivers in the civilian and the agricultural community are capable of receiving a correction signal known as Wide- Area Augmentation System (WAAS). This signal was developed by the U.S. Federal Aviation Administration (FAA), and is available free of charge to anyone with a compatible receiver. Autonomous (non-corrected) positions are calculated and compared to target coordinates distributed throughout the United States, along with satellite and atmospheric error-compensation models; all these factors combine to develop a new correction model across the continental United States, and this correction model is transmitted by geosynchronous satellites across the country on the same frequency as the GPS signals. The result is that a WAAS-capable receiver typically has a better position accuracy than if the position were calculated autonomously. With a high-quality GPS receiver, static accuracy (or the difference between the predicted positions versus the actual location) ranges from ±61 to 66 cm 95% of the time over a 24-hour period (Hest, 2007); however, a low-cost GPS receiver, such as those found in personal navigation devices (PND) utilizing WAAS, may only be accurate to between 1 and 5 m (Stombaugh *et al*., 2005).

2.3.3 JOHN DEERE STARFIRE 1 (SF1) AND STARFIRE 2 (SF2)

Some equipment manufacturers provide proprietary correction signals. John Deere® offers two such DGPS-based corrections that are compatible with their StarFire™

DGPS receiver. These signals are referred to as SF1 and SF2, referring to single-frequency and dual-frequency capabilities, respectively. The method of operation for SF1 and SF2 is similar to that of WAAS, but private companies have the capabilities of offering more robust error modeling or worldwide signal transmission for which WAAS was neither configured nor intended. The static accuracy for SF1 is approximately 76 cm, while the static accuracy for SF2 is approximately 25 cm (Hest, 2007). An SF1-capable receiver is generally regarded in the same category as a WAAS-capable receiver (deemed "sub-meter"), while an SF2-capable receiver is in another category (deemed "decimeter"). Apart from the costs incurred by purchasing John Deere equipment, the SF1 correction signal is offered free of charge to customers, while the SF2 correction signal requires a yearly subscription fee to maintain signal access.

2.3.4 REAL-TIME KINEMATIC (RTK)

The real-time kinematic (RTK) correction signal is regarded in the GPS community as being the most accurate and the most reliable signal available. The principles behind generating the RTK correction are a bit different than other DGPS correction signals. A stationary dual-frequency GPS receiver (referred to as a base receiver) is configured to observe the position error from a known position; this position error, which only consists of three numeric values relating to error in each of three spatial dimensions, is transmitted by radio link to a second compatible dual-frequency receiver that travels with the operator (referred to as the rover receiver), along with a timestamp for each observation. Given the theoretical assumption that most of the errors witnessed at the base receiver are virtually identical to those witnessed at the rover receiver, then

most of the errors can be filtered out in the rover position solution. Static accuracy can be ±3 cm in many situations (Hest, 2007). In order to obtain an RTK correction, two high-quality receivers are required, as well as a communications link between the two receivers; initial equipment costs can range into the tens of thousands of dollars, but the correction signal itself is free to use with compatible receivers.

2.4 Overview of Dynamic GPS

Statistical methods exist to quantify GPS accuracy and precision in static situations, but what about when the GPS receiver is in motion? Static performance of receivers is not indicative of dynamic performance; in addition, techniques used to monitor dynamic performance vary greatly from one researcher to the next (Stombaugh *et al*., 2002). Accuracy of a receiver in motion can still be related to how closely a position is determined relative to an accepted "truth", but determining what "truth" is, or should be, in dynamic situations is challenging. The following articles describe how researchers have endeavored to evaluate dynamic GPS performance.

2.4.1 Measures of Accuracy and Precision

According to a manuscript by Buick (2002), for farming operations conducted in conjunction with established equipment or land features, the primary goal of a guidance system is to be able to operate over time such that the equipment or land features are not destroyed (e.g., drip tape, controlled traffic). When a terrestrial-based frame of reference is considered, Buick calls this *absolute accuracy*. The author then presents the term *relative accuracy*, which refers to "accuracy relative to some location other than a surveyed 'truth'." The author uses this term synonymously with *pass-to-pass accuracy*

(P2P); because relative accuracy degrades in a fairly short amount of time, a testing interval of about 15 minutes is recommended. The term *precision* is used only to refer to the exactness of the solution, i.e. the number of decimal places the solution offers, while *variability* is the term used to conceptually define the spread of position data (inversely known as "repeatability"). Statistically, sigma values refer to variability, and RMS error measures spread and offset from the truth.

Because accuracy depends on a comparison to a true value, many researchers have developed testing protocols that involve "truth in motion" procedures. Various researches have been conducted utilizing either mechanical or conceptual travel paths. A mechanical travel path refers to evaluating the receiver through a predictable, repeatable motion; examples included mounting receivers onto a rotating boom apparatus with constant motion and acceleration (Stombaugh *et al*., 2002) and mounting receivers onto a mobile cart that traveled back and forth via rail (Taylor *et al*., 2004). A conceptual travel path refers to comparing receiver performance through mathematical modeling; examples included evaluating several receivers by studying their performance according to post-process filtering (Han *et al*., 2001) and regression modeling of each "attempted" straight-line pass (Ehsani *et al*., 2003; Wu *et al*., 2005). Positioning performance relative to site-specific monumentation would be considered conceptual travel as well.

In order to measure absolute accuracy, most researchers collect cross-track error (XTE) information, which relates to the "distance between the currently measured GPS position and the desired track" (Han *et al*., 2001). This value is typically represented in a direction perpendicular to the orientation of the travel path; as a result, the change in XTE from one end of a travel path to another would be expected to reflect how well the

receiver (guidance system, vehicle) followed the travel path. In order to measure relative accuracy, some researchers evaluate *pass-to-pass error* (P2P), which relates to how well the guidance system can calculate the position of the next anticipated travel path, usually in relation to the previous one. Utilizing mean XTE values on a per-path basis, *pass-to-pass average error*, which is referred to as the difference in mean XTE of the relevant path and the preceding path ($XTE_i - XTE_{i-1}$), can indicate whether a guidance system exhibits skips or overlaps by interpreting the positive or negative values (Han *et al*., 2004; Ehsani *et al*., 2002).

When measuring dynamic accuracy, precautions and caveats have been offered by researchers. For example, some authors describe an increase in XTE when the mobile test vehicle traveled latitudinally (parallel with the Equator) versus longitudinally (oriented with the North and South Poles) (Wu *et al*., 2005; Ehsani *et al*., 2003). Because GPS satellites are not placed in an orbit relative to the north and south poles, a "hole" exists in satellite coverage for mid-latitude users in the U.S.; the result is smaller cross-track errors when driving north/south versus driving east/west (Buick, 2002). Other factors to consider when evaluating guidance performance in agricultural settings involve vehicle speed, swath width/length, field conditions, different test days and different times during the day, presence of potential multipath objects, and operator bias (Ehsani *et al*., 2002; Han *et al*., 2004); those factors are in addition to the potential error sources that affect overall GPS accuracy (timing errors, constellation shift, etc.).

2.4.2 PREVIOUS RESEARCH TO MODEL ACCURACY AND PRECISION

Most researchers are convinced of the reliability and repeatability of RTK correction such that solutions derived through RTK correction are considered as the "reference" positions by which to compare other systems or GPS receivers (Buick, 2002; Ehrl *et al*., 2003; Ehrl *et al*., 2004; Ehsani *et al*., 2002; Ehsani *et al.*, 2003: Taylor *et al*., 2004). Also, according to Ehrl *et al*. (2004), an independent reference system should have at least three times the accuracy as the systems being evaluated; however, standard testing practice suggests accuracy of a measurement system should be at least ten times greater than what is being evaluated (ION, 1997). For sub-meter and decimeter-level GPS receivers, an RTK-based measuring system may be adequate, but validating the performance of an RTK-based guidance system with an independent RTK-based measuring system may not provide adequate basis for analysis, especially if local site conditions serve to adversely affect both the reference and the measured solutions (Adamchuk et al., 2007). A positioning system that offers greater accuracy than RTK should be considered.

Han *et al.* (2001) utilized a mathematical "filter" to improve position and velocity data on a DGPS navigation system. The filtering technique is useful for reducing effects from random GPS error but not GPS "bias" error---a term that is defined but not addressed by this study. The authors believe that anticipated accuracy of GPS positions should be 0.04 to 0.12 meter for chemical application and 0.02 to 0.04 meter for seeding, row-crop cultivation, and harvesting applications. Along with summarizing results using mean XTE and standard deviation, maximum XTE per dataset is also presented, presumably in an effort to illustrate how the observed position was so contrasting from

the mean and was witnessed by the operators. These values could reflect the amount of non-statistical variation that a farmer may witness during a single random guidance event.

Buick (2002) suggested that high relative accuracy can be expected shortly after establishing a reference, or AB, line for the first time, but a different position solution should be expected when returning to the starting point after a large passage of time. If an operator desires no greater than 1- to 2-inch P2P error for farming operations, then RTK-based guidance is recommended, along with an autosteer system. Buick also states that a GPS system that has low absolute accuracy will be undesirable for controlled-trafficking situations, because the system cannot be relied upon to re-determine the positions for the established vehicle paths consistently.

Among other concepts, Wu *et al*. (2005) discussed the relationship between the GPS constellation and position accuracy. Several Dilution of Precision (DOP) terms were discussed and modified to explain effects from N/S and E/W travel directions. The authors were able to verify that there was a difference between North DOP and East DOP in "mid-latitude" locations. Standard deviations of error were always less in the northerly orientation than in the easterly orientation.

A study by Ehsani et al. (2002) outlined the issues that need to be considered in comparing the accuracy of different lightbar guidance systems; their contention is that, while the ideal situation is to have mean P2P error of zero, generally some overlap is more desirable in farming operations than skip. Also, when trying to evaluate the performance of guidance systems, both the RMS error and standard deviation "range of variation should be very close" for these values.

A later study by Ehsani *et al*. (2003) introduced a method of dynamic accuracy testing for DGPS receivers and compared the dynamic accuracy of five commonly used low-cost DGPS receivers. RTK GPS positions were utilized as the reference positions; to measure cross-track error, standard deviation of error, and root mean square error of positions from the tested receivers, a regression line was modeled from a subset of positions mapped per driving path. (Pass-to-pass accuracy was not studied in this test.) The testing vehicle (a Chevy Suburban) was equipped with a lightbar computer to assist the driver with the location of the desired paths. Accuracy and precision of the systems are defined similarly to their paper in 2002; RMSE was considered as "absolute" cross-track error, but the "relative" cross-track error was not clearly stated---presumably, this value was witnessed by mean XTE. Cross-track error (relative or absolute) was also observed to be worse (higher) when driving east-west direction instead of north-south direction, so one of their conclusions was to measure error in both directions for future evaluations.

In Taylor's study (Taylor *et al*., 2004), testing methods for the compared GPS receivers involved mounting the receivers on a rail cart that traveled in an east/west direction. Cross-track error was deemed the "most important measure" for guidance evaluation and, in this testing scenario, northing error was considered synonymous with cross-track error. Error was determined by finding the regression line that passed through a sample of RTK-based positions collected while the rail cart was in motion.

Ehrl *et al.* (2004) investigated the performance of an RTK-based guidance system that utilized two independent RTK GPS receivers (three in total on the test vehicle). The purpose of this was to capture roll-and-pitch information while the vehicle was in motion

through a winter-wheat seeding; XTE results were ±25 mm, with a max. deviation of 100 mm, on some straight paths; planting on the side of a slope resulted in vehicle yaw and implement drift up to 240 mm between passes, illustrating that vehicle terrain can impact path accuracy significantly in an agricultural environment.

2.5 Overview of Total Station

In the surveying industry, a total-station unit offers target positioning that can be correlated with GPS-derived positions and, more commonly, physical on-site monuments providing a local frame of reference. While surveyors generally collect positions with a stationary target (like a prism), in recent years, total-station technology has progressed such that the target can be in motion as well. Through redundant position calculation across fixed on-site monumentation, the potential exists to utilize total-station technology to document the travel path of a vehicle equipped with a guidance system.

2.5.1 Principles of Operation

A total station, also known as a tachymeter, offers very precise angular and distance measurements. Through electronic distance measuring, a laser pulse is transmitted by the total station and reflected back to the total station by the target, which can be a mirrored prism or some form of highly-reflective material. A distance measurement can be derived by recording the amount of time required for the laser pulse to return to the device from its origin. Also, as the sighting mechanism on the total station pivots horizontally and vertically, vector measurements can be recorded and associated with each recording (Ehrl *et al*., 2004). In the surveying profession, the total station is often oriented over a stable monument upon which the positioning coordinates

are either known or can be easily assumed; in addition, the total station can be oriented relative to north. The result is that any observations made of the target by the total station can be related to the total station's position in three dimensions and over time. Recent advances in total-station technology allow for passive autonomous tracking of the assigned target by the total station, resulting in a hands-off approach by the operator in following the target. Some potential sources of error include radial inaccuracy, or how accurately each degree of horizontal or vertical rotation can be measured, and atmospheric distortion over long distances (Ehrl *et al*., 2004).

2.5.2 PREVIOUS RESEARCH TO MODEL DYNAMIC GPS PERFORMANCE

Freimann (2000) and Bittner (2000) utilized a total station with tracking capabilities to corroborate the driving performance of an experimental "autonavigating" tractor, reporting that the tractor performed better than ± 8 cm when required to follow a preprogrammed path. In order to study characteristics between and within agricultural-vehicle components, Ehrl *et al.* (2002) developed a system to synchronize output between CAN-based communication, GPS positioning information, and controller software performance. The positioning system utilized for this test incorporates both RTK-based positioning and a "target tracking tachymeter" (total station). Results were that, either stationary or in motion, the combined reference system provided an "absolute" accuracy of less than ± 3 cm. In a later study, Ehrl *et al.* (2004) posed potential deficiencies with using a total station as a referencing system for autoguidance testing: acute angle measurements reduce accuracy, downrange measurements lose accuracy after 200 to 300 meters, and tracking-vehicle speeds can exceed servo-motor performance of the

positioning device. Potential dusty conditions in most agricultural settings could also hinder observations with a total station (Bell, 2000).

2.6 SUBSURFACE-DRIP IRRIGATION (SDI)

Subsurface drip irrigation is a method of applying precise amounts of water to agronomic crops by delivering the water directly to the plants' root zone via underground tape or tubing, often referred to as "drip tape", "drip line", or "drip tube". In its various forms, drip tape offers water-use savings due not only to its reduced application volume but also to its reduced evaporative losses. The research topics discussed below involve the uses and benefits of SDI, and previous attempts to study SDI performance in laboratory and field situations.

2.6.1 USES AND BENEFITS

SDI can be adapted to many typical crop applications, both agronomic and horticultural in nature. In a review of all published research pertaining to SDI, crop yields were found to be either comparable or higher than other conventional forms of supplemental irrigation (center-pivot, overhead sprinkler, etc.), and usually less water was required (Camp, 1998). Other studies have focused on utilizing SDI for fertigation or effluent disposal (Lamm *et al.*, 2001; Lamm *et al.*, 2004; Song *et al.*, 2003; Trooien *et al.*, 2000), determining optimum lateral spacing and lateral depth for various crop systems (Enisco-Medina *et al.*, 2002; Bryla *et al.*, 2003; Charlesworth and Muirhead, 2003; Camp *et al.*, 1997), and studying SDI effects on crop water-use efficiency (Bordovsky and Porter, 2003; Lamm and Trooien, 2003). Increased yields and greater application efficiency add up to better profits for producers. For example, in western

Kansas, corn irrigated via SDI provided substantial net returns on a per-hectare basis compared with center-pivot sprinkler irrigation (O'Brien *et al.*, 1998). However, the authors of that study determined that SDI was unprofitable relative to center-pivot sprinklers for SDI product life of less than ten years.

In economic terms, the initial costs associated with designing and installing an extensive SDI system can be daunting. While installation costs may be considered a drawback in some situations, the cost of drip irrigation can be reduced by using both wider lateral spacings and the same laterals for multiple years, as with subsurface placement. From this point of view, there could be a financial incentive to install and maintain an SDI system that could last a great deal longer than ten years (Dougherty *et al.*, 2009).

2.6.2 EVALUATING SDI PERFORMANCE

While much research has focused on improved agronomic growth, relatively few studies discuss the longevity of the drip tape systems themselves. Effects on crop yield and crop quality of SDI tape design (from five manufacturers) and position along 152-m lateral runs were investigated by Steele *et al*. (1996) for three consecutive years. Yields were not statistically different between tape designs for any upstream distance transect in any year. However, measured emitter discharge rates decreased dramatically with distance downstream from the start of the tape.

Camp *et al.* (1997) used three drip irrigation systems; two with lateral lines on the soil surface and one with laterals about 30 cm below the soil surface for several experiments from 1985 to 1992. Emitter plugging, system uniformity, and overall

performance were evaluated via several methods. All uniformity values were lower for the subsurface system, primarily because of plugged emitters. Entry of soil particles into an eight-year-old subsurface system during construction and/or repair operations probably caused the emitter plugging, according to the authors.

Ayars *et al*. (1999) operated several SDI experimentation plots throughout California over a fifteen-year period, testing fertigation regimes against crops such as cantaloupe, corn, cotton, and tomato. The authors reported that some of their plots performed comparably to initial installation after as much as nine years. The presumption was that when the system was flushed and maintained in a proper manner root intrusion was minimized to the emitters.

A commonly-referenced standard pertaining to SDI performance is ASAE S553: Collapsible Emitting Hose (Drip Tape) --- Specifications and Performance Testing (ASAE, 2008). This testing standard outlines methods for certifying performance and quality characteristics of drip tape products. The methods were developed such that industry testing (or consumer testing) could take place under laboratory conditions---specifically, the tape product should be above ground in a controlled environment as opposed to field conditions. Lesikar *et al.* (2004) adopted this standard to a field setting to evaluate drip-tape flow rates from SDI products that had been used for wastewater effluent for up to five years; this required the authors to excavate the soil to such an extent that small catch pans could be placed underneath the emitters in order to perform in-field application uniformity tests. The authors did not refer to any plants of agronomic value that were removed or relocated during excavation; however, the presumption is that soil was disturbed within several inches of the drip tape. In an effort to protect

neighboring plants, Steele *et al.* (1996) employed a less-intrusive method of exposing a few emitters in order to make a rough determination about in-field application uniformity. Catch pans were also placed under the exposed emitters in this situation, and collected volumes were averaged and extrapolated to an equivalent flow rate based on manufacturer's stated flow rates and emitter spacing.

CHAPTER THREE

DEVELOPING A TERRESTRIAL-BASED PROCESS FOR MEASURING ACCURACY OF GPS CORRECTION SERVICES IN GUIDANCE-SYSTEM APPLICATIONS

3.1 ABSTRACT

Navigational satellite services (GPS, GNSS) provide real-time position information for autoguidance applications used today in agriculture production. Under dynamic situations (i.e. when the GPS/GNSS rover receiver is in motion), performance assessments are often based on measured positions relative to a target "path". Creating a testing method that is not reliant on satellite positioning may serve to reveal the potential drift component of any GPS/GNSS-based correction signal when an autoguidance system is in operation. The objective of this study was to evaluate techniques for using an optical total station to provide terrestrial-based, dynamic accuracy testing of an autoguidance system when using different GPS-based correction services. An optical total-station with target-tracking capability was utilized in conjunction with a tracking prism mounted to an autoguidance-equipped tractor to provide an absolute frame of reference for comparing accuracy and repeatability of Wide-Area Augmentation System (WAAS), John Deere® SF1 and SF2, and Real-Time Kinematic (RTK). Several techniques relating to test-site preparation, data collection, and office processing are

presented. Recommended techniques for proper correction-signal testing by the total-station instrument included conducting site calibration, establishing semi-permanent monumentation for reference purposes, and conducting guidance tests in neutral-easting or neutral-northing path orientations. Short-term and long-term testing can be accomplished with this technology for SF1, SF2, and WAAS; tracking capability of the total station was only four to five times more accurate than typical RTK performance, so this process may not be sufficient for RTK evaluation. Total-station positioning accuracy can potentially be degraded unless prism tilt is considered. Therefore, a digital elevation model (DEM) served to capture slope and aspect characteristics for the test site such that derived positions could be adjusted based on the roll and pitch modeled by the DEM; however, for our test site, the prism positions were only improved by about 2 cm.

3.2 INTRODUCTION

The benefits of autoguidance systems include reducing driver fatigue, extending operational hours, increasing field efficiency and potentially lowering fuel usage. A common industry standard involves utilizing a navigational satellite service to derive vehicle location in real time, such as the United States' Global Positioning System (GPS), or the more inclusive Global Navigation Satellite System (GNSS), which includes satellites from the United States (GPS) and Russia (GLONASS) currently but could include future operational systems developed by other governments.

Accuracy and precision measurements of GPS- or GNSS-capable receivers have traditionally been derived from static-operation tests, and internationally-accepted engineering testing standards exist for making such evaluations (Institute of Navigation, 1997). Terms such as Circular Error Probable (CEP), Spherical Error Probable (SEP), and Root Mean Square (RMS) error pertain to differences in measured positions from a known target position (Upadhyaya *et al.*, 2003). Today, no engineering test standard has yet been developed to quantify GPS/GNSS positioning accuracy under dynamic conditions, yet most manufacturers report accuracy and performance values such as pass-to-pass error (P2P) (also known as *relative accuracy*, or *short-term error*), which typically refers to accuracy of a new position relative to a position previously determined within a short period of time, such as fifteen minutes. The assumption is that some form of dynamic testing must have taken place in order to derive such values, but as there is no accepted test standard in place, comparing guidance systems among manufacturers in equal terms becomes a challenge.

Under dynamic situations (i.e. when the GPS receiver is in motion), performance assessments are often based on measured positions relative to a target "path". Stombaugh *et al*. (2002) proposed various testing methods for GPS receivers under dynamic conditions, either by repeatedly driving a vehicle over known predictable paths or by mounting a receiver to an apparatus with a fixed travel path. Taylor *et al*. (2004) also mounted a receiver to a fixed-path apparatus in order to investigate accuracy through straight-line tests. These methods have their advantages in that most of the measurements generated through these processes can be easily evaluated and compared with an intuitive path template; also, evenly-spaced, straight-line drive patterns are often desired with everyday farming operations. Conversely, several equipment- and terrain-related variables can influence the performance of a system; Ehsani *et al*. (2002) advised that dynamic evaluations should be conducted under field conditions representative of standard operational performances and at typical operational speeds.

In recent years, farmers across the U.S. have invested in autoguidance systems to use in their cropping systems. Some farming practices require more accurate positioning from the autoguidance system than others; for example, applying manure with a broadcast spreader would not require autoguidance accuracy on the order of a few cm; accuracy to that order would be essential for banded-fertilizer applications, however. The tasks desired by the operator often determine what level of accuracy is required, and an appropriate autoguidance system or correction signal is selected.

By utilizing high-quality GPS- or GNSS-capable receivers with conventional surveying techniques, positions can be derived to a high order of accuracy under static conditions. When these techniques are not available to autoguidance operators, an

element of drift may be introduced into the positioning error. GPS drift can have an effect on field operations that rely heavily on autoguidance technologies. Han *et al*. (2004) observed that a receiver's dynamic performance fluctuates over time, whether by different hours of the test day or by different test days. This trait could be problematic over the course of several seasons in situations where controlled traffic or conservation tillage is practiced requiring repeatable, accurate equipment paths from year-to-year.

Han *et al.* (2004) and Ehsani *et al*. (2002) utilized multiple GPS sensors receiving multiple decimeter- and sub-meter wide-area differential GPS (DGPS) correction signals mounted onto an agricultural vehicle in an effort to measure their performance; for these studies, the paths mapped via Real-Time Kinematic (RTK) correction were considered the "absolute" or "reference" paths from which to compare the other receivers' paths. Autoguidance operations conducted with RTK correction are often regarded as "repeatable" from one season to the next due to the operating parameters and assumptions maintained in the RTK correction. However, when one GPS receiver is established as an independent "base" from which to generate corrected positions, and few or no redundancies exist to support the position derivations made in the autoguidance software, the potential exists for GPS drift to occur under RTK operation, albeit a small effect. Additionally, if local site conditions contribute to a less-than-optimum correction signal, then this phenomenon will be present in both the "reference" positioning as well as the autoguidance-established positioning (Adamchuk *et al*., 2007). Therefore, creating a testing method that is not reliant on satellite positioning may serve to reveal more accurate and absolute measures of performance for any GPS/GNSS-based correction signal when an autoguidance system is in operation.

In the surveying industry, a total-station unit (also referred to as a tachymeter) offers target positioning that can be correlated with GPS-derived positions and, more commonly, physical on-site monuments providing a local frame of reference. While surveyors generally collect positions with a stationary target (like a prism), in recent years, total-station technology has progressed such that the target can be in motion as well. This characteristic provides the potential to plot the driving path of a vehicle. Ehrl *et al.* (2004) discussed concerns regarding the use of total-station technology (referred to as Terrestrial Positioning Systems or TPS) as a form of absolute-position referencing. Their concerns included the drop in accuracy from a tilted prism, down-range limitations beyond 200 to 300 m, and issues related to the travel speed of the target vehicle.

3.3 SUB-OBJECTIVE

The objective of this study was to evaluate techniques for using an optical total station to provide terrestrial-based, dynamic accuracy testing of an autoguidance system when using different GPS-based correction services.

3.4 MATERIALS AND METHODS

The tractor used for this study was a John Deere® 6420 (Deere and Co., Moline, IL, USA; see Appendix A) factory-equipped with the StarFire® ITC™ GPS receiver (part no. PF80732; software ver. 2.52A; Deere and Co., Moline, IL, USA) and the GreenStar™ autoguidance system (hardware ver. PF80444 2.5; software ver. PF303192F; Deere and Co., Moline, IL, USA: see Appendix D). The tractor was also outfitted with a Trimble® EZ-Guide™ lightbar guidance computer (firmware ver. 4.10.002 Feb 22 2007 11:53:46 for 2007 tests; Trimble Agriculture, Sunnyvale, CA, USA) and an EZ-Steer™ assisted-

steering system (software ver. 3.00.01 for 2007 tests; Trimble Agriculture, Sunnyvale, CA, USA: see Appendix D).

In order to capture moving-vehicle position data with a terrestrial frame of reference, we used a Trimble® 5603 DR+ total station (firmware ver. 696-03.08; Trimble Engineering, Sunnyvale, CA, USA) in combination with a Trimble® TSCe field data collector (part no. 45185-20; Trimble Engineering, Sunnyvale, CA, USA) utilizing Trimble® Survey Controller software (versions 11.20 – 11.40; Trimble Engineering, Sunnyvale, CA, USA: see Appendix B). Point of measurement on the tractor was maintained using a Trimble® RMT ATS Multi-Channel tracking prism (part no. 571233035; Trimble Engineering, Sunnyvale, CA: see appendix C), mounted to the rear frame hitch approximately 66 cm above the ground and aligned with the vehicle's centerline. Distance measurements were calculated via Electronic Distance Measurement (EDM) technique; the stated accuracy of such measurements was ± (5 mm + 2 ppm; Trimble Engineering, 2001). In addition, our total station was equipped with Trimble's AutoLock™ function such that the total station, via servo motors integrated within its base, could automatically track the moving target prism and simultaneously collect distance data.

Four different GPS-based correction signals were evaluated: Wide-Area Augmentation System (WAAS), John Deere SF1 (SF1), John Deere SF2 (SF2), and Real-Time Kinematic (RTK). Position accuracies typically reported by manufacturers and/or system users are referenced in Table 3.1. Measures of short-term error (P2P) and long-term error are often reported; however, long-term error is often reported from static tests, not dynamic tests. No implements were attached during the tests, so draft or drag was

not considered; also, the tractor had performed only light-duty tasks during its life, so steering and/or transmission wear was considered negligible.

Table 3.1. Typical reported accuracies for correction signals used in this study.

Correction Signal	*Type of Correction*	*Accuracy*
WAAS	wide-area	±15 to 30 cm short-term (P2P); ±61 to 66 cm long-term (static)
SF1	wide-area	±33 cm P2P; ≈76 cm static
SF2	wide-area	±10 cm P2P; ≈25 cm static
RTK	local-area	≤3 cm P2P; ≤3 cm static

Source: Hest, 2007. For additional details, see Appendix E.

3.4.1 GENERAL TEST-SITE PREPARATIONS

This study was performed in Auburn, Alabama (32.6º N, 85.5º W) beginning in February 2006 and ending in August 2007. A different testing site was selected each year (see Appendices F and G). Except for differences in local terrain, both sites shared the characteristics of minimal overhead obstruction (desired for maximum reception of available satellites), minimal sources of radio interference (desired for maximum reliability of positioning data), and allowances for line-of-sight testing (desired for uninterrupted prism tracking by the total station).

Semi-permanent position monuments, or "benchmarks," were installed at each testing site to serve as points of reference for total-station data collection. In order to best relate total-station derived positions to the local terrain, a four-point site-calibration technique was employed via Site Calibration procedure in Trimble Survey Controller program (Trimble Surveying, 2007). Additional monumentation was installed and

documented as necessary for consistent total-station viewing location and station backsight monument(s).

For both sites, guidance "paths" were input to the guidance computers at the first data-collection event (referred to as "AB" line placement) by parking the tractor at the start of the path, recording a coordinate at this location (point "A"), driving to the end of the path, parking, and recording a subsequent coordinate (point "B"). Path placement and direction of travel were optimized for total-station line-of-sight availability. Positions were collected via the total station during tests when all the following conditions were met:

1. The tractor operator selected the relevant correction service.
2. The operator aligned the tractor on the relevant pass (1, 2, etc.).
3. The autoguidance device was engaged by the operator.
4. The guidance system steered the tractor on path. Total-station positioning was terminated before the tractor reached the end of the pass.

Five straight-line parallel paths were navigated by the guidance system(s) for each correction signal being evaluated. Vehicle speed was maintained at 2.2 m s^{-1} for all tests. A testing "event" was represented by traversing all five reference lines within a 15-minute time period. A different correction signal was enabled prior to each testing event.

3.4.2 TEST SITE ONE PREPARATIONS

The RTK base receiver/radio was installed atop a standard instrument tripod over a dedicated benchmark at the start of each testing day, located approximately 36 m south of the AB line with clear line-of-sight to the vehicle at all times. A GPS-derived

coordinate for the base receiver was determined instantaneously on the first day of testing and stored in the guidance-system program as a designated base location.

AB-line establishment was made for both the John Deere GreenStar system and the Trimble EZ-Guide system concurrently. However, these systems operated independently of one another; the GreenStar system computed an AB line using RTK-quality positioning, while the Trimble system computed an equivalent AB line using WAAS-quality positioning. Guidance lines were established at 6.1-m spacing; direction of travel was approximately 80.1 degrees azimuth relative to true north (Appendix F).

3.4.3 TEST SITE TWO PREPARATIONS

For the second site, a semi-permanent base-receiver mount was installed with a clear line-of-sight of the testing site, located approximately 30 m from the AB line(s). In the effort to further maximize RTK repeatability, instead of collecting an instantaneous coordinate, the base receiver was programmed to store a coordinate representative of mean position after a 24-hour data compilation.

While we utilized the same John Deere GreenStar system for SF1, SF2, and RTK corrections, the Trimble EZ-Guide computer used in 2006 for WAAS correction was different from the one used in 2007 (but make and model were identical for both). Two additional configuration changes were made to the newer Trimble EZ-Guide. First, we devised a method of outputting the NMEA-0183 data stream (an ASCII standardized data format developed by the U.S. National Marine Electronic Association) from the StarFire iTC receiver and into the Trimble system. This modification served two purposes: (1) while maintaining an RTK-quality position fix, AB-line establishment was conducted

concurrently with both systems utilizing the same vehicle receiver, thereby reducing potential offset error between the systems, and (2) while the StarFire receiver and the GreenStar system could still process WAAS, the signal was sent via NMEA output to the Trimble system so that the EZ-Steer module could function. The second change to the EZ-Guide configuration was the addition of a Terrain-Compensation Module (TCM: see Appendix D); the belief was that roll/pitch conditions exhibited by the vehicle throughout the testing area would tend to not adversely affect position accuracy as may have been the case in the previous year's tests.

More intensive topographic surveys were conducted at this site than the previous one, as the intent for the second year of tests was to attempt to compensate for prism-tilt error. Utilizing a survey-grade RTK receiver, elevation data were recorded throughout the plot.

Finally, this test site allowed both north-to-south and east-to-west orientations for vehicle paths to be studied. This setup provided a means to evaluate whether drive-path orientation impacted dynamic positioning accuracy. A swath width of 12.2 m was used during this testing; directions of vehicle travel were approximately 179.4 degrees and 271.3 degrees relative to true north for the north-to-south and east-to-west tests, respectively (Appendix G).

3.4.4 TEST SITE ONE: DATA ANALYSIS

During both years of testing, positions derived using the total station were converted into Universal Transverse Mercator (UTM) coordinates (Northing and Easting,

in meters). Ground distances could be easily derived with UTM coordinates, and the UTM projection allowed for easy transfer to existing data imagery of the sites.

While the guidance computers used stored AB line information on each successive test, no clear method of documenting the AB line with the total station was determined in 2006. Referencing research conducted by Taylor *et al*. (2004), a linear-regression model was used to evaluate path placement on successive testing events relative to the first path created by the guidance system on the first day of testing at Site 1. For example, the first pass along the AB line when using the RTK signal generated about 30 total-station derived point coordinates. The linear regression equation obtained from those 30 points became the "reference" by which to compare cross-track error (XTE) and pass-to-pass error (P2P) for RTK performance throughout the season. An illustration of XTE determination is presented in Figure 3.1. Furthermore, the target positions were "rotated" about a predicted point on the regression line in order to relate all the vehicle paths relative to a positive easting and zero northing direction by using the following equations:

$$X_f = X_i \left[\cos\left(\tfrac{\pi}{180}(360-\theta)\right)\right] - Y_i \left[\sin\left(\tfrac{\pi}{180}(360-\theta)\right)\right] \qquad (1)$$

$$Y_f = Y_i \left[\cos\left(\tfrac{\pi}{180}(360-\theta)\right)\right] + X_i \left[\sin\left(\tfrac{\pi}{180}(360-\theta)\right)\right] \qquad (2)$$

where (X_i , Y_i) are initial prism coordinates (Easting, Northing), (X_f , Y_f) are modeled prism coordinates, and θ represents a degree conversion of the arc-tangent of the slope parameter from the regression-line equation. The results were that the northing error was equivalent to XTE for a given path, making performance calculations much easier to conduct. (Additional details are in Appendix L.)

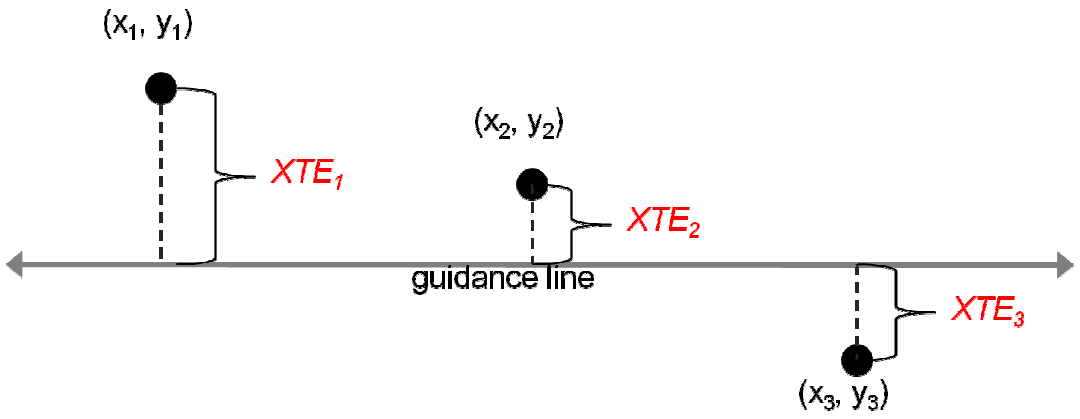

Figure 3.1. Depiction of cross-track error (XTE) determination.

3.4.5 TEST SITE TWO: DATA ANALYSIS

To account for prism movement during the second-year testing, a digital elevation model (DEM), produced using ArcMap GIS Ver. 9 (ESRI, Redlands, CA, USA) was created to represent the study site. The DEM was produced with a 1.0-m^2 resolution. Further, slope and aspect models were also generated. The benefit of these models was that, when tracking positions were included, a derived slope (in degrees) and aspect (related to true north) could be associated with the tracking positions to account for prism tilt. Further details regarding production of slope/aspect models and adjusting target coordinates for prism tilt are available in Appendix M.

While no equivalent AB line was recorded with the total station in the first year, a representative AB line was recorded for the tests in the second year. On the initiation date, target-prism positions were recorded concurrently with the establishment of the guidance-system field records (under RTK correction) via an "A + B" method. Relating this information to the slope and aspect models used to adjust position data, any total-

station-derived position could be modeled from an [$A_{unadj.} + B_{unadj.}$] or [$A_{adj.} + B_{adj.}$] target path.

Example target position data are illustrated in Figure 3.2. One additional change to XTE derivations was made in the second year of testing. Target positions (represented by point coordinates) were exported as GIS-compatible files for further analyses in ArcMap. Through GIS procedures, polyline files were modeled according to anticipated swath width and corresponding with total-station-derived AB line model (expected guidance path). To obtain XTE, we used a GIS procedure that provided perpendicular distance offset of each point coordinate relative to the expected guidance path. (Details of ArcMap procedures are provided in Appendix M.) For further visual representation, polyline files were created by connecting consecutive points per swath, reinforcing the concept of observed vehicle travel compared to expected guidance path (Figure 3.3).

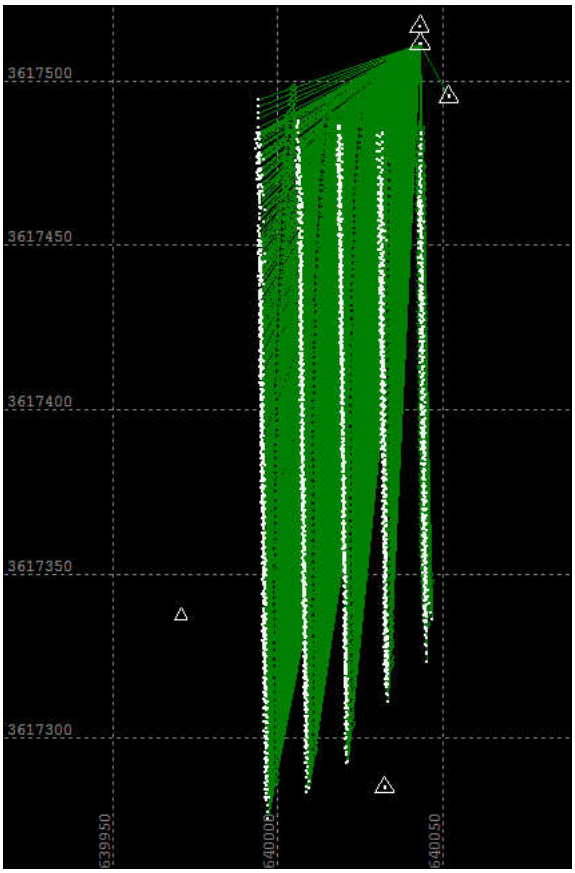

Figure 3.2. Example dataset produced from total-station observations. The labels for the gridded lines represent local grid coordinates, projected into the Universal-Transverse Mercator (UTM) coordinate system (units are in meters). The triangular markers represent stable reference monuments used in site calibration. The green lines represent the vectors from the total station monument to the observed prism positions (illustrated as white dots).

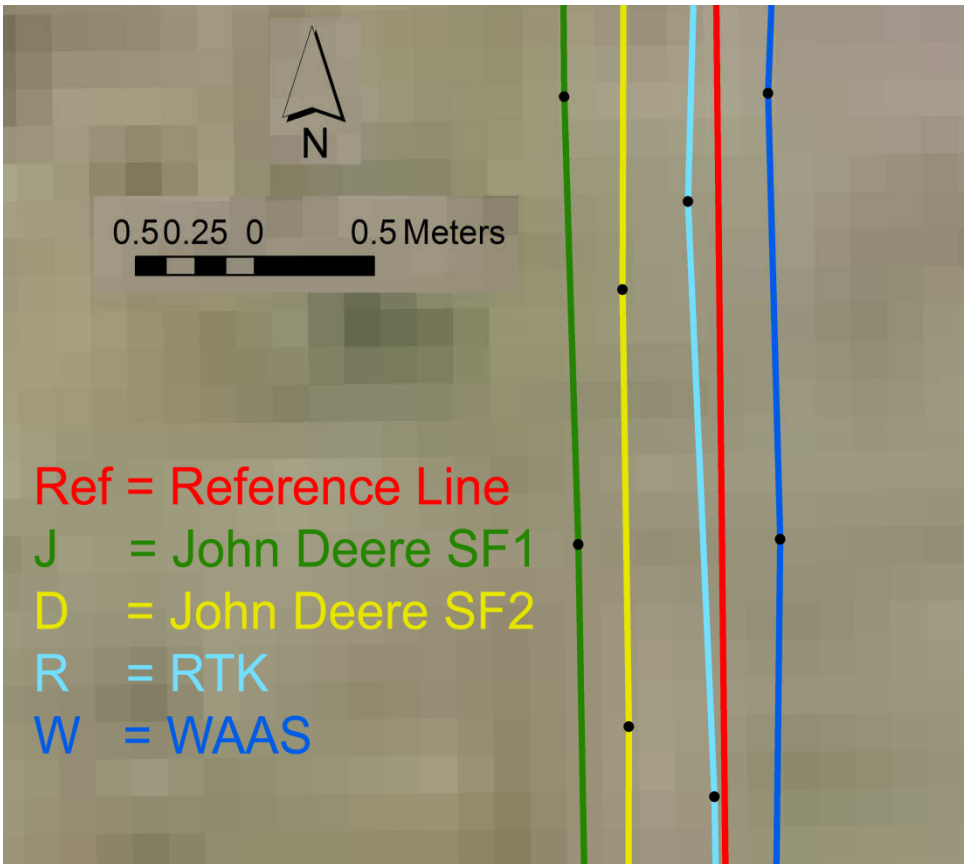

Figure 3.3. Example test dataset in GIS format. Black dots within each line refer to position data recorded by the total station; lines drawn between dots represent travel "paths" made by the test vehicle. Paths are separated by color according to correction signal used for each traverse in relation to the relevant reference guidance line.

3.4.6 STATISTICAL ANALYSES

For both years of the study, mean XTE, standard deviation of XTE (SD), and root mean square error of XTE (RMSE), were calculated as outlined by Ehsani *et al*. (2002) (also outlined in Appendix K). Pass-to-pass errors (P2P) were calculated by subtracting the signed value of the mean XTE of a row from the preceding row. Per-event observations were screened for potential outliers, defined by "any observation farther than 1.5 [Inter-Quartile Range] from the closest quartile" (Devore and Farnum, 2005). Basic statistical measures of XTE and tests for normality were derived through the

univariate-statistics procedure (PROC UNIVARIATE; SAS Institute, Cary, NC, USA). Graphical depictions were generated in MS Excel 2007.

3.5 Results and Discussion

3.5.1 Site One Results

Data collection dates and times are referenced in Table 3.2. Implementation of the desired correction signals was a large challenge throughout the test period. While the intention was to navigate the five drive paths within a 15-minute time period, select a different correction signal, and repeat the navigation, certain correction signals would not initiate in a timely manner between RTK, SF1, and SF2. One potential reason may have been that the processor in the GreenStar computer could not re-compile the satellite data, filter the data using the newly-chosen correction-signal algorithm, and re-compute a vehicle position as quickly as was demanded. This conjecture does not relate to WAAS data collection being unavailable after March 28, however; the Trimble EZ-Guide computer and EZ-Steer accessory had been loaned to the Biosystems Department for the first half of the study and had to be returned. Because of time constraints, problematic signals were abandoned during a testing day.

Table 3.2. Data collection events for each correction signal in 2006 (Site 1).

Test Name[a]	*Date*[b]	*Time of Day*[c]	*Test Name*[a]	*Date*[b]	*Time of Day*[c]
R_{11}	February 22	2:30 pm	R_{51}	April 7	1:33 pm
J_{11}	---	---	J_{51}	April 7	1:59 pm
D_{11}	---	---	D_{51}	April 7	1:45 pm
W_{11}	February 22	2:45 pm	W_{51}	---	---
R_{21}	February 27	3:03 pm	R_{52}	April 7	2:15 pm
J_{21}	---	---	J_{52}	April 7	2:36 pm
D_{21}	February 27	3:28 pm	D_{52}	April 7	2:25 pm
W_{21}	February 27	3:16 pm	W_{52}	---	---
R_{22}	February 27	3:40 pm	R_{61}	June 14	12:28 pm
J_{22}	---	---	J_{61}	---	---
D_{22}	February 27	4:00 pm	D_{61}	June 14	12:42 pm
W_{22}	February 27	3:50 pm	W_{61}	---	---
R_{31}	March 8	1:47 pm	R_{62}	June 14	3:22 pm
J_{31}	---	---	J_{62}	June 14	3:49 pm
D_{31}	March 8	2:15 pm	D_{62}	June 14	3:35 pm
W_{31}	March 8	2:04 pm	W_{62}	---	---
R_{32}	March 8	2:30 pm	R_{71}	June 16	9:43 am
J_{32}	---	---	J_{71}	June 16	10:07 am
D_{32}	March 8	2:52 pm	D_{71}	June 16	9:55 am
W_{32}	March 8	2:42 pm	W_{71}	---	---
R_{41}	March 28	T_1[d]	R_{72}	June 16	12:21 pm
J_{41}	---	---	J_{72}	June 16	12:43 pm
D_{41}	March 28	T_1	D_{72}	June 16	12:32 pm
W_{41}	March 28	T_1	W_{72}	---	---
R_{42}	March 28	T_2			
J_{42}	---	---			
D_{42}	March 28	T_2			
W_{42}	March 28	T_2			

[a] Test name is in the format A_{xy}, where *A* represents correction signal used (R=RTK, J=StarFire SF1, D=StarFire SF2, W=WAAS), *x* represents testing day, and *y* represents event number for that day.
[b] Dashed lines represent absence of data for that iteration.
[c] Time of Day refers to local time at which data collection began, recorded by program clock embedded in datalogger.
[c] Events T_1 and T_2 have no time stamps.

Correction-signal results for all signals will be discussed in more detail in Chapter 4; however, a summary of XTE measures for the 2006 season is presented in Table 3.3. Statistical evidence implied that XTE data did not always follow a normal distribution. XTE generated through RTK correction had the greatest number of testing events (85%) that were normally distributed (if [Pr<W] > 0.05 for Shapiro-Wilk test); 40 to 50 percent of the test events evaluating other correction signals suggested normal XTE distributions. Negative or positive XTE median and XTE mean values represent XTE trends that were to the northern or southern side of the reference line, respectively. RTK correction offered very low position error in terms of variability (5-cm SD, 6-cm IQR), location (5-cm XTE median/XTE mean), and overall accuracy (7-cm RMSE), but the values are slightly higher than values typically reported for RTK performance. SF1 correction varied over a meter throughout the season, yet tended to be centered close (5 cm) to the desired path; however, high RMSE suggested that this signal was the most inaccurate for the time period used in this study. SF2 correction offered XTE farthest from the reference lines (37-cm XTE median; 35-cm XTE mean). Finally, WAAS correction offered good general location throughout the season (9-cm XTE median/mean) despite the overall accuracy (31-cm RMSE), which was consistent with typical reported accuracy for this correction signal.

Table 3.3. Measures of location and assumption of normality for 2006 XTE data.

Correction Signal	Σ Test Events	# Events Rejecting Normality	Median XTE (cm)	Inter-Quartile Range (IQR) of XTE (cm)	Mean XTE (cm)	SD (cm)	RMSE (cm)
RTK	13	2	-5	6	-5	5	7
SF1	5	3	5	116	38	68	78
SF2	12	6	37	30	35	22	41
WAAS	7	4	-9	38	-9	30	31

Considerations should be made concerning the measured accuracy of the RTK correction signal as related to the measurement accuracy of the total station. The "tracking" capabilities of the total station were accurate to ±0.5 cm under ideal circumstances (Trimble Engineering, 2001). While position bias may have been introduced from a tilted targeting prism, we nonetheless believed we were achieving optimum performance of the total station. However, typical static-testing standards for GPS receivers require that measurement devices should be at least one order of magnitude more accurate than the product being evaluated (Institute of Navigation, 1997); ergo, a correction signal that was expected to achieve an accuracy of 3-cm should have been evaluated with a unit or process that could achieve 0.3-cm accuracy or better. Standard (static) total station measurements would have met this criterion, but a stationary prism measurement could only be made if the tractor were stationary as well. More modern total stations may be able to provide necessary accuracy under target-tracking conditions, but the unit used during this study could not meet this threshold. Therefore, for "typical" RTK-derived XTE observations, this measuring process was

considered questionable. RTK statistics are nevertheless presented in this and the next chapter to offer comparisons with the wide-area correction signals.

Several points can be made regarding the lessons learned from first-year data collection. Unfortunately for our testing regime, the autoguidance controller system integrated into the tractor was unable to operate using the WAAS correction with the StarFire iTC receiver. It was this limitation that required the use of a secondary "hands free" guidance system solution to evaluate WAAS, namely, the Trimble EZ-Guide and EZ-Steer hardware bundle. Of course, this platform was entirely independent of the GreenStar computer and StarFire iTC receiver used for the other three correction signals. A second antenna was used for the Trimble guidance system, and while the ideal antenna placement for optimum system performance was the point corresponding to the vehicle centerline and the forward-most point on the cab roof, this location was used by the StarFire receiver. Additionally, the Trimble autoguidance package used for this study was not equipped with terrain-compensation capability like the StarFire iTC receiver. The consequences of this scenario were not apparent in the overall performance of WAAS (as represented by mean XTE per event), but instead were apparent when a close evaluation of the drive paths over time was conducted (Figure 3.4). In Figure 3.4, there is a negative relationship between XTE and distance from the origin. This information led us to consider the possibility that the trend was indicative of roll/pitch error from the site, and therefore needed to be accounted in future tests. However, another possibility that would have explained this trend was that XTE observations were not perfectly adjusted after subjecting the positions to rotation equations (1) and (2). This tendency was

witnessed in other datasets as well; therefore, an alternative method of calculating XTE had to be considered.

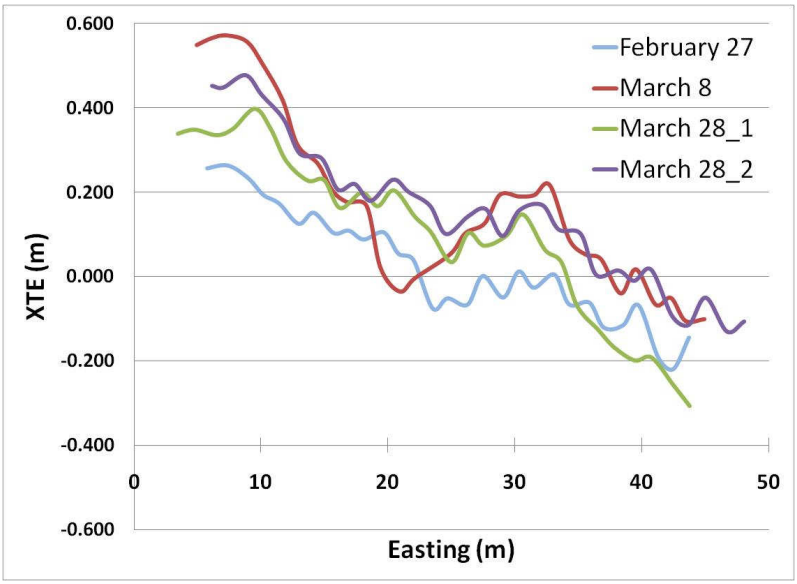

Figure 3.4. Portions of drive paths under WAAS correction for 2006 (site 1). The negative relationship between XTE and Easting values suggests roll/pitch error and/or insufficient XTE calculations.

Regarding data processing, using the regression-line technique to evaluate repeatability of correction signals was not intuitive from an operator's point of view. In a production setting, an operator would not have had the capabilities of documenting an AB line by this procedure, but rather by the AB-line establishment method described above. Therefore, we considered the feasibility of capturing the prism positions concurrently with future AB-line establishment, allowing for a total-station-derived AB-line equivalent that could serve as an absolute path reference during office processing calculations.

Site conditions in 2006 led to several set-up changes that were implemented in 2007. For example, conditions were not conducive to leaving the RTK base receiver in

its original location throughout the duration of this study, or for establishing a permanent monument to accommodate the receiver. While the coordinate stored in the guidance computer referred to a three-dimensional location (represented as latitude, longitude, and altitude), no precise measures were undertaken to reposition the receiver at the identical vertical height or in the identical orientation relative to true north; either condition may have contributed to reduced repeatability of RTK positioning. Only replication of reset relative to latitude and longitude was conducted by centering the base receiver over an established benchmark using a plumb-bob. Therefore, in an effort to reduce potential measurement error, one of the improvements sought for the next season was to provide a semi-permanent receiver mount such that latitude, longitude, altitude, and receiver orientation could be repeated throughout all tests.

Due to size limitations, an average of 187 observations per test event were documented with the total station; while this number was considered sufficient to provide evidence of a normal distribution, more observations were desired for each pass during a test. Also, previous research (Wu *et al.*, 2005) had suggested that path orientation affected XTE trends, so we wanted to find a larger test site that would allow for neutral easting (north-to-south or south-to-north) and neutral northing (east-to-west or west-to-east) comparison studies.

Finally, measurement error contributing from a tilted prism was not considered for 2006 tests. From a conventional-surveying perspective, in order to accurately relate surface positions relative to existing monumentation (or simply to the total station position), the leading assumption is that the total station and the targeting prism are plumb. Given that assumption, ground positions would be consistent horizontally and

adjusted vertically based on instrument and/or target height above the ground. Having either the total station or the target prism out of plumb violates this assumption, and horizontal and vertical accuracy is degraded. Internal sensors in the total station provided immediate indication of instrument error if the device was not plumbed within acceptable tolerances; however, no such mechanism existed for the target prism. Therefore, we wanted to find a method of predicting prism tilt as the vehicle traveled throughout the test plot.

3.5.2 SITE TWO RESULTS

Data collection dates and times are referenced in Appendix J. While initializing the SF1 correction signal was problematic in 2006, initializing the RTK signal was more problematic in 2007. Because of the overall lack of testing events recorded on a correction-signal basis in the previous year, the research objective for the 2007 study was to observe twenty testing events per signal and per orientation; only 13 events were recorded for east-to-west RTK, but all other signal-orientation combinations had 17 to 20 test events.

The size of the second test site allowed for much longer traverses in the north-to-south direction than was witnessed at the earlier site, but the traverses in the east-to-west direction were about the same length as those at the earlier site. An average of 289 observations was recorded per north-to-south testing event, while east-to-west testing events averaged 157 observations.

Summary positioning statistics for all correction signals for north-to-south and east-to-west path orientations are presented in Table 3.3. Similar to 2006, XTE generated

through RTK correction had the greatest number of testing events (70%) that were normally distributed (if [Pr<W] > 0.05 for Shapiro-Wilk test); only 20 to 25 percent of the test events evaluating SF1 and SF2 correction signals suggested normal XTE distributions, and only about 30 percent of test events evaluating WAAS exhibited normality. As evidenced from IQR values, the drive-path orientation tended to influence XTE; as this tendency had already been suggested by previous research efforts, the validation of the concept through the total-station-derived data was acceptable. However, this tendency was not observed for the SF2 signal. Given that variability of SF2 signal was about equal (43-cm southward, 45-cm westward) and that XTE median values of the SF2 signal were closer to zero (expected value) than with either SF1 or WAAS, the suggestion is that the SF2 correction was the most reliable sub-meter correction signal evaluated. Measure of variability for SF2 in 2006 supports this suggestion as well (Table 3.2). SF1 offered consistent position error regardless of path orientation (21-cm XTE median), but the variability in the southward orientation was more than twice that observed in the westward orientation. XTE from WAAS correction tended to be more "on target" throughout the season in the southward, as opposed to the westward, orientation, but XTE variability was about equal to that observed under SF1 correction.

Table 3.4. Measures of location and assumption of normality for 2007 XTE data.

Correction Signal [a]	Σ Test Events	# Events Rejecting Normality	Median XTE (cm)	Inter-Quartile Range (IQR) of XTE (cm)	Mean XTE (cm)	SD (cm)	RMSE (cm)
RTK_S	17	4	-1	10	-1	8	8
RTK_W	13	7	4	19	5	15	15
$SF1_S$	20	15	21	83	12	47	48
$SF1_W$	19	15	21	38	17	33	37
$SF2_S$	20	16	3	43	5	29	29
$SF2_W$	20	16	6	45	3	52	52
$WAAS_S$	20	13	-10	56	-13	65	67
$WAAS_W$	19	14	40	75	27	73	78

[a] Subscripts 'S' and 'W' refer to southward-oriented and westward-oriented reference lines, respectively.

3.5.3 INVESTIGATIONS INTO NORMALITY OF XTE

Because several testing events for the 2006 and 2007 seasons produced non-normal XTE, further analyses were performed to understand this result. Outlier filtering was performed as described by Devore and Farnum (2007) for XTE observations per testing event; an alternative approach was to perform a similar outlier filtration across the *entirety of each season*. This approach was investigated; depending on the correction signal being evaluated, the results were that entire testing events should have been omitted. This scenario was unacceptable for our project goal of comparing XTE trends on a per-event basis; further, we believed that, as a producer does not necessarily have the capability or the time to simply "omit" and "redo" a guidance-based operation that may not be indicative of typical correction-signal performance, we wanted to document and evaluate XTE observations in a similar fashion.

Outlier filtration on a per-testing-event basis did prove useful in spotting XTE observations that should not have been included in the datasets. Usually these

observations were located at the beginning or the ending of individual guidance rows, implying that prism targeting occurred before the tractor "locked" on the guidance (AB) line, or that prism targeting continued briefly (and erroneously) after the autoguidance feature was disabled at the end of the guidance line, respectively. In a few situations, outlier flagging suggested evidence that XTE observations were different on a per-row basis. From the 2006 study, out of a total 178 rows across all correction signals, observations from Row 1 during a June 16 SF2 test event were flagged and removed from analysis (see Appendix N); a graph of XTE observations for this event (with XTE from Row 1 included) is presented in Figure 3.5. In 2007 from a total of 385 rows involved with north-to-south path orientation across all correction signals, only 6 rows were flagged and omitted from analyses (Rows 1 and 2 from two SF1 testing events; Row 2 from an SF2 event; three instances of Row 1 from separate WAAS events; see Appendix O). Out of 355 rows involved with east-to-west path orientation, only 2 rows were omitted from analyses (two instances of Row 1 from SF1 and SF2 testing events; see Appendix O).

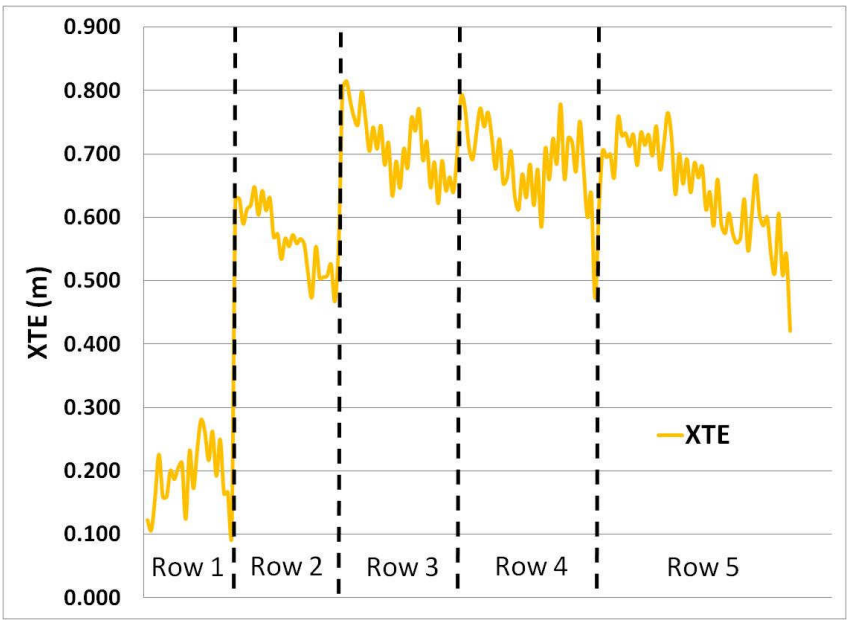

Figure 3.5. Graph of XTE observations per row for SF2 testing event on June 16, 2006. Observations from Row 1 were flagged as potential outliers and omitted from analyses.

Despite these evaluations, XTE observations still suggested evidence of non-normality on a test-event basis. A contributing factor to this tendency was likely from poor satellite geometry or low satellite count at the time of data collection; situations that are generally regarded as adverse to GPS positioning. Neither satellite number nor measures of geometry were recorded during testing events.

Another factor contributing to non-normality may have been the strong dependence of XTE performance to the error-modeling accuracy (or lack thereof) of the wide-area correction signals. In differential GPS techniques, a wide-area correction refers to modeling timing, satellite, and atmospheric error over a "wide area" of the earth. For WAAS, base stations throughout the United States contribute to an error-mitigation model representative of the United States (Hurn, 1993), and for SF1 and/or SF2, base stations are distributed around the world to create three wide-area correction models; one of which models North and South America from 76 degrees north latitude to 76 degrees

south latitude (Navcom Technology, 2003). Error modeling for a very small, specific portion of the planet's surface is best served through "local area" corrections like RTK. The algorithms that comprise SF1 and/or SF2 error modeling are proprietary to Navcom Technology (a subsidiary of John Deere), so an evaluator would be unlikely to simulate or replicate the error modeling of these services. In fact, due to the dynamic nature of the GPS satellite constellation, true testing replications are impossible to achieve, but approximate replications may be possible.

3.5.4 POSITION ADJUSTMENTS VIA SLOPE AND ASPECT MODELING

Digital elevation modeling for the test site revealed that the site, although level in appearance, had a uniform negative slope almost directly towards the west (see Appendices F and G). The average slope value was 1.5 degrees. Given that the tracking prism, mounted on the rear hitch of the tractor, was 90 cm above ground at this site (in order to overcome line-of-sight issues from ground vegetation such as weeds), this translated to a theoretical eastward position adjustment of approximately 2.4 cm. The positions were not adjusted in such a broad manner, however; each unadjusted total-station position was adjusted based on the grid value from its underlying DEM. By adjusting the positions in this manner, overall XTE error was more representative of autoguidance performance. Average position adjustment with the southward drive paths was 2 cm, while average adjustment with the westward drive paths was <1 cm.

One issue that was introduced during the conceptualization and implementation of the slope/aspect modeling involved choosing the DEM resolution. Because the vehicle speed during these tests was 2.2 m s^{-1}, and, because the total station could only process

positions no faster than 1 Hz, slope and aspect values were calculated on a 1.0-m^2 grid. A greater DEM resolution would serve to capture a more complete picture of the ground surface in the test plot but require far greater labor resources to accurately produce and ground-truth the model. On the other hand, as the tractor footprint is far larger than 1.0 m^2, a less-resolute DEM may better explain the characteristics of a suspension-enabled vehicle in motion. We believe a far simpler solution to capturing prism tilt information would have been to install accelerometers or gyroscopic devices at the prism. Acquiring additional equipment would have incurred more project costs, so we wanted to utilize tools that were "in-house" (like GIS software and survey-grade GPS units) to account for the phenomenon.

3.5.5 CONSIDERATIONS FOR CONTINUING RESEARCH

Using a total station with target-tracking capability served us well for documenting the drive path of our autoguidance-equipped tractor. This technique served particularly well in evaluating SF1, SF2, and WAAS. Because RTK correction is typically regarded as accurate to less than 3-cm, the tracking capabilities of our total station were, at best, five times more accurate than RTK observations. However, a measurement accuracy of 10 times better than typical RTK could have provided more robust statistical details about RTK. Modern total stations may satisfy this requirement.

Documenting vehicle prism positions during AB-line establishment served as a more intuitive reference method for XTE distribution throughout subsequent test events. Also, XTE observations supported the notion that position determination has different error levels between the northing and easting components, so evaluating correction-signal

performance with easting-neutral and northing-neutral path orientations should be strongly considered for future testing. While accounting for potential prism tilt may not have contributed greatly to position accuracy in our study, reducing error is nonetheless good policy, so some form of error mitigation should always be considered when travel conditions become more representative to typical farming applications.

3.6 SUMMARY

The techniques evaluated for this study involved following a GPS-based autoguidance-assisted vehicle with an optical total station with target-tracking capability in order to create a terrestrial absolute frame of reference when comparing correction signals. Recommended techniques for proper correction-signal testing by the total-station instrument include conducting site calibration, establishing semi-permanent monumentation for reference purposes, and conducting guidance tests in neutral-easting or neutral-northing path orientations. Proper application of a total station can be used to investigate autoguidance behavior using correction signals with typical decimeter accuracy or greater, like SF1, SF2, and WAAS; XTE error from RTK correction signal could not be sufficiently documented in comparison to inherent tracking-mode error of the total station. Due to the potential measurement errors derived from a tilted tracking prism, a digital elevation model served to capture slope and aspect characteristics for the test site such that derived positions could be adjusted. This adjustment method relies strongly on the susceptibility of the tracking prism to excessive pitch/roll of the vehicle, and this susceptibility can be minimized by installing the prism as close to the ground surface as possible,or by adding accelerometer/gyroscopic hardware to the prism.

CHAPTER FOUR

ACCURACY OF GPS CORRECTION SERVICES OVER TIME FOR GUIDANCE-SYSTEM APPLICATIONS

4.1 ABSTRACT

Navigational satellite services (GPS, GNSS) provide real-time position information for autoguidance applications. Under dynamic situations (i.e. when the GPS/GNSS receiver is in motion), performance assessments are often based on measured positions relative to a target "path". The objective of this study was to compare short-term and long-term accuracies of an autoguidance system when using different GPS-based correction services. An optical total-station with target-tracking capability was utilized to provide an absolute frame of reference when comparing accuracy and repeatability of Wide-Area Augmentation System (WAAS), John Deere® StarFire 1 (SF1) and SF2, and Real-Time Kinematic (RTK) during 2006 and 2007 seasons. Cross-track error (XTE) was influenced by drive-path orientation for RTK, SF2, and WAAS correction signals; SF1 performance was consistent regardless of orientation. Southward XTE was typically more accurate than westward XTE. SF2 short-term and long-term errors were much greater than typically reported values. XTE derived under SF1 and WAAS correction were more representative of typical manufacturer's claims. Unsigned

95% short-term and unsigned 95% long-term error was preferred to describe guidance performance over signed P2P and Y2Y, respectively.

4.2 INTRODUCTION

One of the most significant advancements introduced into the precision-agriculture market has been that of assisted-steering, or autoguidance, for farm machinery. Primarily this technology allows the vehicle operator to focus his or her efforts on monitoring real-time operations other than navigating the vehicle, such as implement activity. A few of the many benefits of autoguidance systems include reducing driver fatigue, extending operational hours, and potentially lowering fuel usage. A common industry practice involves utilizing a navigational satellite service to derive vehicle location in real time, such as the United States' Global Positioning System (GPS), or the more inclusive Global Navigation Satellite System (GNSS), which includes satellites from the United States (GPS), Russia (GLONASS), and other governments as more compatible satellite vehicles are launched into space and positioned into orbits. Unlike many geo-stationary satellites used for communications purposes, GNSS satellites are in constant motion relative to Earth's surface; therefore, many satellite vehicles can come in to and drop out of view of a user's GPS/GNSS receiver over the course of several minutes. A GPS/GNSS receiver, or sensor, operates by "receiving" radio signals from GNSS satellites overhead, and sensor software calculates the distance from each satellite to the user; of course, because of the movement of the GNSS constellation, position solutions fluctuate.

Although an inexpensive personal navigation device (PND), equipped with a GPS/GNSS sensor, can provide the user with his or her location over the majority of the planet, the accuracy of such a location could be several meters from the true geographical location. Several conditions relating to the quality of the PND, the amount of signal interference, and even local environmental conditions may accumulate this error. However, several of these conditions can be managed to a large extent allowing the error to be mitigated. Several manufacturers offer "correction signals" that serve to enhance the real-time positioning of GPS/GNSS sensors; autoguidance systems almost exclusively require some form of correction signal to operate at a performance level acceptable to most users. Correction signals do not necessarily provide consistent, repeatable results for mitigating error, however; Han *et al*. (2004) observed that, when comparing multiple GPS sensors operating on different wide-area (non-RTK) correction signals, a sensor's dynamic performance was extremely variable throughout time, whether by different hours of the test day or by different test days.

Accuracy and precision measurements of GPS- or GNSS-capable sensors are derived from static-operation tests using internationally-accepted engineering testing standards to estimate such determinations (Institute of Navigation, 1997). Static-accuracy terms such as Circular Error Probable (CEP), Spherical Error Probable (SEP), and Root Mean Square (RMS) Error pertain to differences in measured positions from a known target position (Upadhyaya *et al.*, 2003). Today, no engineering test standard has been developed to quantify GPS/GNSS positioning accuracy under dynamic conditions, yet most manufacturers report performance of their system in terms of pass-to-pass error (P2P). Also known as *relative accuracy*, or *short-term error*, P2P refers to a guidance

system's accuracy in determining a new position (point, drive path, etc.) relative to a recently-determined position within a short period of time (about 15 minutes). This concept expresses to the operator how closely the current drive path should relate to the previous drive path, which is a direct relation to skip and overlap in most tillage and sprayer operations. The assumption is that some form of dynamic testing must have taken place in order to derive such values, but as there is no accepted test standard in place, comparing guidance systems among manufacturers in equal terms becomes a challenge. Adamchuk *et al.* (2007) discussed how several parametric and non-parametric statistical values are utilized to describe autoguidance error. The authors preferred to describe both types of values when they reported findings, so that readers may choose for themselves which values are more representative of autoguidance system performance.

Under dynamic situations (i.e. when the GPS/GNSS receiver is in motion), performance assessments are often based on measured positions relative to a target "path". Several researchers have followed this template for guidance testing (Stombaugh *et al.*, 2002; Taylor et al., 2004). These methods have their advantages in that most of the measurements generated through these processes can be easily evaluated and compared with an intuitive path template. Also, some researchers prefer to evaluate dynamic autoguidance tests in field conditions at suitable operating speeds, as several equipment- and terrain-related variables can influence the performance of a system (Ehsani *et al.*, 2002). A commonly-used response variable for assessing guidance error is Cross-Track Error (XTE), which refers to the shortest possible distance between an observed receiver position and its theoretical, or anticipated, position in relation to a mathematical line model. With this variable, other statistical measures of location and variability can be

computed, such as mean XTE, standard deviation of XTE (SD), root mean square error of XTE (RMSE), P2P, and year-to-year accuracy (Y2Y). (Definitions for these terms are in Appendix K.)

By utilizing high-quality GPS- or GNSS-capable sensors with conventional surveying techniques, positions can be derived to a high order of accuracy under static conditions; when these techniques are not available to autoguidance operators, an element of drift may be introduced into the positioning error. This position drift is largely a direct result of fluctuating position solutions caused by the motions of the GNSS constellation. Position drift can have an effect on field operations that rely heavily on autoguidance technologies, such as seasonal crop-seed placement over underground irrigation tubing. No accepted method of quantifying position drift in dynamic situations exists; however, it is generally accepted by researchers that this phenomenon can be measured in terms of Y2Y and/or long-term error by comparing the amount of XTE variability over a long period of time, providing some measure of how "repeatable" a guidance system would be in traversing a known path from season to season. Han *et al.* (2004) and Ehsani *et al.* (2002) utilized an array of vehicle-mounted GPS sensors receiving multiple decimeter- and sub-meter wide-area differential GPS (DGPS) correction signals in an effort to measure their performance; for these studies, the paths mapped via Real-Time Kinematic (RTK) correction were considered the "absolute" or "reference" paths from which to compare the other receivers' paths. Autoguidance operations conducted with RTK correction are often regarded as sub-inch accurate from one season to the next due to the operating parameters and assumptions maintained in the RTK correction. However, when one GPS receiver is established as an independent "base" from which to generate

correction data or position errors, and few or no redundancies exist to support the position derivations made in the autoguidance software, the potential exists for GPS drift to occur under RTK operation, albeit a small effect or negligible for some users in agricultural field operations. Because of this error potential, another form of absolute positioning was investigated by utilizing a total station, or tachymeter. In the surveying industry, a total-station unit offers target positioning that can be correlated with GPS-derived positions and, more commonly, physical on-site monuments providing a local frame of reference. While surveyors generally collect positions with a stationary target (like a prism), in recent years, total-station technology has progressed such that the target can be in motion as well. This characteristic provides the potential to plot the driving path of a vehicle or any moving target in which the prism is mounted.

4.3 SUB-OBJECTIVE

The objective of this study was to compare short-term and long-term accuracies of an autoguidance system when using different GPS-based correction services.

4.4 MATERIALS AND METHODS

The tractor used for this study was a John Deere® 6420 (Deere and Co., Moline, IL, USA; see Appendix A) factory-equipped with the Starfire® ITC™ GPS receiver (part no. PF80732; software ver. 2.52A; Deere and Co., Moline, IL, USA) and the GreenStar™ autoguidance system (hardware ver. PF80444 2.5; software ver. PF303192F; Deere and Co., Moline, IL, USA: see Appendix D). The tractor was also outfitted with a Trimble® EZ-Guide™ lightbar guidance computer (firmware ver. 4.10.002 Feb 22 2007 11:53:46 for 2007 tests; Trimble Agriculture, Sunnyvale, CA, USA) and an EZ-Steer™ assisted-

steering system (software ver. 3.00.01 for 2007 tests; Trimble Agriculture, Sunnyvale, CA, USA: see Appendix D).

In order to capture moving-vehicle position data with a terrestrial frame of reference, we used a Trimble® 5603 DR+ optical total station (firmware ver. 696-03.08; Trimble Engineering, Sunnyvale, CA, USA) in combination with a Trimble® TSCe field data collector (part no. 45185-20; Trimble Engineering, Sunnyvale, CA, USA) utilizing Trimble® Survey Controller software (versions 11.20 – 11.40; Trimble Engineering, Sunnyvale, CA, USA: see Appendix B). Point of measurement on the tractor was maintained using a Trimble® RMT ATS Multi-Channel tracking prism (part no. 571233035; Trimble Engineering, Sunnyvale, CA: see appendix C), mounted to the rear frame hitch approx. 66 cm above the ground and aligned with the vehicle's centerline. Distance measurements were calculated via Electronic Distance Measurement (EDM) technique; the stated accuracy of such measurements was ± (5 mm + 2 ppm; Trimble Engineering, 2001). In addition, the total station was equipped with Trimble's AutoLock™ function such that the total station, via servo motors integrated within its base, could automatically track the moving target prism under dynamic conditions and simultaneously collect vector (angle and distance) data.

Four different GPS-based correction signals were evaluated: Wide-Area Augmentation System (WAAS), John Deere StarFire 1 (SF1), John Deere StarFire 2 (SF2), and Real-Time Kinematic (RTK). Position accuracies typically reported by manufacturers and/or system users are referenced in Table 4.1. No implements were attached during the tests, so draft or drag was not considered; also, the tractor had

performed only light-duty tasks during its life, so steering and/or transmission wear was considered negligible.

Table 4.1. Typical reported accuracies for correction signals used in this study.

Correction Signal	Type of Correction	Accuracy
WAAS	wide-area	±15 to 30 cm short-term (pass-to-pass); ±61 to 66 cm long-term (static)
SF1	wide-area	±33 cm short-term; ≈76 cm long-term
SF2	wide-area	±10 cm short-term; ≈25 cm long-term
RTK	local-area	≤3 cm short-term; ≤3 cm long-term

Source: Hest, 2007. For additional details, see Appendix E.

4.4.1 TEST-SITE PREPARATIONS

This study was performed in Auburn, Alabama (32.6º N, 85.5º W) beginning in February 2006 and ending in August 2007. A different testing site was selected each year (see Figures 4.1, 4.2, and 4.3). Except for differences in local terrain, both sites shared the characteristics of minimal overhead obstruction (desired for maximum reception of available satellites), minimal sources of radio interference (desired for maximum reliability of positioning data and correction-service reception), and allowances for line-of-sight testing (desired for uninterrupted prism tracking by the total station). For the 2006 study, guidance lines were established at 6.1-m spacing; direction of travel was approximately 80.1 degrees azimuth relative to true north (Figure 4.1). For the 2007 study, a swath width of 12.2-m was used during this testing; directions of vehicle travel were approximately 179.4 degrees (Figure 4.2) and 271.3 degrees (Figure 4.3) relative to true north.

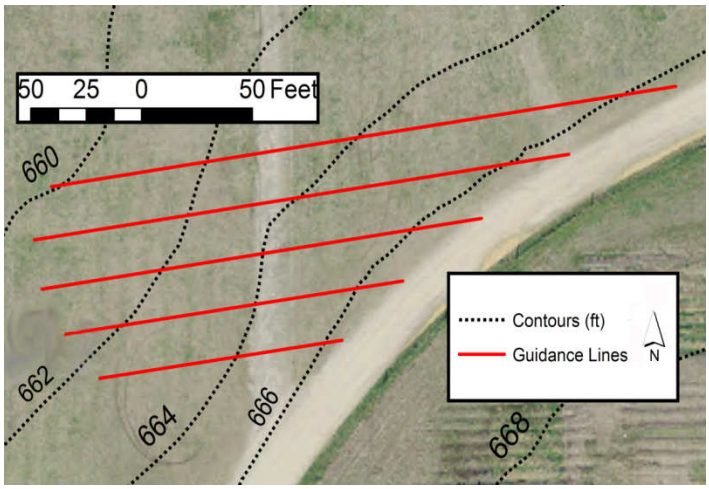

Figure 4.1. Guidance testing site one, used in 2006. Elevation contours are in 2-ft (0.6-m) intervals; guidance lines are spaced 20 ft (6.1 m). Direction of vehicle travel was westerly to easterly (approx. 80.1 degrees azimuth from true north; aerial imagery and contour data courtesy of City of Auburn GIS Department, Auburn, AL).

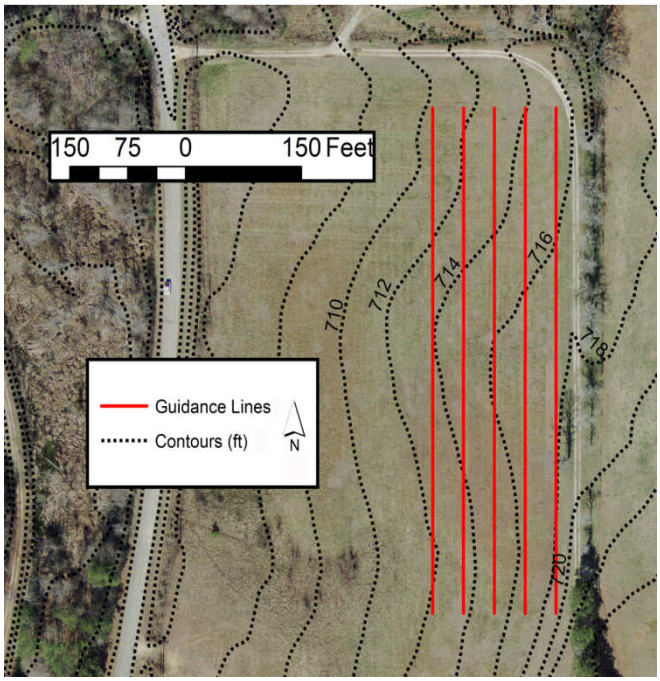

Figure 4.2. Guidance testing site two, used in 2007. Elevation contours are in 2-ft (0.6-m) intervals; guidance lines are spaced 40 ft (12.2 m). Direction of vehicle travel was northerly to southerly (approx. 179.4 degrees azimuth from true north; aerial imagery and contour data courtesy of City of Auburn GIS Department, Auburn, AL).

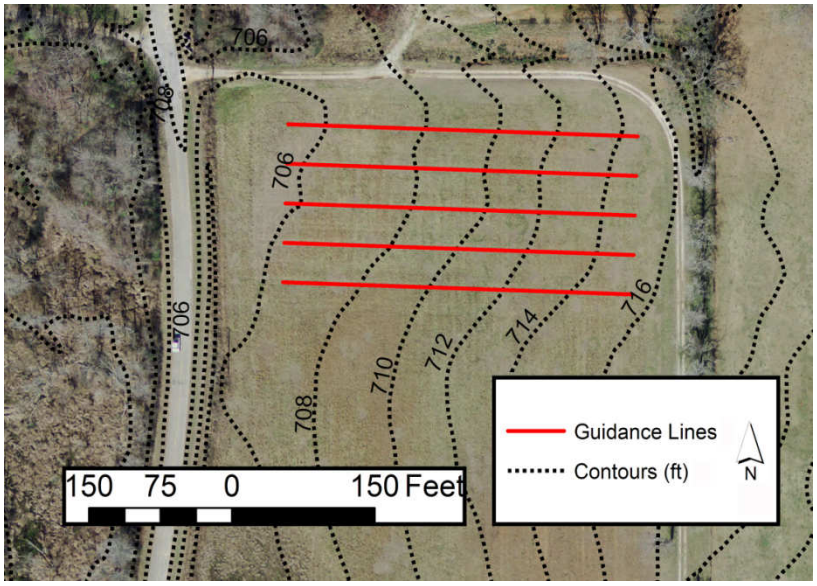

Figure 4.3. Guidance testing site two, used in 2007. Elevation contours are in 2-ft (0.6-m) intervals; guidance lines are spaced 40 ft (12.2 m). Direction of vehicle travel was easterly to westerly (approx. 271.3 degrees azimuth from true north; aerial imagery and contour data courtesy of City of Auburn GIS Department, Auburn, AL).

Five straight-line parallel paths were navigated by the guidance system(s) for each correction signal being evaluated. Vehicle speed was maintained at 2.2 m s^{-1} for all tests. A test "event" was represented by traversing all five reference lines within a 15-minute time period. A different correction signal was enabled prior to each test event. Field set-up and data analysis procedures for each year of testing are discussed in Chapter 3 and Appendices L and M. XTE values were derived from positioning data and rounded to the nearest centimeter. Testing event schedules are presented in Appendix I (2006) and Appendix J (2007).

4.4.2 STATISTICAL ANALYSES

For both years of the study, mean cross track error (XTE), standard deviation of XTE (SD), and root mean square error of XTE (RMSE), were calculated as outlined by Ehsani *et al*. (2002; also outlined in Appendix K). Pass-to-pass errors (P2P) were calculated by subtracting the signed value of the mean XTE of a row from the preceding row; year-to-year errors (Y2Y) were calculated as the range between the signed testing-event XTE across a season. Unsigned short-term error was calculated as the absolute difference from average XTE per testing event (Adamchuk *et al*., 2007); unsigned long-term error was considered the same as unsigned XTE. Individual testing events and Y2Y observations were screened for potential XTE outliers, defined by "any observation farther than 1.5 [Inter-Quartile Range, or IQR] from the closest quartile" (Devore and Farnum, 2005). Basic statistical measures of XTE were derived through the univariate-statistics procedure (PROC UNIVARIATE; SAS Institute, Cary, NC, USA). Box-and-whisker plots were created to illustrate signed XTE comparisons of individual testing events across a given season as well as year-to-year XTE assessment. Cumulative frequency distributions of short-term and long-term error were created to illustrate unsigned XTE trends for each correction signal. Graphical depictions were generated in MS Excel 2007.

4.5 RESULTS AND DISCUSSION

4.5.1 FIRST-YEAR EVALUATIONS OF XTE

As mentioned in Chapter 3, XTE evaluations under the RTK correction are offered solely as comparisons to the other correction signals, since the total station used

in this study was not considered accurate enough to evaluate dynamic RTK situations.

Cumulative short-term and long-term errors for the 2006 season are presented in Figure 4.4. The values at which the 95%-probability lines intersect each error curve are presented as 95% short-term and long-term error in Table 4.2. This method of presenting

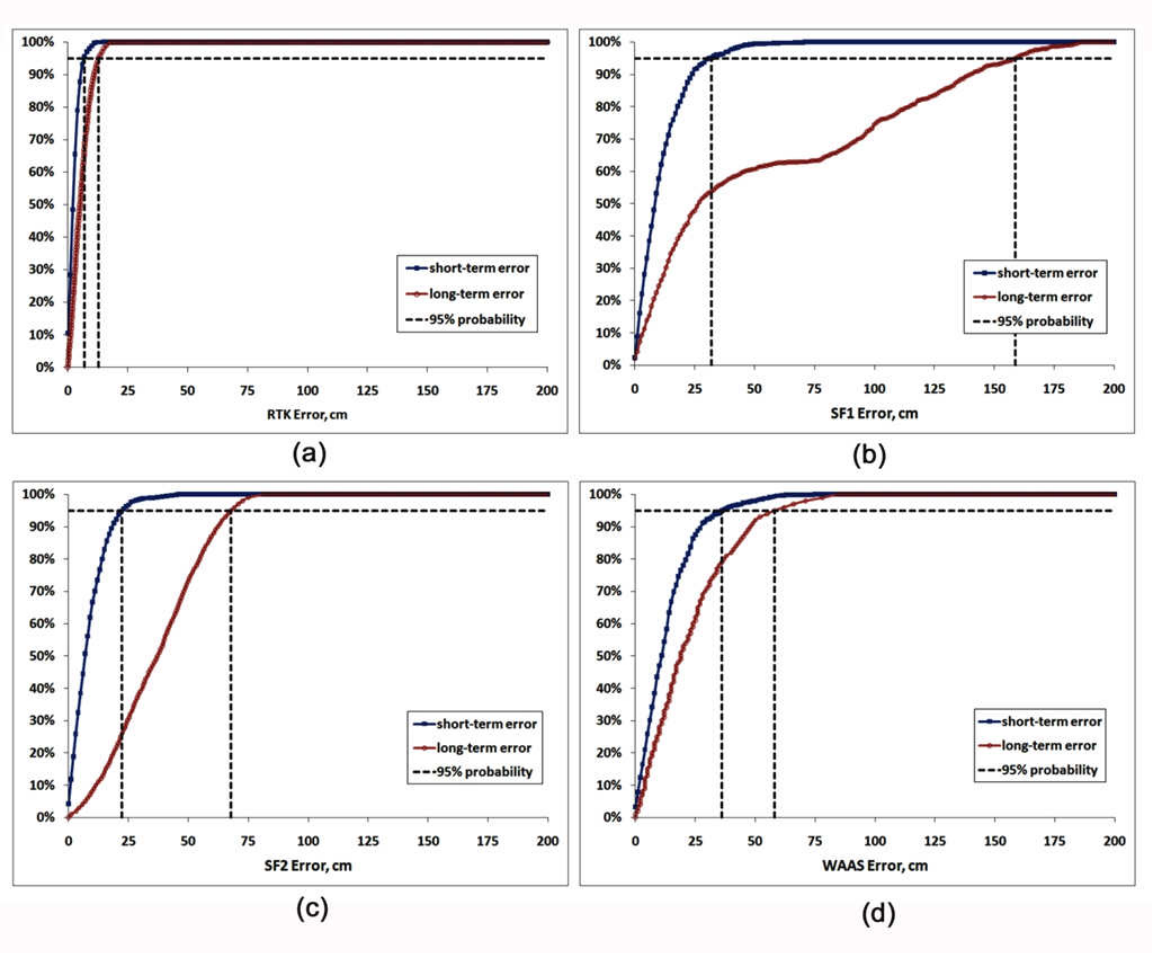

Figure 4.4. Cumulative distributions of unsigned short-term and long-term error (cm) for (a) RTK, (b) SF1, (c) SF2, and (d) WAAS corrections in the 2006 study.

unsigned short-term error is similar to the method discussed by Adamchuk *et al.* (2007), in that short-term error was considered the amount of path deviation witnessed from the average XTE value of the testing event on which the deviation was recorded. For

example, if an individual XTE value of 12 cm from the target path was observed during a testing event in which all XTE averaged 10 cm from the target path, then the short-term error for the individual XTE value was 2 cm. However, Adamchuk *et al.* (2007) used a different calculation for deriving long-term error that depended on finding the amount of

Table 4.2. Summary of 2006 XTE data.

Correction Signal	Median XTE (cm)	XTE IQR (cm)	Mean XTE (cm)	SD (cm)	RMSE (cm)	95% Short-term error (unsigned), cm	95% Long-term error (unsigned), cm
RTK	-5	6	-5	5	7	7	13
SF1	5	116	38	68	78	32	159
SF2	37	29	36	21	41	22	68
WAAS	-9	37	-10	27	29	36	58

path deviation witnessed from the average XTE value of the entire testing season. To extend the previous example, if all XTE values for the entire season averaged 5 cm, then the individual XTE value would have a long-term error of 7 cm. This technique of evaluating long-term error was changed to reflect simple unsigned XTE across the testing season. Firstly, it was apparent that the locations of the GPS-derived drive paths changed, or "drifted", across the season. It was surmised that, by adjusting individual XTE relative to a seasonal average, this "drift" would not be as readily recognized in the datasets. Secondly, we wanted to use values more reflective of what a vehicle operator may witness over time in a typical autoguidance operation, and individual XTE was suitable. However, the 2006 study was considered as more of a procedural evaluation for data collection, and the lessons learned during these tests helped us to refine our

procedures and expand upon other concepts and variables that may have helped to better quantify short- and long-term error.

RTK correction offered very low position error in terms of variability (5-cm SD, 6-cm IQR), location (5-cm XTE median/XTE mean), and overall accuracy (7-cm RMSE), but the values were slightly higher than values typically reported for RTK performance (Table 4.2). Short-term and long-term errors were also greater than anticipated. SF1 correction varied over a meter throughout the season, yet tended to be centered close (5 cm) to the desired path; however, high RMSE suggested that this signal was the most inaccurate signal of the season, and this inaccuracy contributed to a high long-term error. SF2 correction offered XTE farthest from the reference lines (37-cm XTE median; 35-cm XTE mean). Finally, WAAS correction offered good general location throughout the season (9-cm XTE median/10-cm XTE mean) despite the overall accuracy (29-cm RMSE), which was consistent with typical reported accuracy for this signal (Table 4.1).

Box-and-whisker plots for all testing events in 2006 are presented in Figure 4.5; values pertaining to creation of box-and-whisker plots are in Appendix N. The "summary" box-and-whisker plot for each correction signal corresponds with median and IQR values presented in Table 4.2. As mentioned above, positioning for SF1 correction signal had the greatest error of all other signals tested; however, XTE variability between individual testing events was somewhat consistent (Fig. 4.5b). XTE median varied considerably on events J71 and J72 from the previous three events. On these occasions, XTE suggested that SF1 is consistent in a short-term sense but not very repeatable in the long-term sense. Only one individual testing event under SF2 correction was considered

more “on target” than other events (D62; Fig. 4.5c); apart from that event, XTE median was somewhat consistent at 37 cm throughout the period tested. WAAS-derived XTE had consistent variability throughout the period tested, as represented by individual IQR per testing event.

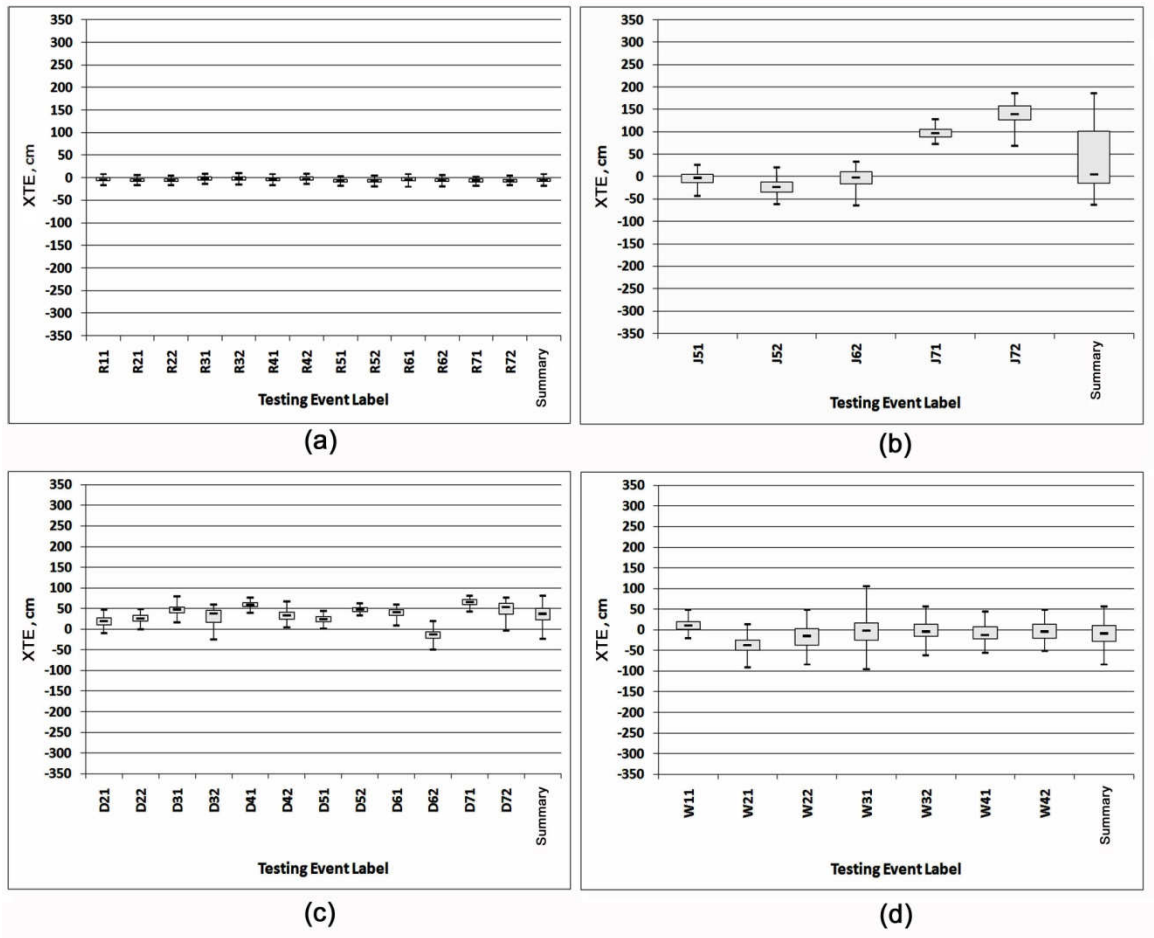

Figure 4.5. Box-and-whisker plots for individual testing events and Y2Y (2006) for (a) RTK, (b) SF1, (c) SF2, and (d) WAAS correction signals. Testing Event Label corresponds to testing events listed in Appendix I.

4.5.2 SECOND-YEAR EVALUATIONS OF XTE

Cumulative short-term and long-term errors for the 2007 season are presented in Figure 4.6. The values at which the 95%-probability lines intersect each error curve are presented as 95% short-term and long-term error in Table 4.3. RTK correction provided

close short-term and long-term error in the southward direction, while the westward short-term and long-term errors were not similar (Figure 4.6a). Short-term and long-term

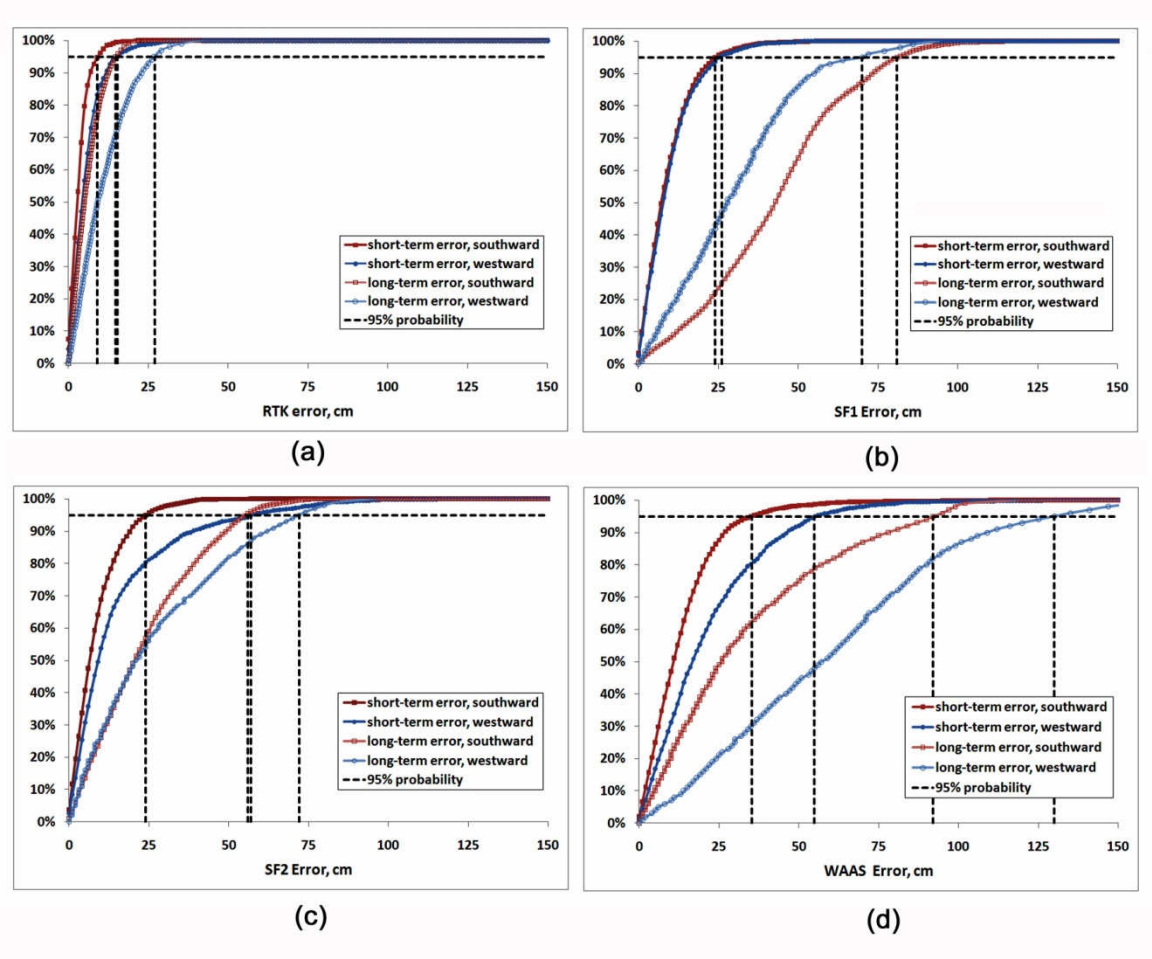

Figure 4.6. Cumulative distributions of unsigned short-term and long-term error (cm) for (a) RTK, (b) SF1, (c) SF2, and (d) WAAS corrections in the 2007 study.

errors were considerably different for the SF1 (Figure 4.6b) and WAAS (Figure 4.6d) corrections and for each drive-path orientation. Westward SF2 provided closer short-term and long-term error than southward SF2 (Figure 4.6c). Both SF1 and SF2 had similar maximum 95% long-term error of around 70 cm, suggesting that both John Deere correction signals performed equally.

As evidenced from RMSE values, the drive-path orientation tended to influence XTE (Table 4.3). Southward drive paths yielded more accurate XTE than westward drive paths for 3 of the 4 correction signals tested. RTK short-term and long-term errors were much larger than values typically reported. Median XTE and mean XTE values suggested, however, that the target path was closely obtained throughout the season. Given that variability of SF2 signal was about equal (43-cm southward, 39-cm westward) and that XTE median values of the SF2 signal were closer to zero (expected value) than with either SF1 or WAAS, the suggestion was that the SF2 correction was the most reliable sub-meter correction signal evaluated. (Measure of variability for SF2 in 2006 supported this suggestion as well---Table 4.2.) Short-term and long-term errors observed for SF2 did not support this suggestion, however;

Table 4.3. Summary of 2007 XTE data.

Correction Signal [a]	XTE Median (cm)	XTE IQR (cm)	XTE Mean (cm)	SD (cm)	RMSE (cm)	95% Short-term error (unsigned), cm	95% Long-term error (unsigned), cm
RTK_S	-1	10	-2	7	7	9	15
RTK_W	4	18	4	13	14	17	27
$SF1_S$	21	83	12	47	48	24	81
$SF1_W$	18	36	18	31	36	26	70
$SF2_S$	3	43	5	29	29	24	56
$SF2_W$	7	39	6	35	35	57	72
$WAAS_S$	-10	49	-8	43	43	35	92
$WAAS_W$	44	66	38	59	70	55	130

[a] Subscripts 'S' and 'W' refer to southward-oriented and westward-oriented reference lines, respectively.

SF1 offered consistent position error regardless of path orientation (21-cm XTE median southward/18-cm XTE median westward; Table 4.3), but the variability in the southward orientation was more than twice that observed in the westward orientation; a

histogram of XTE for the southward SF1 dataset revealed that, instead of XTE being normally distributed about a single mean XTE, there were two distinct "peaks" in the distribution at approximately 60 cm and -50 cm locations. Signed statistics are likely confounded as a result, but unsigned short-term and long-term errors for SF1 are consistent regardless of path orientation. SF1 short-term and long-term errors agree closely with typical reported accuracy of this signal as well (Table 4.1).

Long-term XTE error from WAAS correction was approximately one meter regardless of direction (Table 4.3). To determine whether WAAS correction performed according to typical reports for this signal, some interpretation of Table 4.1 must be considered. Typical WAAS errors are ±15 to 30 cm short-term and ±61 to 66 cm long-term (Table 4.1); if ±15 to 30 cm for short-term error means that the position could be either 15 to 30 cm on one side of the target line or the other, then the error "spread" could be considered 30 to 60 cm. Likewise, long-term WAAS error could be considered as a spread of 122 to 132 cm. Unsigned error represents this error spread, therefore, WAAS short-term and long-term errors agree with those typically reported by manufacturers and researchers regardless of travel direction.

Box-and-whisker plots for all testing events in 2007 are presented in Figures 4.7 – 4.10; values pertaining to creation of box-and-whisker plots are in Appendix O. The "Summary" box-and-whisker plot for each category corresponds with median and IQR values presented in Table 4.3. For each drive-path orientation, XTE spread under RTK correction appeared similar across the season (Figure 4.7); however, westward RTK events exhibited more variability and less accuracy than southward events. Presentation of southward RTK performance over the season provides strong support that RTK

correction had the greatest accuracy and reliability from one event to the next, yet westward RTK performance tends to counter-act this notion.

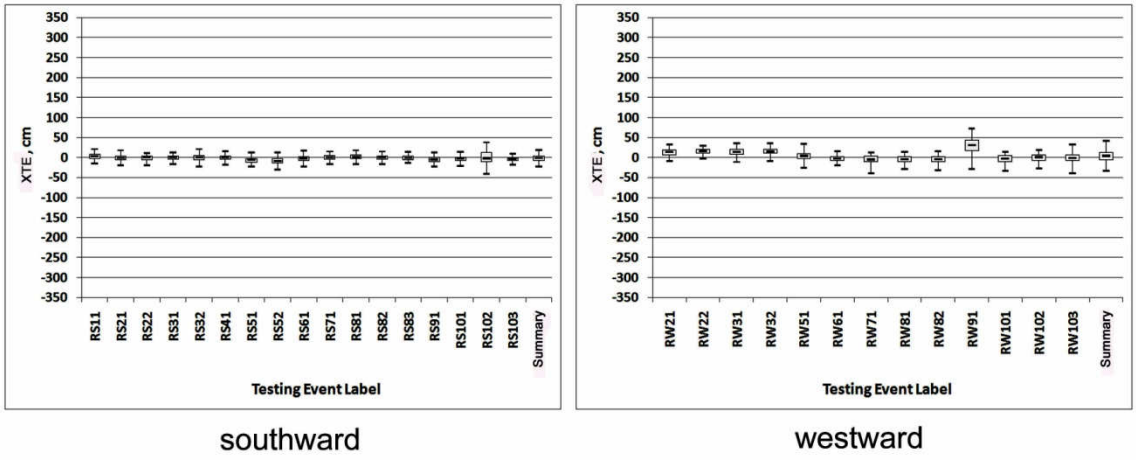

Figure 4.7. XTE box-and-whisker plots for RTK correction signal in 2007, comparing southward orientation (left) and westward orientation (right). Testing Event Label corresponds to testing events listed in Appendix J.

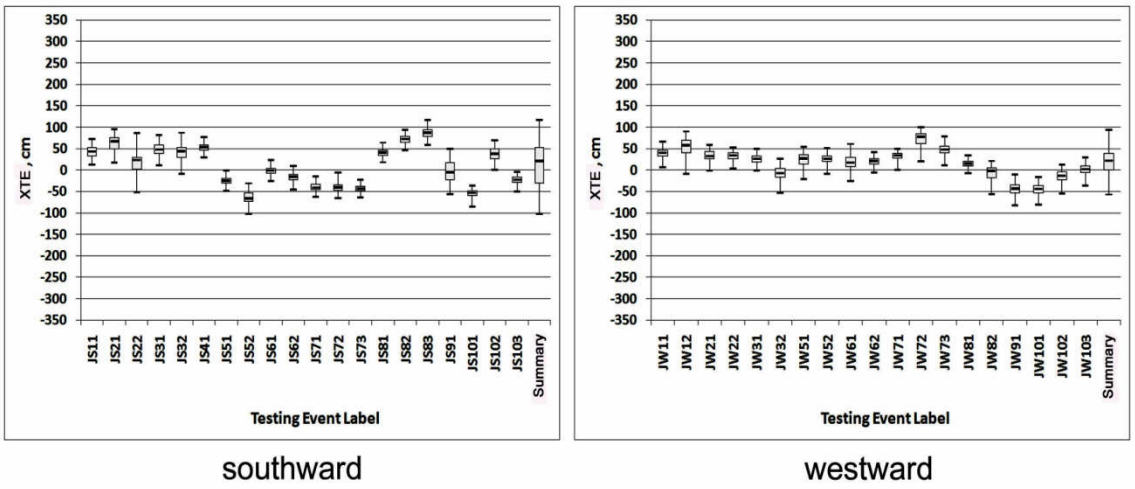

Figure 4.8. XTE box-and-whisker plots for SF1 correction signal in 2007, comparing southward orientation (left) and westward orientation (right). Testing Event Label corresponds to testing events listed in Appendix J.

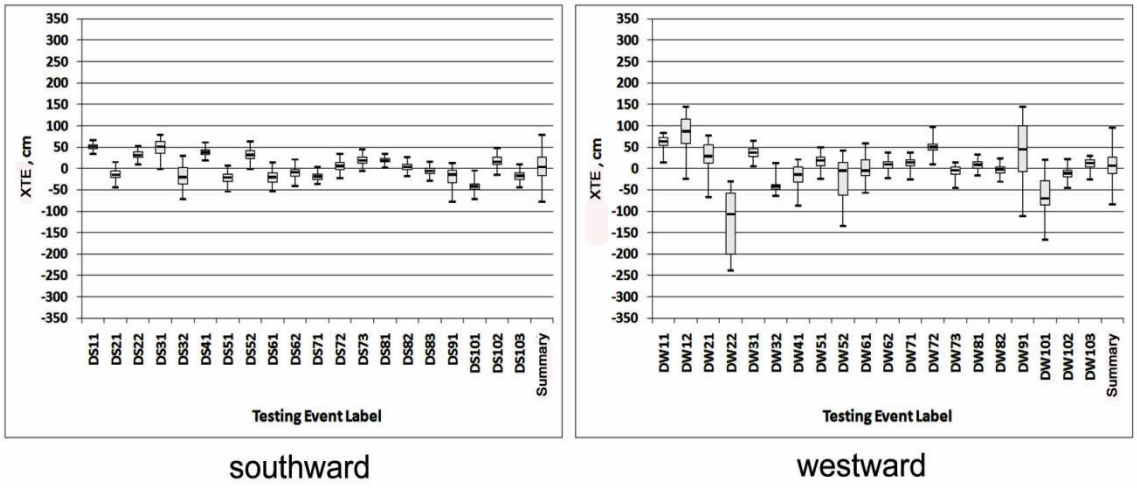

Figure 4.9. XTE box-and-whisker plots for SF2 correction signal in 2007, comparing southward orientation (left) and westward orientation (right). Testing Event Label corresponds to testing events listed in Appendix J.

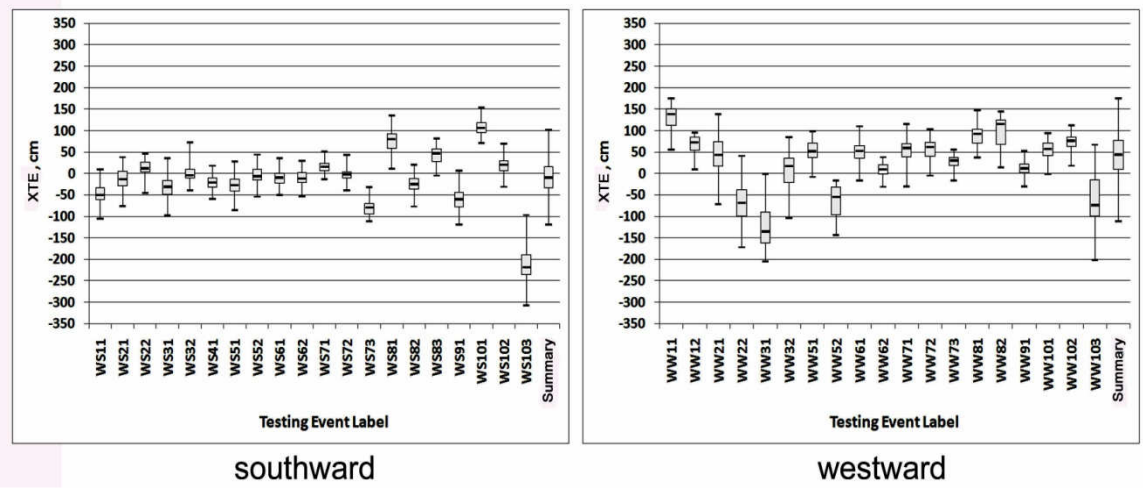

Figure 4.10. XTE box-and-whisker plots for WAAS correction signal in 2007, comparing southward orientation (left) and westward orientation (right). Testing Event Label corresponds to testing events listed in Appendix J.

By studying Figures 4.8 – 4.10, there was the tendency for testing-event XTE median to fluctuate throughout time in an almost-regular sine-wave fashion. SF1 and SF2 illustrated this phenomenon more strongly than WAAS, but this trend was witnessed for WAAS as well. No explanation can be offered to explain this behavior; however, more investigation should be considered to better document this trend and to determine whether a more precise method of evaluating short-term or long-term error could be derived.

Concerning the WAAS correction (Figure 4.10), XTE for testing events that occurred on or after July 31, 2007 (events W*8*, W*9*, and W*10*) may have been influenced by the scheduled removal of one of the two available communications satellites that broadcasted the WAAS correction signal. The GreenStar guidance system, that relayed WAAS correction from the StarFire iTC receiver to the EZ-Guide system, could not be configured or reviewed to determine whether a particular communications satellite was being monitored, or whether the system received the correction without regard to its source. If this incident provided an additional source of error, then per-event XTE for the southward drive path reflected this concept, starting at event WS81. While this incident may have affected per-event XTE for the westward drive paths, starting at event WW81, assessment was difficult considering the large amount of per-event XTE variability witnessed previously in the season.

4.5.3 SIGNED P2P VERSUS UNSIGNED SHORT-TERM ERROR EVALUATIONS

In 2006, RTK correction resulted in no skip and only 2-cm overlap (Table 4.4). Under SF2, signed P2P averaged 2 cm for the study, but separate events witnessed either a skip as great as 12 cm or an overlap as great as 8 cm. Unsigned short-term error for

SF2 was 22 cm (Table 4.2), and both values were consistent with typical reports under this correction (Table 4.1). SF1 correction exhibited greatest amount of overlap throughout the study, and signed P2P under WAAS correction varied greatly.

Table 4.4. Signed pass-to-pass error (P2P, cm) throughout the 2006 study.

Event No.[a]	RTK	SF1	SF2	WAAS
1	-2			7
2	-2		5	-1
3	0		1	-5
4	-1		4	-35
5	-1		0	-2
6	-2		-2	3
7	-1		1	4
8	-2	-2	5	
9	-1	-8	2	
10	-1		-1	
11	0	0	-8	
12	0	-5	12	
13	-1	-15	11	
Avg. P2P	**-1**	**-6**	**2**	**-4**

[a] Events are numbered in sequential order by time and date of collection (see Appendix I).

In 2007, southward P2P under RTK correction ranged from neutral to 8-cm overlap, and westward P2P ranged from 2-cm skip to 2-cm overlap throughout the study (Table 4.5). SF2 correction yielded skip and overlap as high as 8 cm traveling southward, while skip was as high as 39 cm and overlap was as high as 26 cm traveling westward. Under SF1, both path orientations averaged neutral P2P. WAAS correction yielded overlap in the southward direction and skip in the westward direction; southward P2P illustrated an overlap as high as 19 cm, and westward P2P illustrated overlap and skip nearing a half meter. To compare the signed short-term error to the unsigned short-

Table 4.5. Signed pass-to-pass error (P2P, cm) throughout the 2007 study.

Test Date[a]	RTK_S[b]	$SF1_S$	$SF2_S$	$WAAS_S$	RTK_W[c]	$SF1_W$	$SF2_W$	$WAAS_W$
March 7	-2	6	-2	4		0	-8	14
						-10	-25	-9
March 14	-2	9	4	-4	-2	4	14	-1
	-1	-17	2	-13	-1	-4	39	8
April 13	-1	7	8	-13	0	-3	-5	25
	-2	7	1	-4	-1	8	0	16
April 30	-2	-4	-6	-2			-4	
June 5	-2	-4	3	-4	2	4	-2	-8
	-3	-1	-5	-6		0	-12	58
July 10	0	-6	2	-5	0	-11	-13	-7
		4	6	-6		-3	-6	3
July 18	-2	4	3	0	-2	-1	-1	-10
		-6	-3	-9		2	6	5
		-2	2	6		-3	-1	-4
July 31	-2	-3	1	2	-2	-2	3	9
	-1	1	4	-8	-1	6	-2	22
	0	0	-2	2				
August 3	-2	9	-8	1	-1	5	-26	3
August 23	-2	-1	-8	4	0	3	-24	12
	-8	-5	-6	-1	-2	-6	-1	4
	0	-2	3	-19	-1	1	2	-42
Avg P2P	**-2**	**0**	**0**	**-4**	**-1**	**0**	**-3**	**5**

[a] Events are numbered in sequential order by time and date of collection (see Appendix J).

[b] Correction signals labeled with "S" refer to tests conducted while driving southward.

[c] Correction signals labeled with "W" refer to tests conducted while driving westward.

term error documented in Table 4.3, southward RTK, westward SF2, and either SF1 orientation had similar values.

Neither signed nor unsigned short-term error as calculated in this analysis can be sufficiently compared to one another. Average P2P, as presented in Tables 4.4 and 4.5, do not adequately represent the situations witnessed during autoguidance trials, although the range of signed P2P is somewhat representative. Most researchers consider P2P and short-term error as similar in the sense that both testing methods typically require a limited timeframe for data collection, such as 15 minutes, however.

4.5.4 SIGNED VERSUS UNSIGNED YEAR-TO-YEAR ERROR (Y2Y) EVALUATIONS

Year-to-year errors are presented in Table 4.6. When comparing these values to 95% long-term error in the same categories for the 2006 study, some similarities were observed for the SF1, SF2, and WAAS corrections. For the 2007 study, Y2Y was not similar to any of the long-term error values derived. The unsigned long-term error value may be a more representative method to quantify guidance drift.

Table 4.6. Year-to-year error (Y2Y, cm) from the 2006 and 2007 studies.

Correction Signal	2006 Y2Y (cm)	Correction Signal [a]	2007 Y2Y (cm)
RTK	5	RTK_S	12
		RTK_W	34
SF1	163	$SF1_S$	151
		$SF1_W$	113
SF2	78	$SF2_S$	91
		$SF2_W$	204
WAAS	49	$WAAS_S$	316
		$WAAS_W$	261

[a] Subscripts 'S' and 'W' refer to southward-oriented and westward-oriented reference lines, respectively (2007 data).

4.5.5 CONSIDERATIONS FOR CONTINUING RESEARCH

Further research would involve evaluating other factors that may influence short-term and long-term error, such as vehicle ground speed. Factors that have been known to affect general position accuracy, such as GPS/GNSS satellite geometry or satellite count, should be collected for future evaluations in order to more consistently compare experimental conditions from one test to another. An ambitious research prospect would be to conduct time-series analyses for dynamic XTE in an effort to better understand if there is a cyclical nature to correction-signal performance as was suggested in the 2007 study.

4.6 SUMMARY

An autoguidance-assisted vehicle was tracked with an optical total station in order to measure short-term and long-term error under four correction signals. Cross-track error was influenced by drive-path orientation (North-South vs. East-West) for RTK, SF2, and WAAS correction signals; SF1 performance was consistent regardless of orientation. Southward XTE was typically more accurate than westward XTE. RTK and SF2 short-term and long-term errors were much greater than typically reported values by manufacturers. XTE derived under SF1 and WAAS correction were more representative of typical manufacturer's claims. Unsigned 95% short-term and unsigned 95% long-term error was preferred to describe guidance performance over signed P2P and Y2Y, respectively.

CHAPTER FIVE

EVALUATING APPLICATION UNIFORMITY OF AN IN-SITU PRESSURE-COMPENSATING SUBSURFACE-DRIP IRRIGATION PRODUCT

5.1 ABSTRACT

In the southeast U.S., an available agricultural irrigation practice is Subsurface Drip Irrigation (SDI). Research performed at the Tennessee Valley Research and Extension Center (TVREC), Belle Mina, AL indicated moisture variability after irrigation in an active experimental plot equipped with pressure-compensated SDI. The need therefore exists to quantify the uniformity of the SDI product without disrupting the ongoing crop research. A study was conducted to develop and validate an *in-situ* testing technique to assess application uniformity of SDI products, and to evaluate if variable operating pressure or terrain slope impacted application uniformity. Laboratory investigations indicated that new pressure compensated SDI tape of the type used at TVREC had an emitter discharge of 1.04 L h^{-1} at 5% coefficient of variability (CV), above the manufacturer's specification of 0.98 L h^{-1} at 2.5% CV. A field testing apparatus was fabricated to interface with the *in-situ* SDI product in order to deliver water over a range of operating pressures while measuring sample discharge. This apparatus was tested under laboratory conditions to compare emitter-discharge estimates

with per-emitter discharge from drip-tape samples; apparatus accumulated measurements agreed to within a half-percent of per-emitter discharge rates. Global Positioning System (GPS) and Geographic Information System (GIS) technologies were utilized to quantify surface slope conditions and to target SDI samples throughout the field test plot based on irrigation system use frequency and terrain slope. Drip-tape discharge was affected by an interaction between operating pressure and system use frequency ($p=<0.0001$). Lowest discharge was observed for the irrigated SDI product operating at 48 kPa pressure. Discharges from non-irrigated SDI product and from irrigated product, both operated at 83 and 117 kPa, were not statistically different ($\alpha=0.05$) from one another. Emitter discharge estimates were within ±5% of the baseline discharge rate determined from laboratory evaluations (1.04 L h^{-1}) regardless of operating pressure or system use frequency, except for irrigated samples operating at 48 kPa (-7%). Certain tested samples exhibited flows exceeding ±5% of the baseline discharge that may prompt a system manager to investigate situations more closely. Spatial yield estimates suggested that cotton lint yield was adversely affected by poor SDI uniformity. Techniques and equipment developed in this study provide SDI researchers and users a prototype field method to evaluate *in-situ* SDI performance.

5.2 INTRODUCTION

Subsurface drip irrigation (SDI) is a method of applying precise amounts of water to agronomic crops by delivering the water directly to the plants' root zone via underground tape or tubing, often referred to as "drip line", "drip tape", or "drip tube". Previous studies have focused on utilizing SDI for fertigation or effluent release (Lamm *et al.*, 2001; Lamm *et al.*, 2004; Song *et al.*, 2003; Trooien *et al.*, 2000), determining optimum lateral spacing and lateral depth for various crop systems (Enisco-Medina *et al.*, 2002; Bryla *et al.*, 2003; Charlesworth and Muirhead, 2003; Camp *et al.*, 1997), and studying SDI effects on crop water-use efficiency (Bordovsky and Porter, 2003; Lamm and Trooien, 2003). While much research has focused on improved agronomic growth, relatively few studies discuss the longevity of drip tape systems. Ayars *et al.* (1999) operated several SDI experimentation plots throughout California over a fifteen-year period, testing fertigation regimes against crops such as cantaloupe, corn, cotton, and tomato. The authors reported that some of their plots performed similarly to initial installation after nine years, and when the system was flushed and maintained in a proper manner, root intrusion and overall emitter clogging was minimized. The case was presented by O'Brien *et al.* (1998) that longevity of an SDI system became an economic factor; when compared to center-pivot irrigation the implementation of the SDI system was not deemed profitable if the system did not function for at least ten years.

Much research has focused on evaluating emitter discharge uniformity and efficiency. One often-used testing standard pertaining to SDI performance is ASAE S553 (2008). This standard outlines methods for quantifying performance of drip tape

products, and includes testing criteria for selecting sample populations and evaluating emitter discharge rates at constant pressure or by pressure response. Testing criteria documented in this standard are most favorable to laboratory conditions; specifically, the tape product should be above ground in a controlled environment as opposed to *in-situ* field conditions. Several researchers have adapted the criteria from this testing standard to evaluate drip tape products under field conditions. When Lesikar *et al.* (2004) followed the ASAE standard to evaluate drip-tape flow rates from tape products that had been used for wastewater effluent for up to five years, the authors were required to excavate the soil to such an extent that small catch pans could be placed underneath the emitters in order to perform in-field application uniformity tests. The authors did not refer to any plants of agronomic value that were removed or relocated during excavation. However, in an effort to protect neighboring plants, Steele *et al.* (1996) exposed a reduced number of emitters in order to make an estimate of in-field application uniformity. Catch pan volumes were averaged and extrapolated to an equivalent flow rate based on manufacturer's flow rates. A similar practice of placing catch pans under exposed emitters was employed by Safi *et al.* (2007) to evaluate emitter-discharge uniformity between new and 3-year used drip-tape product across a range of operating pressures; the authors also relied upon evaluation procedures and terminology documented in ASAE EP458 (1996) and ASAE EP405 (2005).

In recent years, manufacturers have developed SDI products that are "pressure compensated," meaning that regardless of pressure changes caused by system surges or rolling terrain, emitter discharge rates are consistent. There is a lack of research literature available regarding pressure-compensated SDI performance in agronomic settings, while

some research has been conducted in wastewater or sewage-effluent settings (Li *et al*., 2009; Liu and Huang, 2009). The primary reason for the lack of research may be that pressure-compensated SDI products are still relatively new, and manufacturers continue to refine designs as products are released into the marketplace. Additionally, acceptance of SDI technology by producers may be relatively slow.

At the Tennessee Valley Research and Extension Center (TVREC, Belle Mina, Alabama), station-management practices involved the utilization of pressure-compensated SDI in conjunction with precision agriculture technology to grow cotton and other crops. Research by Sullivan *et al*. (2007) indicated that moisture variability existed within a study site containing plots using pressure compensated SDI tape in ways that suggested either clogged emitters or flow rate differences between emitters. In theory, pressure compensated SDI emitters should maintain equivalent flow rate regardless of pressure differences over a specified range. The surface of the TVREC study site exhibits rolling terrain (0% to 5% slope range) that may influence water distribution from one end of the lateral to the other if the pressure-compensation feature was inadequate or had deteriorated over time. The tape product selected in this study had been operational for six years and had not been evaluated for specific in-field performance; however, as a long-term experiment was being conducted on this test plot, major disruption through excavation was not a preferred option. From a research perspective, the need existed to quantify the *in-situ* performance of selected portions of drip tape coinciding with locations identified as having undesirable moisture distribution. A scenario such as this could provide either preliminary diagnostic information for SDI

system-management or independent data for moisture variability and precision-agriculture related crop yield studies.

5.3 SUB-OBJECTIVES

The objectives of this investigation were to (1) develop and validate *in-situ* testing techniques to assess application uniformity of SDI products, and (2) evaluate whether variable operating pressure or terrain slope impacted application uniformity.

5.4 MATERIALS AND METHODS

5.4.1 LABORATORY INVESTIGATIONS

To determine a feasible method to assess application uniformity of the SDI product at the TVREC, we conducted laboratory evaluations of new drip tape of identical design. The SDI product evaluated was Netafim® DripNET PC™, 0.381 mm tape thickness, 2.2 cm I.D. For this product, each emitter was rated by the manufacturer to distribute 0.984 liter hr^{-1} at 0.6-m spacing (Netafim USA, 2010; see Appendix P). Adapting from ASAE S553 (2008), a portion of drip tape containing 20 contiguous emitters was selected and subjected to specified performance tests. A tape sample containing 20 emitters was the desired number for *in-situ* field tests.

The municipal water supply provided in the laboratory offered a higher operating pressure than was desired; therefore, pressure was reduced and regulated via a system bypass (ball valve) and a brass-body pressure regulator (Model 26A; Watts Regulator Co., No. Andover, MA, USA), capable of adjusting from 21 to 344 kPa pressure range. Operating pressure was monitored throughout the tests via analog pressure gauges plumbed on the upstream and downstream ends of the tape sample. Emitter discharge

values were recorded over a period of five minutes by suspending the product over an array of catch cups in order to validate manufacturer specifications. In order to test potential slope effects on discharge uniformity, a sample of new drip tape was subjected to a constant operating pressure of 117 kPa at a horizontal (0% slope) grade and a 6% slope grade uphill of the water supply. Then, another sample of drip tape was subjected to a range of operating pressures (48, 83, 117, and 138 kPa) while also subjected to a 6% slope grade to evaluate potential discharge differences according to pressure. Three replications were conducted during this testing. Per-emitter discharge and coefficients of variation (CV) were collected and tabulated using MS Excel 2007. A studentized t-test was conducted in MS Excel 2007 to determine if a discharge difference existed (α=0.05) between slope classes, and a General Linear Model (GLM) procedure was conducted using SAS ver. 9.1.3 to determine if discharge differences existed (α=0.05) between pressure classes. Mean discharge values were separated according to Tukey's Studentized Range (SAS Institute, Cary, NC, USA).

5.4.2 SDI TESTING APPARATUS

Because the premise behind this study was to evaluate application uniformity with minimal soil-profile disturbance, we needed to determine whether a discharge value could be derived for previously installed SDI tape without having access to per-emitter flow rates, thereby avoiding complete excavation of SDI tape to access each emitter within the test specimen. Based on the manufacturer's specifications, twenty emitters per drip-tape sample distributes 19.7 L h^{-1} under the recommended operating conditions (Netafim USA, 2010). It was therefore necessary to design and construct a portable field

apparatus that would supply water to the drip-tape samples over a suitable range of operating pressures; in addition, this apparatus needed to be equipped such that the quantity of water distributed through the drip-tape samples could be recorded to within ±2% of actual discharge (ASAE, 2003). The result was a trailer-mounted apparatus with a 12V, low-flow (10.6 L min^{-1}) centrifugal pump (Model 2088; SHURflo, Cypress, CA, USA) to deliver water from a 19-L reservoir to the drip-tape sample (Figure 5.1) and a low-flow pressure regulator in-line with the pump discharge (Figure 5.2). This equipment configuration allowed for sustainable operating pressures from 20 - 310 kPa.

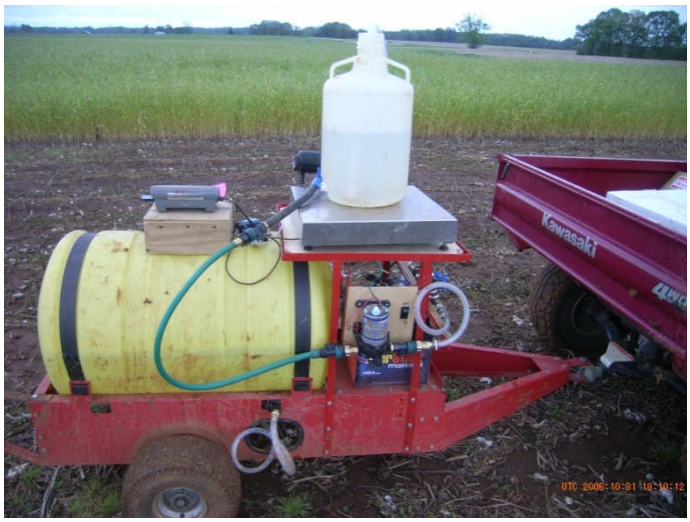

Figure 5.1. Illustration of the portable, in-field SDI testing apparatus. The white vessel atop the bench scale served as the water supply reservoir during testing. The bench scale provided vessel mass, which equated to sample discharge. The 12-volt battery-powered pump was mounted on the side and provided the operating pressure for the SDI sample tested.

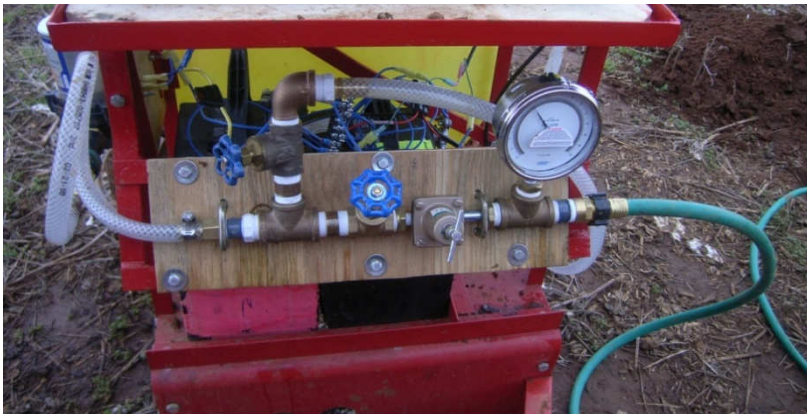

Figure 5.2. Pressure and flow regulation system for the SDI testing apparatus. Most of the water from the pump (left side) was recirculated to the white reservoir (not shown) and remaining water was distributed to the *in-situ* SDI sample section through an adjustable pressure regulator (center right) and the green hose (right side). The gate valve (center left) and the adjustable pressure regulator (center right) served as a means to target and sustain the necessary operating pressure.

Due to power consumption by the water pump and on-board measurement devices, field testing was performed over a relatively short time interval. Apart from initially conditioning the drip line samples at 5- to 15-minute intervals, data collection events were limited to 5 minutes per pressure level tested. Because of this limitation, the design criteria for the apparatus required that a method of measuring a small flow rate (approx. 1.64 L 5 min^{-1}) be incorporated. In order to obtain the temporal resolution of data collection, we devised a method of measuring the water mass as it was distributed to the drip line. A water vessel was placed atop a 100-kg capacity, 0.02-kg resolution digital bench scale (model B100S platform with model CD-11 indicator, software ver. 1.22; Ohaus Corp., Pine Brook, NJ, USA) during tests (Figure 5.1). Water mass (kg) was converted into a volumetric value (mL) and then into an equivalent sample discharge rate per emitter given the number of emitters per unit length of tape tested.

Operating pressure had to remain constant during each test, yet pressure settings needed to be adjustable from test to test. Pressure regulation was achieved using a 2-way

brass-body adjustable pressure regulator (Model 26A; Watts Regulator Co., No. Andover, MA, USA), capable of adjusting from 21 to 344 kPa pressure range (Figure 5.2). An analog precision pressure gauge (Type 332.54; F.N. Cuthbert, Inc., Toledo, OH, USA) was installed immediately after the pressure regulator, the gauge served primarily as a quick approximation of operating pressure. More accurate pressure monitoring was achieved through two digital pressure sensors (Model 1501B02EZ50PSIG; PCB Piezotronics, Depew, NY, USA) capable of detecting a pressure range from 0 to 344 kPa with an accuracy of ±0.15%. Each pressure sensor was installed at either end of the drip-line sample via plastic fittings that were compatible for connection to the drip line (Figures 5.3a and 5.3b). Pressure-sensor readings were relayed wirelessly from data loggers (Model CR206, PakBus software; Campbell Sci., Logan, UT, USA) to a Topcon X20 field computer (Windows XP platform; Topcon Positioning Systems, Inc., Livermore, CA, USA) mounted on the apparatus. A real-time sensor-monitoring software program (LoggerNet 3.4.1; Campbell Sci., Logan, UT, USA) was installed on the X20 computer to allow an operator to view instantaneous operating pressure exhibited on the drip-tape sample. (Equipment specifications are listed in Appendix H.)

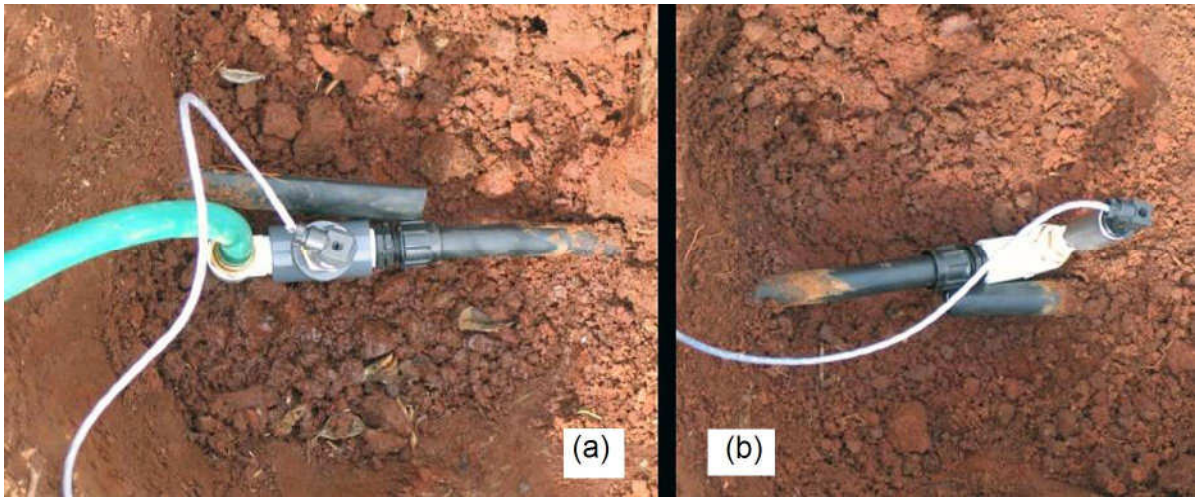

Figure 5.3. Pressure sensors located at the (a) upstream and (b) downstream ends of the drip-tape being sampled.

5.4.3 LABORATORY TESTS FOR SDI TESTING APPARATUS

To validate discharge data obtained from the apparatus, laboratory tests were performed with new SDI product identical to that in the field plot. Emitter uniformity was evaluated for a random sample of 100 contiguous emitters in order to calculate the CV under 48, 83, 117, and 138 kPa operating pressures, adapted from clause 8.2 of ASAE S553 (2008). Tape-section preparation involved >15 min of conditioning at four operating pressures. Operating pressures were monitored via the aforementioned pressure transducers installed upstream and downstream of the drip-tape sample. The drip-tape sample was suspended above the laboratory floor, 152 cm over an array of 100, 240-mL plastic cups. Tests were replicated three times at each pressure level. Discharge values were tabulated and compared in MS Excel 2007, and CVs were computed according to ASAE S553 (2003). Differences in discharge values according to pressure were analyzed using GLM procedure and separated according to Tukey's Studentized Range (SAS Institute, Cary, NC, USA).

5.4.4 FIELD PREPARATIONS

For the field tests, a 3x2 randomized complete block design was developed to select potential sampling locations ranked according to field slope classes (0-2%, 2-4%, and >4% rise) and irrigation-system use frequency ("irrigated" versus "non-irrigated" treatment) with three replications. Topographic data were collected utilizing a Trimble survey-grade, real-time kinematic (RTK) Global Positioning System (GPS) receiver, capable of elevation information within 5 cm relative accuracy (Trimble Navigation, Sunnyvale, CA, USA). The GPS receiver was mounted to an ATV, and position data were recorded on a 2- to 3-m spacing; position data were then imported into ArcGIS ver. 9.3 (ESRI, Redlands, CA, USA) for mapping and further analyses. To classify the test plot according to slope, geospatial data were interpolated first into a digital elevation model (DEM) via 3D Analyst Tools / Raster Interpolation / Topo to Raster function, and then into a slope model via 3D Analyst Tools / Raster Surface / Slope function (Figure 5.4).

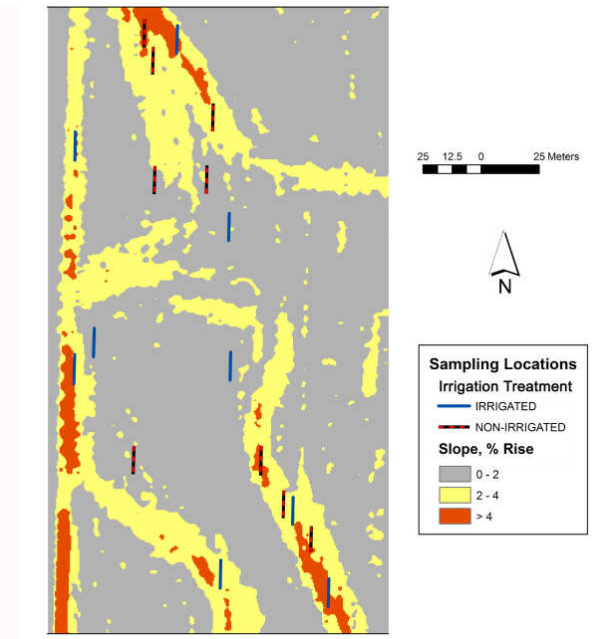

Figure 5.4. Depiction of test plot with respect to slope categories, represented as percent rise. Sampling locations represent 12.2-m drip-line segments blocked according to "irrigated" versus "non-irrigated" treatment effect and slope category.

To clarify the meaning of irrigation-system use frequency, since the experimental plot's inception (fall 2003), a concurrent field experiment involved evaluation of treatment effects ("irrigated" versus "non-irrigated") on an independently-conducted long-term seasonal cotton crop (see Appendix Q). While the entirety of the plot was equipped with SDI tape, only those portions of the system pertaining to the "irrigated" treatment were operated during the growing season according to site-specific pan-evaporation estimates. The portions of the system pertaining to the "non-irrigated" treatment variable were only operated during spring maintenance cycles which involved a sustained clean-and-flush. From a concept of SDI longevity, we wanted to test whether irrigated portions of the drip-line system would be more fatigued than the non-irrigated portions of the system with respect to drip-tape sample discharge.

The resulting GIS depiction also served as a navigational aid during field testing. The map of sampling locations was uploaded into a handheld differential GPS (DGPS) mapping device with a nominal sub-meter horizontal accuracy (Trimble Navigation, Sunnyvale, CA, USA). This device allowed for easy navigation to all sampling locations.

5.4.5 FIELD INVESTIGATIONS

Field investigations were conducted in mid-April, 2009, prior to crop planting. Approximately two weeks earlier, an annual spring maintenance cycle was performed for the SDI system, which consisted of flushing the laterals and running the system uninterrupted for several days in order to locate and repair obvious leaks before the growing season. As a result, the SDI system performance was deemed optimum in mid-April. At each sample location, a small volume of soil was excavated so as to reveal approximately 30 cm of drip line at points along the drip line that were 12.2-m apart; this method would result in 20 contiguous emitters being tested. While the emitters were spaced 0.6-m, an emitter was not always visible after excavation; where an emitter was uncovered, the soil was further excavated so as to not include any exposed emitter in the test. The justification for this action was that application uniformity may have been impacted by the immediate soil microenvironment around the buried emitters, and we wanted to maintain that potential integrity during testing. The drip line was severed at both ends of the 12.2-m test section in order to install the necessary plumbing and pressure transducers for interaction with the testing apparatus (Figures 3a and 3b).

The isolated test section was charged with water from the apparatus for approximately 15 minutes at the first pressure reading of 48 kPa. Obvious leaks were

repaired during this time in order to reliably determine that the only water being lost from the apparatus was through the buried emitters. Data collection then occurred for a 5-minute period; water reservoir mass was recorded at the beginning and ending of this period, and target operating pressure was maintained via pressure regulation and transducer feedback. Vessel-mass differential was equated to cumulative discharge for that sample. After the 5-minute period expired, water pressure was readjusted to the next desired threshold, and the sample line was conditioned to the new pressure setting for > 5 minutes. This process continued for all four desired pressure levels. When the test was completed for the drip-line sample, the interface was removed, and drip-line couplers were used to reattach the sample to the existing drip line. In addition, position readings were recorded for the excavated locations using the RTK GPS system. Positions were recorded for two reasons: 1) to provide documentation of accurate locations of the line couplers for maintenance records, and 2) to provide a "ground-truth" solution to the accuracy of the slope model derived through GIS.

Emitter discharge equivalents for drip-line samples were subjected to GLM procedure and separated according to Tukey's Studentized Range (SAS Institute, Cary, NC, USA) to evaluate differences among operating pressure, irrigation use and field slope effects. Flow-rate versus pressure curves were produced using MS Excel 2007.

5.5 RESULTS AND DISCUSSION

5.5.1 LABORATORY INVESTIGATIONS

At a constant operating pressure of 117 kpa, mean emitter discharge rate was measured for the horizontal drip-tape sample at 1.04 L h^{-1} and 1.06 L h^{-1} for the sloped

sample (CV=3.7% for both conditions); the emitter discharges in both cases were not statistically different (p=0.8081) from one another. Results from variable-pressure tests are presented in Table 5.1. Results indicated that operating pressure significantly affected emitter discharge rate (p=0.0024). Only the discharge at the 48 kPa pressure differed from the other pressures tested by approximately 0.010 L h^{-1}. Because the resolution of per-emitter discharge testing was 1 mL $emitter^{-1}$ $(5\ min)^{-1}$, statistical differences between pressure levels should be regarded as tenuous. For all four operating pressures, the observed mean emitter discharge rate did not exceed ±10% of the nominal discharge rate of 0.984 L h^{-1} (Netafim USA, 2010).

Table 5.1. Emitter discharge rates (L h^{-1}) over a range of operating pressures on 20 contiguous emitters subjected to a 6-percent slope rise (laboratory conditions).

Operating Pressure (kPa)	Mean Emitter Discharge Rate (L h^{-1})[a]	Change from Nominal Rate (%)[b]	Avg. CV (%)
48	1.052 a	+7.3	4.3
83	1.041 b	+6.2	4.3
117	1.043 b	+6.4	4.3
138	1.043 b	+6.4	4.0

[a] Mean separation according to Tukey's Studentized Range. Discharges with the same letter are not significantly different (α<0.05).
[b] Nominal rate = 0.984 L h^{-1} from manufacturer specifications (Netafim USA, 2010).

5.5.2 LABORATORY INVESTIGATIONS OF SDI TESTING APPARATUS

Results from laboratory tests are summarized in Table 5.2. Pressure response was a significant factor (p=<0.0001) in per-emitter sampling. Per-emitter sampling revealed a 0.016 L h^{-1} difference between 48 and 138 kPa, a similarity between 48 and 83 kPa, and a similarity between 83 and 117 kPa (α=0.05). Laboratory emitter discharge rate across all pressure levels was 1.036 L h^{-1}. That value, with a ±5% margin of error, was used as a

baseline performance value in making field management decisions regarding *in-situ* product performance with respect to drip-tape sample discharge.

Table 5.2. Per-emitter and apparatus discharge values over a range of operating pressures on 100 contiguous emitters utilizing SDI testing apparatus (laboratory conditions).

Operating Pressure (kPa)	Mean Emitter Discharge (L h^{-1})[a]	CV (%)	Mean Apparatus Discharge (L h^{-1})[a,b]	SD Apparatus Discharge (L h^{-1})	Change from Emitter Discharge (%)
48	1.028 c	4.8	1.032a	0.012	+0.4
83	1.035 bc	5.0	1.032a	0.012	-0.3
117	1.036 b	5.5	1.032a	0.000	-0.4
138	1.044 a	5.0	1.040a	0.007	-0.4

[a] Mean separation according to Tukey's Studentized Range. Discharges (per column) with the same letter are not significantly different ($\alpha<0.05$).
[b] Derived from kilograms water emitted through drip-tape sample.

Pressure response was not a significant factor ($p=0.5376$) in influencing sample discharge rate utilizing laboratory data derived from the apparatus (Table 5.2). More importantly, apparatus equivalents derived through this process varied less than one-half percent from per-emitter discharge averages. The small variation between per-emitter values and apparatus equivalents provided strong evidence for validating that the testing apparatus could be utilized for estimating *in-situ* drip-line discharge throughout the field.

For the laboratory study, discharge values were recorded for equal to or greater than 95% of the emitter population. On occasion, cups were either misplaced so as to not catch the discharge, or cups were knocked over before a volume could be recorded. Therefore, each replication had between 95 and 100 emitters that contributed to the mean emitter discharge rate and CV. Consistently throughout all laboratory tests, CV was higher than that stated by the manufacturer of 2.5% (Netafim USA, 2010). One explanation for this discrepancy is that CV, measured as standard deviation of a single

emitter's discharge over the same emitter's mean discharge rate, did not exceed 2.5% for above tests. The calculation method of CV we employed was measured as standard deviation of *all contiguous emitters per drip-tape sample* over the mean discharge rate of same. Clause 8.2 of ASAE S553 (2008) may be interpreted to justify either scenario; however, we believe that our method is more useful from a product-evaluation standpoint, as an end-user would be more concerned with application uniformity for a population of emitters rather than individual emitters.

5.5.3 FIELD INVESTIGATIONS

The interaction between operating pressure and system use frequency affected equivalent emitter discharges ($p=<0.0001$). Results are presented in Table 5.3. Lowest discharge was observed for the irrigated SDI product operating at 48 kPa. Six of the eight classifications were not statistically different ($\alpha=0.05$) from one another. Emitter discharge estimates were within ±5% of baseline discharge rate determined from earlier laboratory evaluations, except for irrigated samples operating at 48 kpa (-7%).

Table 5.3. Mean emitter-discharge-equivalent values (L h^{-1}) on 20 contiguous emitters utilizing SDI testing apparatus (field conditions). Values from sites 2 and 9 were omitted from the analysis.

System Use Frequency	Operating Pressure (kPa)	Mean Equivalent Discharge (L h^{-1})	Significance[a]	SD Discharge (L h^{-1})
Irrigated	48	0.967	c	0.082
	83	1.040	ab	0.054
	117	1.064	ab	0.042
	138	1.073	a	0.039
Non-Irrigated	48	1.025	b	0.042
	83	1.043	ab	0.051
	117	1.032	ab	0.019
	138	1.043	ab	0.026

[a] Mean separation according to Tukey's Studentized Range. Discharges with the same letter are not significantly different ($\alpha<0.05$).

Surface-slope modeling was not an accurate depiction of anticipated drip-tape slope. Essentially, the calculated surface-slope model served as a reasonable three-dimensional representation of the field, but the drip-line orientation could be better described in a two-dimensional sense. As the GIS model interpolated slopes between neighboring locations, slope trends were spatially distributed in a 360-degree "view" across the ground surface; however, the drip-line orientation was spatially fixed in two directions opposite to one another. The result was that the slope model, while depicting a given slope in a given area, did not accurately indicate the estimated slope relative to the orientation of the drip tape. Drip-tape samples exhibited slope between 0.3 to 1.9 percent rise; unfortunately, the drip-tape samples collected in the field were unbalanced in regards to the original experimental design, so no proper evaluation of the effect of slope on product performance could be conducted.

Equivalent-discharge data from three testing sections were beyond ±5% of baseline discharge estimate (Figure 5.5) which would warrant further investigation in a diagnostics setting. For example, at site 2, a pin-hole leak appeared during the 83-kPa test, and the leak was not repaired until the final pressure test was concluded; the trend line illustrates the fact that a non-pressure-compensated emission was present. Also, sites 9 and 11 depict potential emitter under- and overwatering, respectively. Having the ability to document flow-rate estimates offers the potential benefit of utilizing this procedure and equipment as a site-specific diagnostic tool for *in-situ* SDI performance.

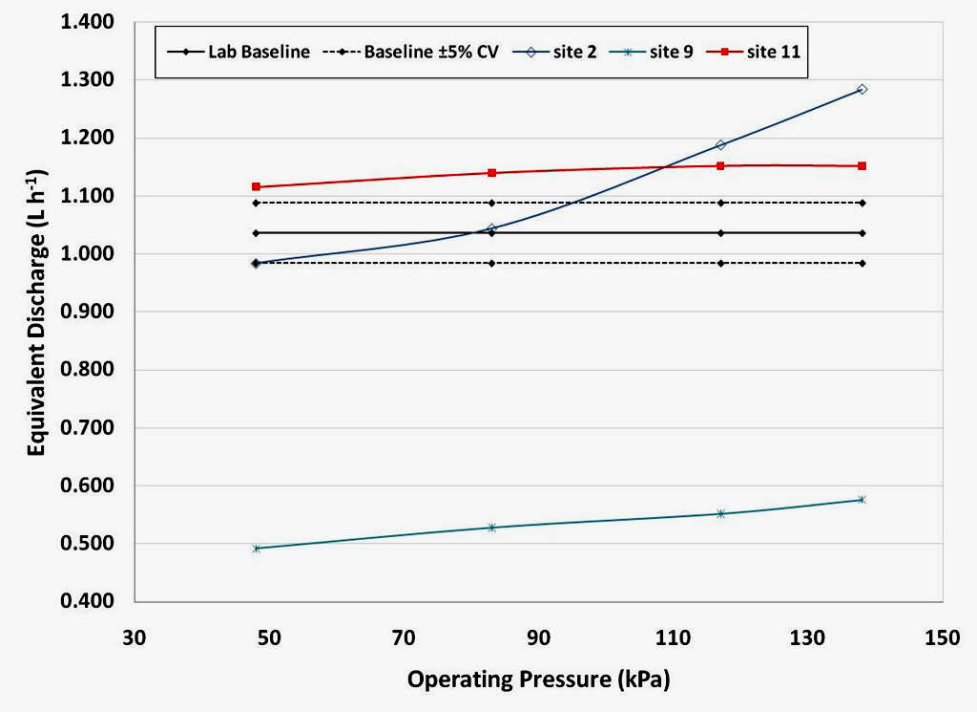

Figure 5.5. Pressure-versus-equivalent-discharge curves for three SDI samples. Per-emitter discharge witnessed from product evaluation in a laboratory setting ("Baseline") is represented as 1.036 L h^{-1} ±5% margin.

One example of how this "site-specific" SDI diagnostics tool can be integrated with supplemental GPS and/or GIS information is represented in Figure 5.6. Cotton is

the marketable crop for this experimental plot, and spatial yield data as bales/ha lint from the 2008 growing season were collected using a yield monitoring system. Referring to the Site 9 example from above, in which the estimated discharge was 48 percent lower than the expected, baseline value, lint yield for the treatment block that contained the Site 9 sample averaged 1.12 bales/ha, while the mean yield for all eight irrigated plots was 1.26 bales/ha. However, summary yield data in the immediate vicinity of Site 9 indicated that 1.26 bales/ha was produced, and the mean yield witnessed in the vicinity of irrigated drip-line samples was 1.29 bales/ha. In addition, the lowest yield observed at an irrigation-active sampling location was 1.09 bales/ha at Site 6, a sample with estimated discharge that corresponded with other drip-line samples. While the implications with the available data suggested that other factors may be contributing to yield variability, site-specific irrigation variability cannot be ruled out for certain locations within the plot. Regardless, the estimated discharge observed with the SDI testing apparatus, along with spatially-referenced yield data, suggests that the drip tape had some degree of clogging for that drip-tape lateral.

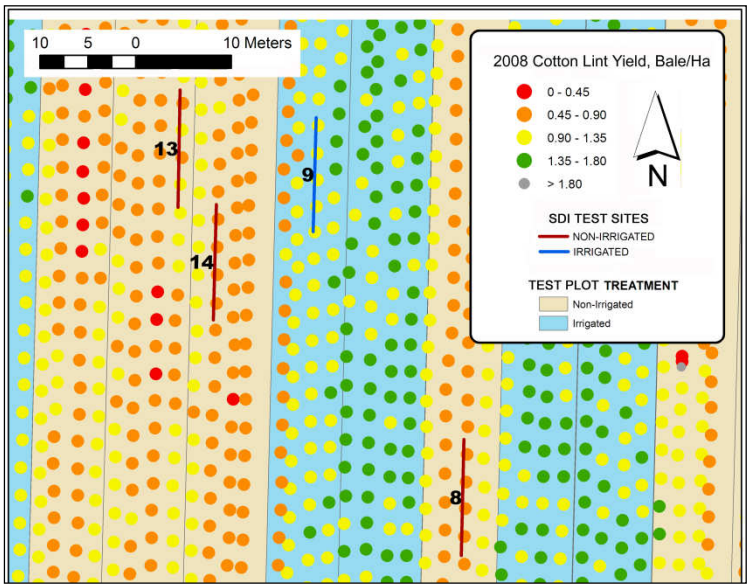

Figure 5.6. Illustration of drip-tape testing sites corresponding to cotton lint yield. Yield variability is suggested in the vicinity of the SDI sample labeled as site "9"; average estimated emitter discharge at site 9 was 0.54 L h^{-1}, which is 48% less discharge than that stated by the manufacturer.

5.5.4 CONSIDERATIONS FOR CONTINUING RESEARCH

For future SDI research, the potential for field product evaluation has been demonstrated using an SDI testing apparatus that can interface with a drip-tape test section over time. As the drip product is used over time, performance could be documented to derive effective or useful design life of the product. This testing technique could be a highly-desirable planning tool for SDI users and researchers. Recommended follow-up studies include larger or smaller drip-tape samples to evaluate precision of the testing apparatus and procedures. Moisture-variation studies can be used to further characterize the site by combining soil-moisture sensors or other moisture-monitoring equipment.

5.6 SUMMARY

In-situ subsurface-drip irrigation performance was evaluated using a mobile, trailer-mounted apparatus consisting of a water reservoir, a digital bench scale, a low-flow centrifugal pump, and a pressure regulator. Laboratory tests were conducted to evaluate behavior of an agricultural SDI product using the portable testing apparatus. Surface terrain and lateral locations were compiled in a GIS program to select representative portions of SDI laterals for field analyses. While laboratory per-emitter discharge values were not statistically different as a function of slope from 0% to 6% ($p=0.8081$), values were typically greater than the discharge of 0.984 L h^{-1} stated by the manufacturer and within ±10% of the manufacturer's value. Operating pressure was found to be a significant factor in per-emitter discharge for SDI tape samples containing twenty emitters ($p=0.0024$) and 100 emitters ($p=<0.0001$), but mean comparisons were not large enough to be considered practical. Mean equivalent discharge determined using the testing apparatus agreed to within 0.5 percent of laboratory results, validating the testing apparatus. Slope effect could not be verified in the field, as observed drip-tape slope did not correspond to surface-slope estimates. Drip-tape discharges were affected by an interaction between operating pressure and irrigation-system use frequency ($p=<0.0001$). The lowest discharge was observed for the irrigated SDI product operating at 48 kPa pressure. Mean discharges from non-irrigated SDI product were not statistically different ($\alpha=0.05$) from irrigated product operating at 83 and 117 kPa. Emitter discharge estimates were within ±5% of baseline discharge rate determined from

laboratory evaluations using 100 emitters (1.036 L h^{-1}), except for irrigated samples operating at 48 kpa. Pressure-versus-discharge curves for three SDI samples indicated the possibility of substandard discharge. By combining sample discharges with supplemental spatially-related information about the laterals (like cotton lint yield), variability in the cropping system can be more fully investigated with regard to precise application of water and nutrients in a field situation.

CHAPTER SIX

CONCLUSION

6.1 CONCLUSIONS

Utilizing total-station technology to document guidance system signal performance was deemed practicable. Site preparation has to be made favorable for the line-of-sight limitations of the total station, and site-specific permanent monumentation must be constructed in order to relate each cross-track error (XTE) dataset to the same terrestrial frame of reference over time. Provided that line-of-sight is not violated, the potential exists for researchers to accurately track the movements of guidance-system-enabled agricultural vehicles over a variety of field conditions, driving speeds, and driving patterns. From an office-processing perspective, two different methods of recording XTE were developed: mathematical rotation of positioning coordinates relative to a regression-line model of the drive path, and offset distance calculation from a terrestrial-based line model in GIS software. Either method may be considered worthy from a research point of view; however, the intuitive nature of using a terrestrial-based line model makes the GIS approach the more desirable option. Utilizing a tracking prism on the target vehicle means accounting for potential positioning error resulting from pitch and roll of the moving vehicle; developing a slope and aspect model of the terrain is one method of quantifying perceived pitch and roll of a vehicle as it traverses the field. As

the test site used in this study had no major slope undulations in the direction of travel, tilt corrections did not significantly improve cross-track error values.

The next objective regarding guidance-system performance was to quantify short-term and long-term accuracies of the four correction signals tested, with the hypothesis that long-term error would quantify the drift phenomenon. RTK correction offered very accurate XTE throughout the durations of each study. Drive path orientation (north-to-south versus east-to-west) had an effect on XTE for RTK, SF2, and WAAS corrections; SF1 was consistent regardless of orientation. XTE derived under SF1 and WAAS correction were more representative of typical manufacturer's claims. Per-event XTE values served as a more instantaneous estimation of signal repeatability, and I believe the variability that is associated from one testing event to the next is what operators are referring to when they talk about "drift" of the guidance system. However, a simpler statistical quantifier of absolute accuracy was unsigned short-term and long-term 95% probability.

Regarding the subsurface-drip irrigation (SDI) performance evaluation, the methodology and principles discussed provide an innovative way of determining SDI product performance in as unobtrusive a manner as possible for field conditions. Because the principle behind the constructed testing apparatus involved using differences in water mass over time to equate per-emitter flow rate, the testing apparatus provided a precise, site-specific SDI flow-rate analysis that agreed to within a half percent of per-emitter discharge tests conducted in the laboratory. For the Netafim® pressure-compensating product being evaluated, lowest discharge was observed for the irrigated SDI product operating at 48-kPa pressure. All discharges from non-irrigated SDI product and from

the irrigated product operating at 83 and 117 kPa (12 and 17 psi) were not statistically different (α=0.05) from one another. Emitter discharge estimates were within ±5% of baseline discharge rate determined from laboratory evaluations (1.036 L h^{-1}), except for irrigated samples operating at 48 kpa (-7% from baseline). Because one drip-line sample had substantially lower flow rate than other samples tested, geospatially-linked cotton yield data was compared relative to the location of the drip-line sample; evidence indicated that yield was affected by reduced SDI output in that location.

6.2 Opportunities for Future Research

Regarding guidance-system testing, several potential research opportunities are available. While the slope and aspect models of the test site were used to estimate potential roll and pitch of the testing vehicle, other means of capturing vehicle roll and pitch should be considered, such as gyroscopic devices or accelerometers. While the guidance systems used for this study provided some form of internal self-correction through pitch and roll, this information was not available for supplemental collection to compare "observed" prism tilt from "expected" prism tilt. Therefore, other guidance systems must either have the capability of providing roll/pitch information to an outside source (like a data logger), or supplemental accelerometers would have to be installed on the target prism. With vehicle pitch/roll information, it may also be possible to mount the target prism in a more accessible location on the vehicle to reduce line-of-sight total-station limitations, such as on the vehicle roof. Such a procedure would also involve some form of synchronizing the prism tilt with the instant at which the target prism is observed by the total station.

For the 2006 and 2007 studies, testing intervals were not as uniform as initially desired. As has been noted from previous research and confirmed through this project, guidance-system accuracy can be affected by time of day. A more precise way of describing this phenomenon may be to conjecture that guidance-system accuracy can be affected by satellite geometry and availability. While Dilution of Precision (DOP) values (particularly Horizontal DOP or Position DOP) are often regarded in the GPS community as a measure of satellite geometry, synchronizing testing events with predicted DOP values may provide a more apples-to-apples comparison of system performance over time. Relating to this topic, the concept of sidereal time refers to the amount of time that a celestial object returns to its original position relative to reference points on Earth; instinctively, one may think that 24 hours constitutes sidereal time, but the GPS constellation has a slightly smaller interval of time than 24 hours. For sake of simplicity, this would suggest that, if a GPS sidereal day is 23 hours instead of 24 hours, a truer replication of a testing event from a previous test may require testing one hour earlier on the second day than the first day, as the GPS constellation would be more consistent throughout the two tests.

For the SDI testing, the methodology presented provides for potential continued product evaluation in terms of sample discharge, as the locations for each interface were documented with accurate positioning equipment, and the SDI testing apparatus can easily interface with the same drip-tape sample over time. As the product ages, reductions in discharge uniformity could be documented accordingly in order to derive an estimated “design life” of the product, which would be a highly-desirable planning tool for SDI users. Further moisture-variation studies can be supplemented by the site-

specific nature of this application, by combining soil-moisture meter data or other moisture-monitoring equipment, in an effort to capture the nature of water movement in the localized soil zone. Also, while one of the motivating factors behind this SDI research was to explain whether certain locations exhibiting within-plot variability existed for the test plot from SDI-emission variability, this evaluation was not specifically conducted.

6.3 FINAL CONSIDERATIONS

Using a total station to document guidance-system performance is, in my opinion, a worthwhile technique to continue. For researchers that wish to evaluate dynamic accuracy, yet may have limited acreage in which to perform large drive tests, a total station is ideal. While the accuracy of our total station was not considered accurate enough to evaluate the RTK correction, the total station would be sufficient to evaluate other available correction signals. Also, while the total station provided 5-mm accuracy in the tracking mode, some of the claims about RTK performance can still be validated regarding excellent accuracy (centimeter level) and repeatability over time, and I would ultimately recommend that farmers invest in this correction signal if their intent is to maintain any row-cropping system. Utilizing RTK correction is an expensive investment initially, but ways exist to reduce costs by utilizing other civilian-owned or government-owned reference stations to obtain an RTK solution. Also, from a producer's perspective, practical positioning accuracy is not only related to how well the vehicle follows a line, but also how well the *implement* follows the same line. If the farming "system," meaning

the vehicle plus the implement, has a limiting performance error of >5 cm, then our total station may be considered as an appropriate measurement tool.

The need exists for researchers and industry to agree on a dynamic testing standard. When quantifying guidance accuracy, there is not one single value that can be offered at this time to describe, in plain language, just how well a guidance system performs. GPS-based dynamic accuracy is a complex topic; many variables contribute to positioning error from a static-observation perspective alone, and when the GPS/GNSS receiver is in motion, additional error sources exist. While my desire was to derive a statistical term for "drift," with one value to capture the fact, the topic is too complex to currently reach that goal.

The techniques presented for *in-situ* SDI evaluations are simple, repeatable, and the values are easily understood. I believe the limiting factor regarding the testing apparatus was its power-consumption and the resolution of the bench scale; however, the premise of *in-situ* uniformity testing is sound, and I would recommend to other researchers that this concept be expanded upon over a range of drip-tape products, operating pressures, fluid temperatures, and fertigation/effluent mixes.

REFERENCES

Adamchuk, V. I., R. M. Hoy, G. E. Meyer, and M. F. Kocher. 2007. GPS-based auto-guidance test program development. Precision agriculture '07: presented at the 6th European Conference on Precision Agriculture, Skiathos, Greece, June 3-6, 2007.

Ayars, J., C. Phene, R. Hutmacher, K. Davis, R. Shoneman, S. Vail, and R. Mead. 1999. Subsurface drip irrigation of row crops: a review of 17 years of research at the Water Management Research Laboratory. *Agricultural Water Management* 42(1): 1-27.

ASAE Standards, 43rd ed. 1996. EP458. Field evaluation of microirrigation systems. St. Joseph, Mich. ASAE.

ASAE Standards. 2008. S553 DEC2000 (R2008): Collapsible emitting hose (drip tape) - specifications and performance testing. St. Joseph, Mich.: ASAE.

ASAE Standards. 2005. EP405.1 FEB03. Design and installation of microirrigation systems. St. Joseph, Mich.: ASAE.

Bell, T. 2000. Automatic tractor guidance using carrier-phase differential GPS. *Computers and Electronics in Agriculture* 25: 53-66.

Bittner, G. 2000. AGRO NAV® autonomous, off-road vehicle navigation and implement control system, using CDGPS and inertial backup. AgEng 2000, *Proceedings of the International Conference on Agricultural Engineering*, Warwick, England. 00-IE-007.

Bryla, D. R., G. S. Banuelos, J. P. Mitchell. 2003. Water requirements of subsurface drip-irrigated faba bean in California. *Irrigation Science* 22(1): 31-37.

Bordovsky, J. P. and D. Porter. 2003. Cotton response to pre-plant irrigation level and irrigation capacity using spray, LEPA, and subsurface drip irrigation. ASAE Meeting Paper No. 032008. St. Joseph, Mich.: ASAE.

Buick, R. 2002. GPS guidance – making an informed decision. *Proceedings of 6th International Conference on Precision Agriculture and Other Precision Resources Management.* Minneapolis, MN, 14-17 July 2002. American Society of Agronomy, Madison, WI.

Camp, C. R., P. J. Bauer, P. G. Hunt. 1997. Subsurface drip irrigation lateral spacing and management for cotton in the southeastern Coastal Plain. *Transactions of the ASAE* 40(4): 993-999.

Camp, C. R., E. J. Sadler, W. J. Busscher. 1997. A comparison of uniformity measures for drip irrigation systems. *Transactions of the ASAE* 40(4): 1013-1020.

Camp, C. R. 1998. Subsurface drip irrigation: a review. *Transactions of the ASAE* 41(5): 1353-1367.

Charlesworth, P. B. and W. A. Muirhead. 2003. Crop establishment using subsurface drip irrigation: a comparison of point and area sources. *Irrigation Science* 22: 171-176.

Deere and Company. 2004. GreenStar™ guidance systems---parallel tracking and AutoTrac assisted steering systems. Moline, Ill.: Deere and Company. Manual OMPC20353: p.146.

Devore, J. and N. Farnum. 2005. Applied statistics for engineers and scientists: second edition. Thomson Brooks/Cole, Belmont, California, USA.

Dougherty, M., A. H. AbdelGadir, J. P. Fulton, E. van Santen, L. M. Curtis, C. H. Burmester, H. D. Harkins, and B. E. Norris. 2009. Subsurface drip irrigation and fertigation for north Alabama cotton production. *Journal of Cotton Science* 13: 227-237.

Downey, D., D. K. Giles, D. C. Slaughter. 2003. Ground based vision identification for weed mapping using DGPS. ASAE Meeting Paper No. 031005. St. Joseph, Mich.: ASAE.

Ehrl, M., M. R. Demmel, H. Auernhammer, W. V. Stempfhuber, W. Maurer, and T. Wunderlich. 2002. Spatio-temporal quality of precision farming applications. ASAE Meeting Paper No. 023084. St. Joseph, Mich.: ASAE.

Ehrl, M., W. V. Stempfhuber, M. R. Demmel, M. Kainz, and H. Auernhammer. 2004. AutoTrac – accuracy of a RTK DGPS based autonomous vehicle guidance system under field conditions. ASAE Publication Number 701P1004.

Ehsani, M. R., M. Sullivan, J. T. Walker, T. L. Zimmerman. 2002. A method of evaluating different guidance systems. ASAE Meeting Paper No. 021155. St. Joseph, Mich.: ASAE.

Ehsani, M. R., M. D. Sullivan, T. L. Zimmerman, T. Stombaugh. 2003. Evaluating the dynamic accuracy of low-cost GPS receivers. ASAE Meeting Paper No. 031014. St. Joseph, Mich.: ASAE.

Enisco-Medina, J., B. L. Unruh, J. C. Henggeler, W. L. Multer. 2002. Effect of row pattern and spacing on water use efficiency for subsurface drip irrigated cotton. *Transactions of the ASAE* 45(5): 1397-1403.

Freeland, R. S., R. E. Yoder, J. T. Ammons, L. L. Leonard. 2002. Mobilized surveying of soil conductivity using electromagnetic induction. *Applied Engineering in Agriculture* 18(1): 121-126.

Freimann, R. 2000. Investigation of position accuracy of an autonomous, off-road vehicle navigation. *AgEng 2000: Proceedings of the International Conference on Agricultural Engineering*. Warwick, England. 00-IE-007ii.

Gan-Mor, S. and R. L. Clark. 2001. DGPS-based automatic guidance – implementation and economical analysis. ASAE Meeting Paper No. 011192. St. Joseph, Mich.: ASAE.

Giles, D. K. and D. Downey. 2003. Quality control verification and mapping for chemical application. *Precision Agriculture* 4(1): 103-124.

Guo, L. S., Q. Zhang, L. Feng. 2003. A low-cost integrated positioning system of GPS and inertial sensors for autonomous agricultural vehicles. ASAE Meeting Paper No. 033112. St. Joseph, Mich.: ASAE.

Han, S., Q. Zhang, H. K. Noh. 2001. Applying filtering techniques to improve GPS positioning accuracy. ASAE Meeting Paper No. 011158. St. Joseph, Mich.: ASAE.

Han, S., Q. Zhang, H. Noh, and B. Shin. 2004. A dynamic performance evaluation method for DGPS receivers under linear parallel-tracking applications. *Transactions of the ASAE* 47(1): 321-329.

Hest, D. 2007. On target? Penton Media, Inc. Available at http:// farmindustrynews.com/ farm-equipment/ precision-farming/ farming_on_target/ . Last accessed February, 2008.

Hurn, J. 1989. GPS: A Guide to the Next Utility. Trimble Navigation, Sunnyvale,CA.

Hurn, J. 1993. Differential GPS Explained. Trimble Navigation, Sunnyvale, CA.

Institute of Navigation (ION) Standards. 1997. Recommended test procedures for GPS receivers, ION STD 101. ION, Alexandria, Virginia, USA.

Lamm, F. R., T. P. Trooien, H. L. Manges, H. D. Sunderman. 2001. Nitrogen fertilization for subsurface drip-irrigated corn. *Transactions of the ASAE* 44(3): 533-542.

Lamm, F. R. and T. P. Trooien. 2003. Subsurface drip irrigation for corn production: a review of 10 years of research in Kansas. *Irrigation Science* 22: 195-200.

Lamm, F. R., A. J. Schlegel, G. A. Clark. 2004. Development of a best-management practice for nitrogen fertigation of corn using SDI. *Applied Engineering in Agriculture* 20(2): 211-220.

Lesikar, B., V. Weynand, and R. Persyn. 2004. Evaluation of the application uniformity of subsurface drip distribution systems. ASAE Publication Number 701P0104.

Li, J., L. Chen, and Y. Li. 2009. Comparison of clogging in drip emitters during application of sewage effluent and groundwater. *Transactions of the ASABE* 52(4): 1203-1211.

Liu, H. and G. Huang. 2009. Laboratory experiment on drip emitter clogging with fresh water and treated sewage effluent. *Agricultural Water Management.* 96(5): 745-756.

Nagasaka, Y., N. Umeda, Y. Kanetai. 2002. Automated rice transplanter with GPS and FOG. *Automation Technology for Off-Road Equipment: Proceedings of the ASAE.* Publication No. 701P0502, pp. 190-195. St. Joseph, Mich.: ASAE.

Navcom Technology, Inc. March 2003. StarFire datasheet. Available at: http://www.navcomtech.com/support/Download/StarFire%20Network_050302-4%20low%20res.pdf. Last accessed April 2010.

Netafim USA. 2010. DripNet PC 875 product specifications. Available at: http://www.netafimusa.com/ files/ literature/ agriculture/ thinwall-dripperline/ DNPC-875.pdf. Last accessed April, 2010.

Noguchi, N., M. Kise, K. Ishii, H. Terao. 2002. Field automation using robot tractor. *Automation Technology for Off-Road Equipment.* Publication No. 701P0502: 239-245. St. Joseph, Mich.: ASAE.

O'Brien, D. M., D. H. Rogers, F. R. Lamm, G. A. Clark. 1998. An economic comparison of subsurface drip and center pivot sprinkler irrigation systems. *Applied Engineering in Agriculture* 14(4): 391-398.

Reid, J. F., Q. Zhang, N. Noguchi, M. Dickson. 2000. Agricultural automatic guidance research in North America. *Computers and Electronics in Agriculture* 25(1): 155-167.

Safi, B., M. R. Neyshabouri, A. H. Nazemi, S. Massiha, and S. M. Mirlatifi, 2007. Water application uniformity of a subsurface drip irrigation system at various operating pressures and tape lengths. *Turkish Journal for Agriculture and Forestry* 31(5): 275-285.

Sharpe, T., R. Hatch, and F. Nelson. 2002. StarFire and real-time GIPSY: a global high-accuracy differential GPS system. Torrance, Cal.: NavCom Technology, Inc. Available at http://www.navcomtech.com/ Support/ Download/ StarFire%20and%20Real-Time%20GIPSY.pdf . Last accessed March 2008.

Song, I., S. Stine, J. Pimentel, C. Y. Choi, C. Gerba. 2003. The role of irrigation and wastewater: comparison of subsurface drip irrigation and furrow irrigation. ASAE Meeting Paper No. 032373. St. Joseph, Mich.: ASAE.

Srivastava, A. K., C. E. Goering, R. P. Rohrbach, and D. R. Buckmaster. 1993. Chapter 6: Precision Agriculture. In Engineering Principles of Agricultural Machines, 2nd ed., p. 123 – 138. St. Joseph, Mich.: ASABE.

Steele, D. D., R. G. Greenland, B. L. Gregor. 1996. Subsurface drip irrigation systems for specialty crop production in North Dakota. *Applied Engineering in Agriculture* 12(6): 671-679.

Stombaugh, T., S. A. Shearer, J. Fulton, R. Ehsani. 2002. Elements of a dynamic GPS test standard. ASAE Meeting Paper No. 021150. St. Joseph, Mich.: ASAE.

Stombaugh, T., D. McLaren, and B. Koostra. 2005. The global positioning system. University of Kentucky Cooperative Extension circular AEN-88. Issued August, 2005.

Sullivan, D. G., J. P. Fulton, J. N. Shaw, and G. Bland. 2007. Evaluating the sensitivity of an unmanned thermal infrared aerial system to detect water stress in a cotton canopy. *Transactions of the ASABE* 50(6): 1963-1969.

Taylor, R. K., M. D. Shrock, J. Bloomfield, G. Bora, G. Brockmeier, W. Burton, B. Carlson, J. Gattis, R. Groening, J. Kopriva, N. Oleen, J. Ney, C. Simmelink, and J. Vondracek. 2004. Dynamic testing of GPS receivers. *Transactions of the ASAE* 47(4): 1017-1025.

Tian, L. 2002. Development of a sensor-based precision herbicide application system. *Computers & Electronics in Agriculture* 36(2): 133-149.

Trimble Engineering. 2001. Trimble 5600 data sheets. Dayton, Ohio: Trimble Engineering and Construction Group. Available at http://www.trimble.com . Last accessed July 2006.

Trimble Surveying. 2007. Trimble survey controller help: version 11.40, revision A. Sunnyvale, California: Trimble Surveying. Available at http:// trl.trimble.com/docushare/dsweb/Get/Document-377255/TSCv1140_Help_ English.pdf. Last accessed April 2010.

Trooien, T. P., F. R. Lamm, L. R. Stone, M. Alam, D. H. Rogers, G. A. Clark, A. J. Schlegel. 2000. Subsurface drip irrigation using livestock wastewater: dripline flow rates. *Applied Engineering in Agriculture* 16(5): 505-508.

Upadhyaya, S. K., G. S. Pettygrove, J. W. Oliveira, and B. R. Jahn. 2003. An introduction – global positioning system. Available at http://www. calspace.ucdavis.edu/Docs/Intro-GPS-Final.pdf . Last accessed March 2008.

Westphalen, M. L., B. L. Steward, and S. Han. 2003. Topographic mapping through measurement of vehicle attitude. ASAE Meeting Paper No. 031008. St. Joseph, Mich.: ASAE.

Wu, C., P. Ayers, and A. Anderson. 2005. Influence of travel directions on the GPS dynamic accuracy for vehicle tracking. ASAE Meeting Paper No. 051088. St. Joseph, Mich.: ASAE.

Yao, H. and R. L. Clark. 2000. Development of topographic maps for precision farming with medium accuracy GPS receivers. *Applied Engineering in Agriculture* 16(6): 629-636.

APPENDIX A

TRACTOR SPECIFICATIONS

A.1. JOHN DEERE 6420 TRACTOR

Figure A.1. John Deere 6420.

Tractor Power:	
PTO rated, kW:	70.3
Engine:	
Manufacturer:	John Deere
Fuel:	Diesel
Aspiration:	Turbocharger with intercooler
Cylinders:	4
Displacement, L:	4.5
Rated engine speed, RPM:	2300
Cooling:	liquid
Oil capacity, L:	15.9
Hydraulic flow rate, LPM:	96
Transmission:	
Type:	Infinitely Variable Transmission
Mechanical:	
MFWD:	Yes
Dimensions:	
Wheelbase, mm:	2400

APPENDIX B

TOTAL-STATION SPECIFICATIONS

B.1 TRIMBLE 5603 TOTAL STATION

Figure B.1. Trimble 5603 Total Station.

Total station specifications:	
Manufacturer:	Trimble
Model:	5603
Firmware version:	696-03.08
Angle measurement:	
Accuracy (standard deviation):	3”
Automatic level compensator:	Dual-axis compensator ±6”
Distance measurement:	
Accuracy (standard deviation), prism:	±(2 mm +2 ppm), standard; ±(5 mm+2 ppm), tracking
Measuring time, prism:	
Standard measurement:	2 s (0.5 Hz)
Tracking:	0.5 s (2 Hz)
Range:	
Under standard clear conditions, 1 prism:	3000 m

B.2 DATALOGGER SPECIFICATIONS

Figure B.2. Trimble TSCe datalogger.

Manufacturer:	Trimble
Model:	TSCe
Part no.:	45185-20
Operating system:	Microsoft Windows CE Version 4.0.12
Internal memory capacity:	16 MB

B.3 DATA COLLECTION SOFTWARE SPECIFICATIONS

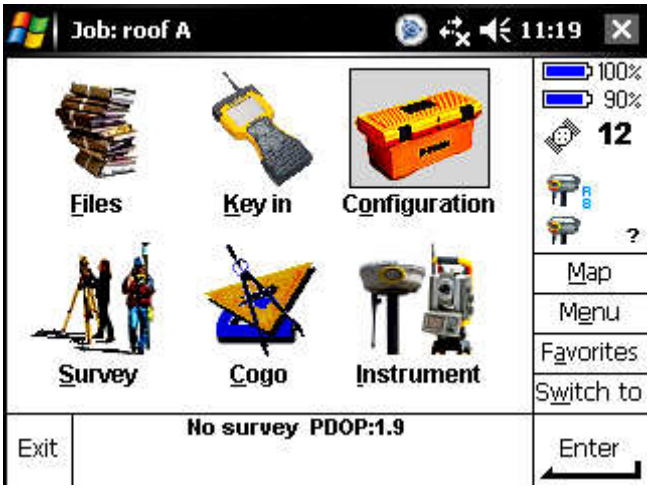

Figure B.3. Trimble Survey Controller.

Manufacturer:	Trimble
Model:	Trimble Survey Controller
Software version:	11.20 – 11.40

APPENDIX C

TARGETING PRISM SPECIFICATIONS

C.1 TRIMBLE RMT PRISM

Figure C.1. Trimble RMT prism.

Manufacturer:	Trimble
Model:	RMT ATS Multi-Channel
Part No.:	571233035
Prism constant, mm:	10
Power supply, V:	12 – 35, external source
Infrared channels:	4

APPENDIX D

GUIDANCE-SYSTEM SPECIFICATIONS

D.1. JOHN DEERE GREENSTAR SYSTEM

Figure D.1. John Deere Greenstar display.

Manufacturer:	John Deere
Model:	Greenstar Mobile Processor
Hardware version:	PF80444 2.5
Software/firmware version:	PF303192F
Loader:	2.30A
Mapping processor software version:	PF301660D
Runtime, hr (until December, 2007):	246.8
Correction signals available:	RTK, SF2, SF1, WAAS

Serial output:

NMEA messages:	GGA, GSA, VTG
Baud:	19200
Output rate:	5 Hz

D.2. JOHN DEERE STARFIRE ITC GPS RECEIVER

Figure D.2. StarFire iTC GPS receiver (yellow dome).

Manufacturer:	John Deere
Model:	StarFire iTC
Hardware part no.:	PF80732
Software app. version:	2.52A
Sofware loader version:	1.04
Position receiver software version:	12.5
Receiver runtime, hr (until December, 2007):	1337.9

Features:

Terrain compensation:	Yes
External port:	RS232 (serial), configurable

D.3. TRIMBLE EZ-GUIDE GUIDANCE COMPUTER

Figure D.3. Trimble EZ-Guide display and accessory GPS antenna.

Manufacturer:	Trimble
Model:	EZ-Guide Plus
Part no.:	52001-00
Software version no. (2007 tests):	4.10.002 Feb 22 2007
11:53:46	

Serial port settings (2007 tests):

Input:	External GPS
Baud:	19200 bps
Parity:	8-N-1
Output rate:	5 Hz

Supplemental information:

For the WAAS drive-path tests in the 2006 study, a Trimble EZ-Guide Plus with accessory GPS antenna was used. The equipment did not include any form of terrain compensation. Also, the EZ-Guide Plus with accessory GPS antenna was loaned to the department on an evaluation basis; at the end of the 2006 tests, the equipment was returned to the owner, and similar equipment was purchased by the department later that year for the 2007 tests. No configuration information was recorded for the equipment bundle used in 2006. For the WAAS drive-path tests in the 2007 study, the accessory GPS antenna was replaced with the John Deere StarFire iTC receiver. Configuration settings in the EZ-Guide computer were adjusted accordingly. In addition, terrain compensation module was available.

D.4. TRIMBLE EZ-STEER ASSISTED-STEERING SYSTEM WITH TERRAIN COMPENSATION MODULE

Figure D.4. Trimble EZ-Steer assisted-steering system.

Manufacturer:	Trimble
EZ-Steer specifications (2007):	
Software version:	3.00.01
Tilt:	Basic
Filter:	Heavy3 (under Terrain Comp.)
Vehicle setup:	
Type:	Tractor 4WD
Steering wheel diameter, in.:	16.0
Angle/turn, deg.:	21
Freeplay left, in.:	1.80
Freeplay right, in.:	1.80
Wheelbase, in.:	95
Engagement:	
Aggressiveness, percent:	120
Minimum / maximum speed, mph:	2 / 15
Maximum angle, deg.:	15
Motor speed:	Auto High
Engage on AB:	On
Minimum number of satellites:	5
Maximum HDOP:	3.0
Features:	
External port:	RS232 (serial), configurable

APPENDIX E

CORRECTION SIGNALS USED IN GUIDANCE-ACCURACY TESTS

E.1 CORRECTION-SIGNAL CHARACTERISTICS

Table E.1. Characteristics of GPS-based correction signals used in 2006 and 2007 tests.

Correction Signal:	**Wide Area Augmentation System (WAAS)**
Type of Correction:	wide-area
Single vs. Dual Frequency:	single frequency
Operating Fee:	free
Accuracy Claims:	±15 to 30 cm pass-to-pass ±61 to 66cm long-term static
Supplemental information:	Service is offered by U.S. government, designed for Federal Aviation Administration (FAA) to offer navigational aid to airplanes; many inexpensive personal navigation devices can utilize WAAS
Correction Signal:	**John Deere SF1**
Type of Correction:	wide-area
Single vs. Dual Frequency:	single frequency
Operating Fee:	free (with compatible John Deere receivers)
Accuracy Claims:	±33 cm pass-to-pass ≈76 cm static
Supplemental information:	SF1 signal is proprietary to John Deere
Correction Signal:	**John Deere SF2**
Type of Correction:	wide-area
Single vs. Dual Frequency:	dual frequency
Operating Fee:	$800 annually
Accuracy Claims:	±10 cm pass-to-pass ≈25 cm static
Supplemental information:	SF2 signal is proprietary to John Deere
Correction Signal	**Real-Time Kinematic (RTK)**
Type of Correction:	local-area
Single vs. Dual Frequency:	dual frequency
Operating Fee:	free (initial set-up costs up to $12K)
Accuracy Claims:	≤3 cm pass-to-pass ≤3 cm static
Supplemental information:	RTK procedure employs two dual-frequency receivers; one is located at a fixed location (“base”), while the other travels with the vehicle (“rover”); most install costs come from 2nd receiver purchase

APPENDIX F

GUIDANCE TESTING SITE ONE

F.1 GUIDANCE TESTING SITE ONE

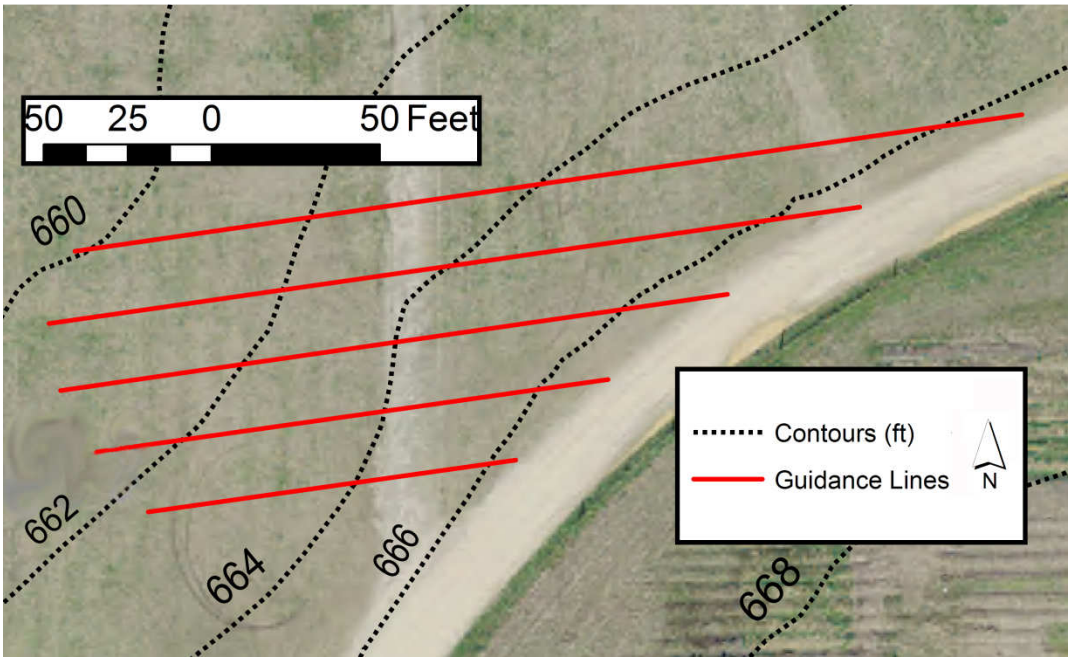

Figure F.1. Guidance testing site one, used in 2006. Elevation contours are in 2-ft (0.6-m) intervals; guidance lines are spaced 20 ft (6.1 m). Direction of vehicle travel was westerly to easterly (approx. 80.1 degrees azimuth from true north; aerial imagery and contour data courtesy of City of Auburn GIS Department, Auburn, AL).

APPENDIX G

GUIDANCE TESTING SITE TWO

G.1 GUIDANCE TESTING SITE TWO

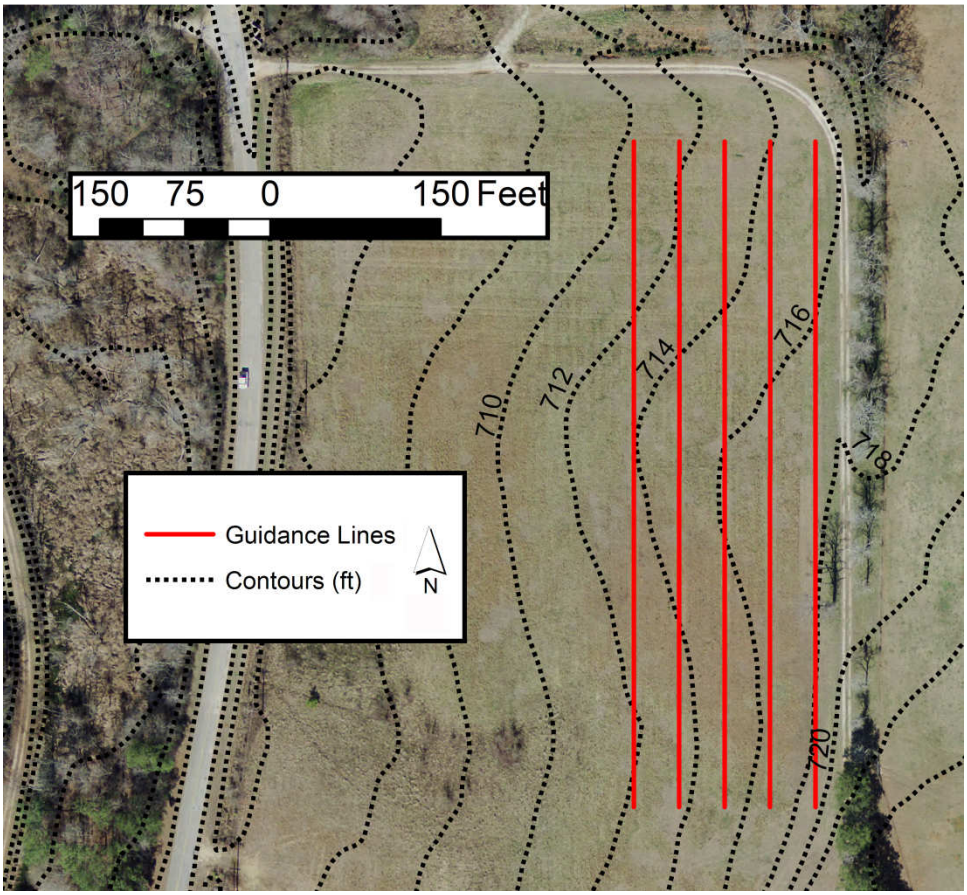

Figure G.1. Guidance testing site two, used in 2007. Elevation contours are in 2-ft (0.6-m) intervals; guidance lines are spaced 40 ft (12.2 m). Direction of vehicle travel was northerly to southerly (approx. 179.4 degrees azimuth from true north; aerial imagery and contour data courtesy of City of Auburn GIS Department, Auburn, AL).

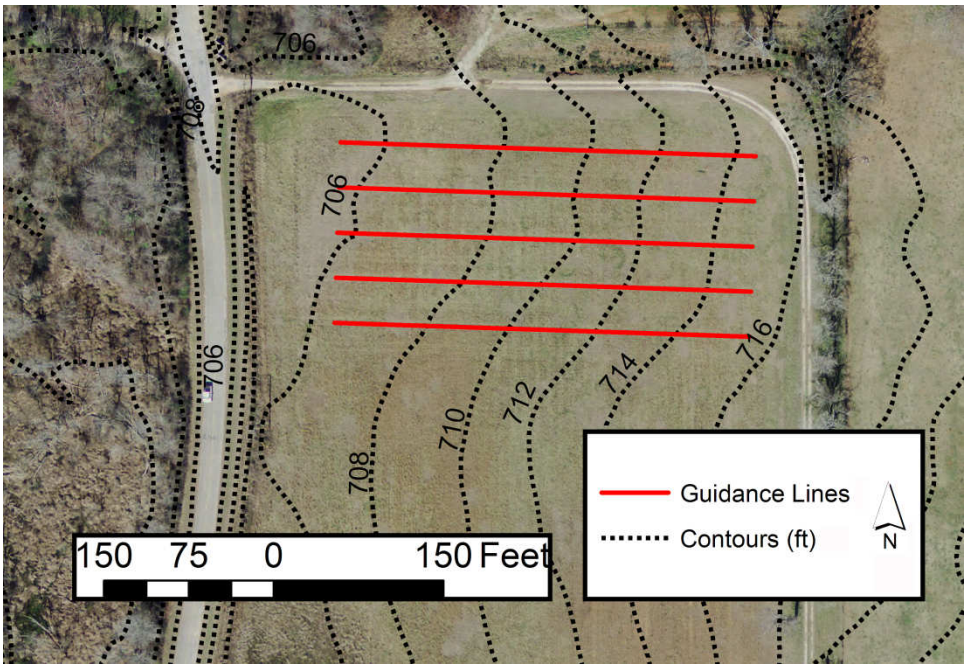

Figure G.2. Guidance testing site two, used in 2007. Elevation contours are in 2-ft (0.6-m) intervals; guidance lines are spaced 40 ft (12.2 m). Direction of vehicle travel was easterly to westerly (approx. 271.3 degrees azimuth from true north; aerial imagery and contour data courtesy of City of Auburn GIS Department, Auburn, AL).

APPENDIX H

SDI TESTING APPARATUS PARTS

H.1. 12-VOLT PUMP

Figure H.1. Shurflo diaphragm pump.

Manufacturer:	Shurflo
Model:	2088
Type:	3 chamber diaphragm
Flow rate, gpm:	2.8
Electrical motor:	12VDC, intermittent-duty
Maximum amps:	7.0
Priming:	Self-priming to 9 ft.
Ports:	½”-14 NPSM-Male
Dimensions (L x W x H), in.:	7.8” x 5.0” x 4.6”
Net weight, lb.:	5

H.2 PRESSURE REGULATOR

Figure H.2. Watts adjustable small-pressure regulator.

Manufacturer:	Watts Regulator
Model:	26A
Operating range, psi:	3 – 50
Ports:	¼", Female
Materials:	
Body:	Brass
Spring Cage:	Aluminum
Disc:	Buna-N stainless steel
Diaphragm:	Reinforced Buna-N

H.3 DIGITAL BENCH SCALE

Figure H.3. Ohaus CD-11 indicator (scale platform not shown).

Manufacturer:	Ohaus
Model:	
Indicator:	CD-11
Bench scale:	B100S
Scale capacity, kg:	100
Resolution, kg:	0.02
Indicator software version:	1.22

H.4 PRESSURE TRANSDUCER

Figure H.4. PCB pressure transducer.

Manufacturer:	PCB Piezotronics
Model:	1501B02EZ50PSIG
Output:	Amplified 0 – 5 VDC FS
Supply voltage:	6.5 – 30 VDC
Accuracy:	± 0.25% FS
Response time:	≤ 1 ms
Pressure port:	¼" – 18 NPT, Male
Electrical connection:	Solder tabs; power, signal, ground
Pressure range:	0 – 50 psig

H.5 DATA LOGGER

Figure H.5. Campbell Scientific CR206 datalogger.

Manufacturer:	Campbell Scientific
Model:	CR206
Operating system:	PakBus protocol
Operating frequency of internal spread-spectrum radio:	900 MHz
Power supply, external:	12 VDC
Communications port:	RS232 (serial)
Sensor input channels:	
Analog, 0 – 5 V, single-ended:	5
Pulse counter:	2
Switched excitation:	2
Digital I/O:	2

H.6 RADIO MODEM

Figure H.6. Campbell Scientific RF401 radio modem.

Manufacturer:	Campbell Scientific
Model:	RF401
Operating frequency:	910 - 918 MHz
I/O data rate:	9600 bps
Power supply, external:	9 to 16 VDC
Communications port:	RS232 (serial)

H.7 TOPCON X20 FIELD COMPUTER

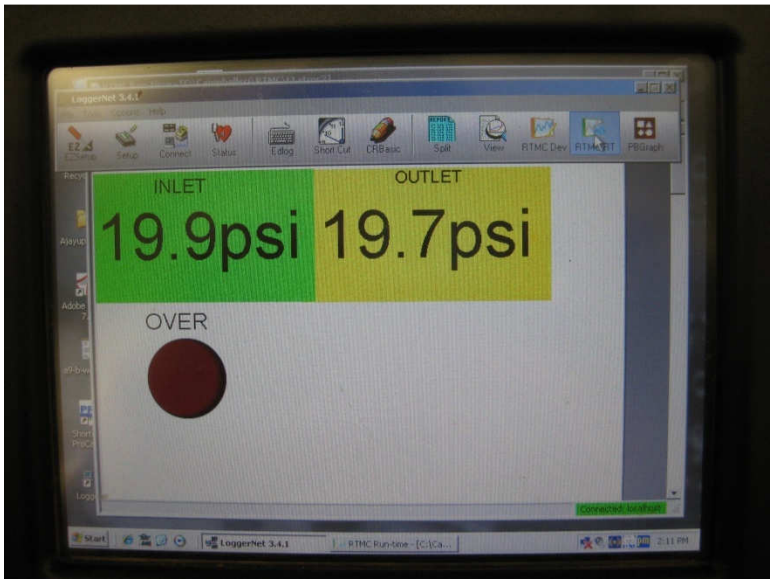

Figure H.7. X20 field computer screen shot illustrating pressure-monitoring software.

Console:

Processor:	1 GHz
Memory:	512 Mb
Operating system:	Windows XP Pro SP2
Display size:	213 mm (8.4 in.)
Solid state drive:	4 GB
Mounting bracket:	RAM mount
USB ports:	4 x USB 2.0
Serial RS232 ports:	4
PS2 ports:	2
VGA ports:	1
10/100 Base T Ethernet port:	1

Pressure-monitoring software:

Manufacturer:	Campbell Scientific
Software:	LoggerNet
Software version:	3.4.1
Capabilities:	Datalogger programming
	Real-time sensor monitoring

APPENDIX I

TEST EVENT SHEDULE (2006)

I.1. GUIDANCE-TESTING EVENT SCHEDULE OF 2006

Table I.1. Testing event schedule of 2006.

Test Name [a]	*Date* [b]	*Time of Day*	***Test Name*** [a]	*Date* [b]	*Time of Day*
R_{11}	February 22	2:30 pm	R_{51}	April 7	1:33 pm
J_{11}	---	---	J_{51}	April 7	1:59 pm
D_{11}	---	---	D_{51}	April 7	1:45 pm
W_{11}	February 22	2:45 pm	W_{51}	---	---
R_{21}	February 27	3:03 pm	R_{52}	April 7	2:15 pm
J_{21}	---	---	J_{52}	April 7	2:36 pm
D_{21}	February 27	3:28 pm	D_{52}	April 7	2:25 pm
W_{21}	February 27	3:16 pm	W_{52}	---	---
R_{22}	February 27	3:40 pm	R_{61}	June 14	12:28 pm
J_{22}	---	---	J_{61}	---	---
D_{22}	February 27	4:00 pm	D_{61}	June 14	12:42 pm
W_{22}	February 27	3:50 pm	W_{61}	---	---
R_{31}	March 8	1:47 pm	R_{62}	June 14	3:22 pm
J_{31}	---	---	J_{62}	June 14	3:49 pm
D_{31}	March 8	2:15 pm	D_{62}	June 14	3:35 pm
W_{31}	March 8	2:04 pm	W_{62}	---	---
R_{32}	March 8	2:30 pm	R_{71}	June 16	9:43 am
J_{32}	---	---	J_{71}	June 16	10:07 am
D_{32}	March 8	2:52 pm	D_{71}	June 16	9:55 am
W_{32}	March 8	2:42 pm	W_{71}	---	---
R_{41}	March 28	T_1 [c]	R_{72}	June 16	12:21 pm
J_{41}	---	---	J_{72}	June 16	12:43 pm
D_{41}	March 28	T_1	D_{72}	June 16	12:32 pm
W_{41}	March 28	T_1	W_{72}	---	---
R_{42}	March 28	T_2			
J_{42}	---	---			
D_{42}	March 28	T_2			
W_{42}	March 28	T_2			

[a] Test name is in the format A_{xy}, where *A* represents correction signal used (R=RTK, J=Starfire SF1, D=Starfire SF2, W=WAAS), *x* represents testing day, and *y* represents starting time of testing.
[b] Dashed lines represent absence of data for that iteration.
[c] Events T_1 and T_2 have no time stamps.

APPENDIX J

TEST EVENT SCHEDULE (2007)

J.1. GUIDANCE-TESTING EVENTS OF 2007

Table J.1. Testing event schedule of 2007 for RTK and John Deere SF1 correction signals.

Test Name[a]	*Date*	*Time of Day*	*Test Name*[a]	*Date*	*Time of Day*
R_{S11}	Mar 7	11:36 am	J_{S11}	Mar 7	10:39 am
---	---	---	J_{W11}	Mar 7	1:18 pm
---	---	---	J_{W12}	Mar 7	2:02 pm
R_{S21}	Mar 14	8:45 am	J_{S21}	Mar 14	9:24 am
R_{S22}	Mar 14	10:14 am	J_{S22}	Mar 14	11:20 am
R_{W21}	Mar 14	1:09 pm	J_{W21}	Mar 14	1:19 pm
R_{W22}	Mar 14	2:02 pm	J_{W22}	Mar 14	2:13 pm
R_{S31}	Apr 13	10:46 am	J_{S31}	Apr 13	10:30 am
R_{S32}	Apr 13	2:00 pm	J_{S32}	Apr 13	1:43 pm
R_{W31}	Apr 13	12:59 pm	J_{W31}	Apr 13	12:39 pm
R_{W32}	Apr 13	2:56 pm	J_{W32}	Apr 13	2:42 pm
R_{S41}	Apr 30	8:19 am	J_{S41}	Apr 30	8:56 am
---	---	---	---	---	---
R_{S51}	Jun 5	1:04 pm	J_{S51}	Jun 5	1:37 pm
R_{S52}	Jun 5	3:52 pm	J_{S52}	Jun 5	4:29 pm
R_{W51}	Jun 5	2:48 pm	J_{W51}	Jun 5	2:33 pm
---	---	---	J_{W52}	Jun 5	5:30 pm
R_{S61}	Jul 10	10:12 am	J_{S61}	Jul 10	10:42 am
---	---	---	J_{S62}	Jul 10	1:45 pm
R_{W61}	Jul 10	11:16 am	J_{W61}	Jul 10	11:40 am
---	---	---	J_{W62}	Jul 10	2:55 pm
R_{S71}	Jul 18	10:22 am	J_{S71}	Jul 18	11:24 am
---	---	---	J_{S72}	Jul 18	1:52 pm
---	---	---	J_{S73}	Jul 18	3:34 pm
R_{W71}	Jul 18	10:36 am	J_{W71}	Jul 18	11:38 am
---	---	---	J_{W72}	Jul 18	2:08 pm
---	---	---	J_{W73}	Jul 18	3:47 pm
R_{S81}	Jul 31	10:20 am	J_{S81}	Jul 31	10:47 am
R_{S82}	Jul 31	1:52 pm	J_{S82}	Jul 31	2:22 pm
R_{S83}	Jul 31	4:11 pm	J_{S83}	Jul 31	4:38 pm
R_{W81}	Jul 31	11:23 am	J_{W81}	Jul 31	11:48 am
R_{W82}	Jul 31	3:05 pm	J_{W82}	Jul 31	3:29 pm
R_{S91}	Aug 3	11:12 am	J_{S91}	Aug 3	11:57 am
R_{W91}	Aug 3	12:43 pm	J_{W91}	Aug 3	1:23 pm
R_{S101}	Aug 23	7:45 am	J_{S101}	Aug 23	8:12 am
R_{S102}	Aug 23	10:04 am	J_{S102}	Aug 23	10:31 am
R_{S103}	Aug 23	1:16 pm	J_{S103}	Aug 23	1:49 pm
R_{W101}	Aug 23	9:05 am	J_{W101}	Aug 23	9:29 am
R_{W102}	Aug 23	11:04 am	J_{W102}	Aug 23	11:24 am
R_{W103}	Aug 23	2:22 pm	J_{W103}	Aug 23	2:55 pm

[a] Test name is in the format A_{Xyz}, where *A* represents correction signal used (R=RTK, J=Starfire SF1, D=Starfire SF2, W=WAAS), *X* represents drive path orientation (S=southward, W=westward), *y* represents testing day, and *z* represents testing event number.
[b] Dashed lines represent absence of data for that iteration.

Table J.2. Testing event schedule of 2007 for John Deere SF2 and WAAS correction signals.

Test Name[a]	*Date*	*Time of Day*	*Test Name*[a]	*Date*	*Time of Day*
D_{S11}	Mar 7	10:21 am	W_{S11}	Mar 7	11:16 am
D_{W11}	Mar 7	1:06 pm	W_{W11}	Mar 7	1:29 pm
D_{W12}	Mar 7	1:50 pm	W_{W12}	Mar 7	2:19 pm
D_{S21}	Mar 14	9:07 am	W_{S21}	Mar 14	9:43 am
D_{S22}	Mar 14	10:38 am	W_{S22}	Mar 14	11:43 am
D_{W21}	Mar 14	12:58 pm	W_{W21}	Mar 14	1:31 pm
D_{W22}	Mar 14	1:49 pm	W_{W22}	Mar 14	2:26 pm
D_{S31}	Apr 13	10:03 am	W_{S31}	Apr 13	11:15 am
D_{S32}	Apr 13	1:28 pm	W_{S32}	Apr 13	2:16 pm
D_{W31}	Apr 13	12:26 pm	W_{W31}	Apr 13	1:14 pm
D_{W32}	Apr 13	2:34 pm	W_{W32}	Apr 13	3:13 pm
D_{S41}	Apr 30	8:37 am	W_{S41}	Apr 30	9:13 am
D_{W41}	Apr 30	11:46 am	---	---	---
D_{S51}	Jun 5	1:23 pm	W_{S51}	Jun 5	1:53 pm
D_{S52}	Jun 5	4:13 pm	W_{S52}	Jun 5	4:45 pm
D_{W51}	Jun 5	2:15 pm	W_{W51}	Jun 5	3:14 pm
D_{W52}	Jun 5	5:13 pm	W_{W52}	Jun 5	5:47 pm
D_{S61}	Jul 10	10:27 am	W_{S61}	Jul 10	10:56 am
D_{S62}	Jul 10	1:28 pm	W_{S62}	Jul 10	2:08 pm
D_{W61}	Jul 10	11:27 pm	W_{W61}	Jul 10	11:53 am
D_{W62}	Jul 10	2:42 pm	W_{W62}	Jul 10	3:12 pm
D_{S71}	Jul 18	10:54 am	W_{S71}	Jul 18	11:55 am
D_{S72}	Jul 18	1:26 pm	W_{S72}	Jul 18	2:31 pm
D_{S73}	Jul 18	3:09 pm	W_{S73}	Jul 18	4:01 pm
D_{W71}	Jul 18	11:08 am	W_{W71}	Jul 18	12:12 pm
D_{W72}	Jul 18	1:40 pm	W_{W72}	Jul 18	2:52 pm
D_{W73}	Jul 18	3:23 pm	W_{W73}	Jul 18	4:15 pm
D_{S81}	Jul 31	10:34 am	W_{S81}	Jul 31	11:05 am
D_{S82}	Jul 31	2:07 pm	W_{S82}	Jul 31	2:41 pm
D_{S83}	Jul 31	4:24 pm	W_{S83}	Jul 31	4:51 pm
D_{W81}	Jul 31	11:35 am	W_{W81}	Jul 31	12:12 pm
D_{W82}	Jul 31	3:17 pm	W_{W82}	Jul 31	3:42 pm
D_{S91}	Aug 3	11:38 am	W_{S91}	Aug 3	12:18 pm
D_{W91}	Aug 3	1:03 pm	W_{W91}	Aug 3	1:47 pm
D_{S101}	Aug 23	7:59 am	W_{S101}	Aug 23	8:42 am
D_{S102}	Aug 23	10:17 am	W_{S102}	Aug 23	10:47 am
D_{S103}	Aug 23	1:34 pm	W_{S103}	Aug 23	2:04 pm
D_{W101}	Aug 23	9:16 am	W_{W101}	Aug 23	9:42 am
D_{W102}	Aug 23	11:14 am	W_{W102}	Aug 23	11:35 am
D_{W103}	Aug 23	2:35 pm	W_{W103}	Aug 23	3:08 pm

[a] Test name is in the format AXyz, where A represents correction signal used (R=RTK, J=Starfire SF1, D=Starfire SF2, W=WAAS), X represents drive path orientation (S=southward, W=westward), y represents testing day, and z represents testing event number.

[b] Dashed lines represent absence of data for that iteration.

APPENDIX K

CONCEPTS AND EQUATIONS USED IN GUIDANCE-SYSTEM PERFORMANCE TESTS

K.1. CROSS-TRACK ERROR (XTE)

Cross-track error (XTE) refers to the shortest possible ground distance between an observed target position and its theoretical, or anticipated, position in relation to a computer-generated drive path. In statistical terms, this value would be analogous to a residual value of an observation relative to a regression line. This is the primary value on which other descriptive statistics are calculated, such as mean cross-track error, standard deviation of error, root mean square error, pass-to-pass accuracy, and year-to-year accuracy (see below).

From the example in figure K.1, three observed target positions are represented according to x,y planar coordinates (analogous to "easting" and "northing" coordinates, respectively, in a gridded map coordinate system). The three observations are plotted relative to a pre-determined guidance line or drive path. The distance perpendicular to the guidance line from the observed position is the cross-track error (XTE) of that observation.

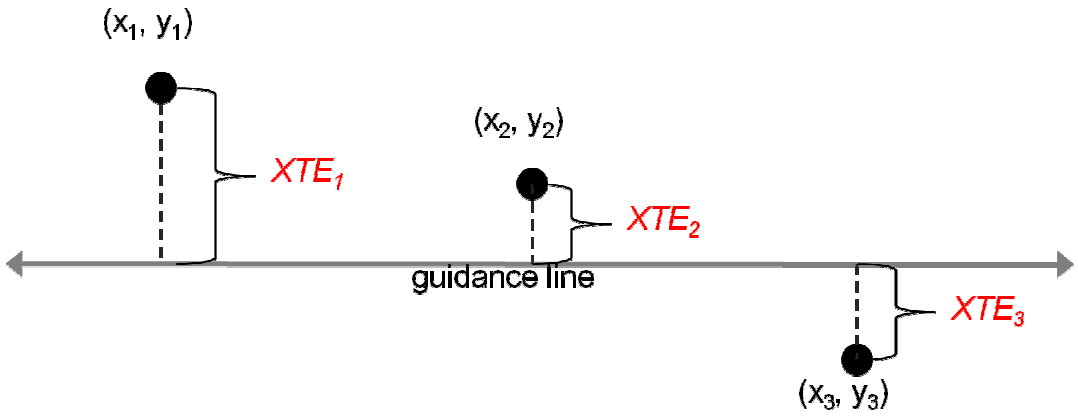

Figure K.1. Depiction of cross-track error.

Depending on the direction of vehicle travel, a "signed" XTE (having a positive or negative value) will refer to which side of the guidance line the observation was taken. Mean cross-track error was calculated by the following equation:

$$\bar{X}_j = \frac{1}{N}\sum_{i=1}^{N} X_{ij} \qquad (1)$$

where N = the number of data obtained from line j, $\bar{X}_j$ = mean XTE, and X_{ij} = the distance from point i to desired line j.

K.2 STANDARD DEVIATION OF ERROR (SD)

Standard deviation of error (SD) is considered as a measure of precision of a guidance system's ability to maintain a vehicle's drive path (Ehsani *et al*., 2002), as this value represents deviation from the mean XTE. Standard deviation of error was calculated by the following equation:

$$SD_j = \sqrt{\frac{1}{N-1}\sum_{i=1}^{N}(X_{ij} - \bar{X}_j)^2} \qquad (2)$$

where N = the number of data obtained from line j, X_{ij} = the distance from point i to desired line j, and $\bar{\bar{X}}_j$ = mean XTE for line j.

K.3 ROOT MEAN SQUARE ERROR (RMSE)

Root mean square error (RMSE) is considered as a measure of accuracy, as this value represents deviation of observed position from its theoretical, ideal position (Ehsani *et al*., 2002). Root mean square error was calculated by the following equation:

$$RMSE_j = \sqrt{\frac{1}{N}\sum_{i=1}^{N} X_{ij}^2} \qquad (3)$$

where N = the number of data obtained from line j, and X_{ij} = the distance from point i to desired line j.

K.4 PASS-TO-PASS ACCURACY (P2P)

Pass-to-pass accuracy (P2P) is regarded as the system's accuracy in determining the location of the next drive path in relation to a recently-traveled drive path, typically within a 15- minute time frame. Pass-to-pass accuracy was calculated by the following equation:

$$P2P_{jk} = \bar{X}_k - \bar{X}_j \qquad (4)$$

where $P2P_{jk}$ refers to pass-to-pass accuracy from line j to line k, $\overline{X_k}$ = mean XTE for line k, and $\bar{X}_j$ = mean XTE for line j.

K.5 YEAR-TO-YEAR ACCURACY (Y2Y)

Year-to-year accuracy (Y2Y) is regarded as the system deviation in determining the location of a repetitious drive path, typically beyond a 15-minute time frame (separation of hours, days, etc.). For a given time interval, Y2Y can best be described as the absolute difference between the minimum and the maximum mean signed XTE of a drive path (field, etc.). Year-to-year accuracy was calculated by using the following equation:

$$Y2Y_j = \left|\left(Max\ \bar{X}_j\right) - \left(Min\ \bar{X}_j\right)\right| \qquad (5)$$

where $Y2Y_j$ is the year-to-year accuracy on line j and $\bar{X}_j$ = mean XTE for line j.

APPENDIX L

GUIDANCE ASSESSMENT OFFICE PROCESSING PROCEDURE (2006)

L.1. NECESSARY SOFTWARE

- Trimble Survey Controller (on the TSCe)
- Microsoft ActiveSync
- Trimble Geomatics Office
- Microsoft Excel

L.2. PROCEDURE STEPS

L.2.1. Uploaded data file from TSCe to Trimble Geomatics Office desktop software.

L.2.2. Checked for obvious errors, measurement blunders, etc.

L.2.3. Converted point data file into a delimited text file in the format Name-Easting-Northing-Elevation-Code. (Elevation and Code values were not required for further calculations.)

L.2.4. Imported the text file into Microsoft Excel.

L.2.5. In Microsoft Excel, a regression analysis was performed on the data set that represented the first established drive path; this data set also corresponded with the initial AB line, zero line, etc. in the guidance computer. From the analysis, the coefficient value that pertains to slope of the model line was recorded. An arc-tangent calculation was made on the coefficient, and this new value was converted to degrees; this newest value represented the slope of the model line in degrees relative to the positive x (easting) axis.

L.2.6. Given the parameters of the regression line, an arbitrary coordinate was derived that fit on the line to the left of the first observed data point; likewise, an arbitrary coordinate was derived to the right of the last observed data point. By using the swath width value, four additional parallel lines were derived to represent the neighboring theoretical drive paths.

L.2.7. UTM coordinate values were normalized by subtracting out the original easting and northing coordinate values from the ensuing data block.

L.2.8. The following equations were used to "rotate" the data set to a model slope of zero:

$$X_f = X_i \left[\cos\left(\tfrac{\pi}{180}(360-\theta)\right)\right] - Y_i \left[\sin\left(\tfrac{\pi}{180}(360-\theta)\right)\right] \quad (6)$$

$$Y_f = Y_i \left[\cos\left(\tfrac{\pi}{180}(360-\theta)\right)\right] + X_i \left[\sin\left(\tfrac{\pi}{180}(360-\theta)\right)\right] \quad (7)$$

where (X_i, Y_i) were initial prism coordinates (Easting, Northing), (X_f , Y_f) were modeled prism coordinates, and θ represented the degree conversion of the arc-tangent of the slope parameter from the regression-line equation.

L.2.9. As a double-check of the accuracy of the rotation function, the newly-derived Northing coordinates for the data set from the initial drive path were compared to the residuals values calculated in the regression analysis; if both sets of numbers were similar, then this rotation model was utilized for every successive drive path and data set.

L.2.10. Because the data sets pertaining to the neighboring drive paths were offset from the X axis by each row's respective swath width, those Northing values were normalized to better reflect uniform cross-track-error values.

L.2.11. Mean cross-track-error, standard deviation of error, root mean square error, pass-to-pass accuracy, and year-to-year accuracy were then calculated according to Appendix K.

APPENDIX M

GUIDANCE ASSESSMENT OFFICE PROCESSING PROCEDURE (2007)

M.1. NECESSARY SOFTWARE

- Trimble Survey Controller (on the TSCe)
- Microsoft ActiveSync
- Trimble Geomatics Office
- ESRI ArcGIS Desktop Version 9 bundle
- XTools Pro Version 5

M.2. PROCEDURE STEPS

M.2.1. Uploaded data file from TSCe to Trimble Geomatics Office desktop software.

M.2.2. Checked for obvious errors, measurement blunders, etc.

M.2.3. Converted point data file into ESRI-compatible shapefile format; formatted data included point name, easting, northing, elevation, and feature code for each data point.

M.2.4. Point data were separated in ArcGIS (ArcMap, ArcCatalog) according to test attributes or site features. If necessary, additional shapefiles were created for those separations for future reference and analyses.

M.3. CREATING A SITE SLOPE/ASPECT MAP

M.3.1. Topographic data were collected across the test site at 5-m-by-5-m spacing using a survey-grade GPS unit, resulting in point data with sub-inch vertical accuracy across the site. Topographic data were uploaded from TSCe to Trimble Geomatics Office desktop software, checked for obvious errors, and converted into ESRI-compatibe shapefile format.

M.3.2. In ArcMap, a map projection was defined for the data set (ArcToolbox / Data Management / Projections and Transformations / Define Projection). Data were then inspected for potential outliers or projection blunders before continuing.

M.3.3. A sub-set of topographic data were isolated from the large set for statistical validation. This was accomplished through Geostatistical Analyst / Create Subsets …; five percent of the topographic data were assigned to the “test” dataset, while the remainder were assigned to the “training” dataset.

M.3.4. A surface raster image (digital elevation model, or DEM) was created from the “training” dataset through ArcToolbox / 3D Analyst Tools / Raster Interpolation / Topo to Raster. Output cell size was defined as “1” so as to produce an image with a 1-square-meter resolution. Drainage Enforcement was turned off (“No Enforce”).

M.3.5. The accuracy of the raster image was tested. From ArcToolbox / Spatial Analyst Tools / Extraction / Extract Values to Points, the "test" dataset was labeled as 'validation' for the raster grid. The "interpolate values at the point locations" feature was active. After the procedure finished, interpolated elevation values were amended to the "testing" shapefile. This batch of numbers was then compared to the original, or measured, elevations from the field work by studentized t-test in Microsoft Excel; the test failed in rejecting the hypothesis that the numbers were not different, so the raster image was considered valid.

M.3.6. Utilizing the raster image, a slope map was created through ArcToolbox / 3D Analyst Tools / Raster Surface / Slope. Slope units were assigned as degrees. This function interpolated the extent of "tilt" for each square meter of the raster image.

M.3.7. Utilizing the raster image, an aspect map was created through ArcToolbox / 3D Analyst Tools / Raster Surface / Aspect. Aspect units were assigned as degrees. This function interpolated the direction of "tilt" for each square meter of the raster image.

M.4. ADJUSTING TARGET COORDINATES FOR PRISM TILT

M.4.1. For each observed target position recorded within the test plot, an interpolated slope and aspect value was also associated. This feature was accomplished through ArcToolbox / Spatial Analyst Tools / Extraction / Extract Values to Points; the relevant point shapefile and the relevant raster were analyzed. The "interpolate values at the point locations" feature was active. After the procedure finished, interpolated slope and/or aspect values were appended to the shapefile attributes.

M.4.2. For each dataset, the point names, northing/easting coordinates, derived slope, and derived aspect values were transferred to Microsoft Excel. Position re-adjustments by slope and aspect were determined for both the easting (X) and northing (Y) coordinates by the initial height of the target prism above the ground.

M.4.3. Utilizing ArcCatalog, a new point-based shapefile was created using the re-adjusted coordinates and identical point names.

M.5. DETERMINING OBSERVATIONAL CROSS-TRACK ERROR

M.5.1. Utilizing shapefile-editor tools in ArcMap, a polyline record was created by connecting the beginning and ending prism observations at the time of guidance-line establishment. Also using the editor tools, four parallel polylines were created to represent the theoretical neighboring drive paths,

separated by a swath-width distance. This polyline file served as the total-station-established reference file for all subsequent tests.

M.5.2. With the desired point file and the reference polyline file available, the Near function was used (ArcToolbox / Analysis Tools / Proximity / Near). When this function finished, each point record had a distance to the nearest reference line appended to its attributes; by leaving the "Angle" feature active during the procedure, a determination could be made as to which side of the reference line the point record was located (through positive or negative angle values).

M.5.3. For ease of further calculation, the Near values were truncated to three decimal places (units in meters), and each value was multiplied by +1 for its corresponding positive angle value or -1 for its corresponding negative angle value. The result was that each point record had an equivalent cross-track error from the desired reference line.

M.5.4. Mean cross-track-error, standard deviation of error, root mean square error, pass-to-pass accuracy, and year-to-year accuracy were then calculated according to Appendix H.

APPENDIX N

SUPPLEMENTAL 2006 XTE DATA

Table N.1. Summary signal-correction quality statistics for testing event 1 (February 22, 2006); tests R_{11} and W_{11}.

Signal[a]	Row 1[b]	Row 2[b]	Row 3[b]	Row 4[b]	Row 5[b]	XTE[c]	N[d]	SD[c]	RMSE[c]	P2P[c]
XTE_R	0	-2	-3	-6	-7	-4				
N_R	22	22	36	39	34		153			
SD_R	4	5	4	5	5			5		
$RMSE_R$	4	5	5	8	9				7	
$P2P_R$	--	-2	-1	-3	-1					-2
XTE_J										
N_J										
SD_J										
$RMSE_J$										
$P2P_J$										
XTE_D										
N_D										
SD_D										
$RMSE_D$										
$P2P_D$										
XTE_W		5	-2	14	26	12				
N_W		31	39	43	45		158			
SD_W		7	10	8	16			15		
$RMSE_W$		9	10	16	31				20	
$P2P_W$		--	-7	16	12					7

[a] Cross-track error by signal (XTE_x) refers to the correction signals evaluated during the test, marked by the subscript R for RTK, J for John Deere SF1, D for John Deere SF2, and W for WAAS. N_x refers to the number of total-station recorded positions available from each path (row).

[b] Values represent average XTE_x (cm), SD_x (cm), and $RMSE_x$ (cm) for this row given N_x datapoints. Negative or positive XTE_x values represent cross-track error to the right or left of the reference line, respectively. $P2P_x$ values are not dependent upon N_x, however.

[c] XTE, SD, and RMSE refer to average values across all five rows with all N_x datapoints for this event. P2P refers to average of four $P2P_x$ values available.

[d] Total N refers to sum of N_x datapoints.

Table N.2. Summary signal-correction quality statistics for testing event 2 (February 27, 2006); tests R_{21}, D_{21}, and W_{21}.

Signal[a]	Row 1[b]	Row 2[b]	Row 3[b]	Row 4[b]	Row 5[b]	XTE[c]	N[d]	SD[c]	RMSE[c]	P2P[c]
XTE_R	-1	-2	-7	-6	-7	-5				
N_R	25	33	43	54	65		220			
SD_R	4	5	4	4	4			5		
$RMSE_R$	4	5	8	7	8				7	
$P2P_R$	--	-1	-5	1	-1					-2
XTE_J										
N_J										
SD_J										
$RMSE_J$										
$P2P_J$										
XTE_D	0	14	25	27	20	19				
N_D	30	33	41	49	65		218			
SD_D	5	4	8	8	7			11		
$RMSE_D$	4	15	26	28	21				22	
$P2P_D$	--	14	11	2	-7					5
XTE_W		-29	-43	-46	-33	-37				
N_W		56	35	60	58		209			
SD_W		20	13	17	29			22		
$RMSE_W$		35	44	49	44				43	
$P2P_W$		--	-14	-3	13					-1

[a] Cross-track error by signal (XTE_x) refers to the correction signals evaluated during the test, marked by the subscript R for RTK, J for John Deere SF1, D for John Deere SF2, and W for WAAS. N_x refers to the number of total-station recorded positions available from each path (row).
[b] Values represent average XTE_x (cm), SD_x (cm), and $RMSE_x$ (cm) for this row given N_x datapoints. Negative or positive XTE_x values represent cross-track error to the right or left of the reference line, respectively. $P2P_x$ values are not dependent upon N_x, however.
[c] XTE, SD, and RMSE refer to average values across all five rows with all N_x datapoints for this event. P2P refers to average of four $P2P_x$ values available.
[d] Total N refers to sum of N_x datapoints.

Table N.3. Summary signal-correction quality statistics for testing event 3 (February 27, 2006); tests R_{22}, D_{22}, and W_{22}.

Signal[a]	Row 1[b]	Row 2[b]	Row 3[b]	Row 4[b]	Row 5[b]	XTE[c]	N[d]	SD[c]	RMSE[c]	P2P[c]
XTE_R	-5	-7	-5	-5	-7	-6				
N_R	32	36	40	57	70		235			
SD_R	3	4	5	4	3			4		
$RMSE_R$	6	7	7	7	8				7	
$P2P_R$	--	-2	2	0	-2					0
XTE_J										
N_J										
SD_J										
$RMSE_J$										
$P2P_J$										
XTE_D	20	35	37	20	23	26				
N_D	31	39	45	59	70		244			
SD_D	4	5	7	8	7			10		
$RMSE_D$	21	36	38	22	24				28	
$P2P_D$	--	15	2	-17	4					1
XTE_W		-10	-17	-11	-26	-18				
N_W		37	45	53	70		205			
SD_W		16	20	31	32			28		
$RMSE_W$		18	27	33	42				33	
$P2P_W$		--	-7	6	-15					-5

[a] Cross-track error by signal (XTE_x) refers to the correction signals evaluated during the test, marked by the subscript R for RTK, J for John Deere SF1, D for John Deere SF2, and W for WAAS. N_x refers to the number of total-station recorded positions available from each path (row).
[b] Values represent average XTE_x (cm), SD_x (cm), and $RMSE_x$ (cm) for this row given N_x datapoints. Negative or positive XTE_x values represent cross-track error to the right or left of the reference line, respectively. $P2P_x$ values are not dependent upon N_x, however.
[c] XTE, SD, and RMSE refer to average values across all five rows with all N_x datapoints for this event. P2P refers to average of four $P2P_x$ values available.
[d] Total N refers to sum of N_x datapoints.

Table N.4. Summary signal-correction quality statistics for testing event 4 (March 8, 2006); tests R_{31}, D_{31}, and W_{31}.

Signal[a]	Row 1[b]	Row 2[b]	Row 3[b]	Row 4[b]	Row 5[b]	XTE[c]	N[d]	SD[c]	RMSE[c]	P2P[c]
XTE_R	0	0	-2	-4	-4	-2				
N_R	30	36	37	45	39		187			
SD_R	3	3	4	5	5			4		
$RMSE_R$	3	3	4	6	6				5	
$P2P_R$	--	0	-2	-2	0					-1
XTE_J										
N_J										
SD_J										
$RMSE_J$										
$P2P_J$										
XTE_D	28	64	47	53	45	47				
N_D	28	23	42	49	55		197			
SD_D	6	9	7	6	8			12		
$RMSE_D$	29	64	47	54	46				49	
$P2P_D$	--	36	-17	6	-8					4
XTE_W		84	0	2	-26	0				
N_W		17	37	45	57		156			
SD_W		10	15	22	33			40		
$RMSE_W$		85	15	22	42				40	
$P2P_W$		--	-84	2	-24					-35

[a] Cross-track error by signal (XTE_x) refers to the correction signals evaluated during the test, marked by the subscript R for RTK, J for John Deere SF1, D for John Deere SF2, and W for WAAS. N_x refers to the number of total-station recorded positions available from each path (row).
[b] Values represent average XTE_x (cm), SD_x (cm), and $RMSE_x$ (cm) for this row given N_x datapoints. Negative or positive XTE_x values represent cross-track error to the right or left of the reference line, respectively. $P2P_x$ values are not dependent upon N_x, however.
[c] XTE, SD, and RMSE refer to average values across all five rows with all N_x datapoints for this event. P2P refers to average of four $P2P_x$ values available.
[d] Total N refers to sum of N_x datapoints.

Table N.5. Summary signal-correction quality statistics for testing event 5 (March 8, 2006); tests R_{32}, D_{32}, and W_{32}.

Signal[a]	Row 1[b]	Row 2[b]	Row 3[b]	Row 4[b]	Row 5[b]	XTE[c]	N[d]	SD[c]	RMSE[c]	P2P[c]
XTE_R	-1	-2	-1	-3	-4	-3				
N_R	31	35	45	46	58		215			
SD_R	5	4	3	5	4			4		
$RMSE_R$	5	5	4	6	6				5	
$P2P_R$	--	-1	1	-2	-1					-1
XTE_J										
N_J										
SD_J										
$RMSE_J$										
$P2P_J$										
XTE_D	14	47	43	40	16	32				
N_D	31	34	41	50	57		213			
SD_D	7	7	5	12	12			17		
$RMSE_D$	15	48	44	42	20				36	
$P2P_D$	--	33	-7	-3	-24					0
XTE_W		5	-3	-2	-2	-1				
N_W		37	46	44	52		179			
SD_W		25	15	21	30			23		
$RMSE_W$		25	15	20	29				23	
$P2P_W$		--	-8	1	0					-2

[a] Cross-track error by signal (XTE_x) refers to the correction signals evaluated during the test, marked by the subscript R for RTK, J for John Deere SF1, D for John Deere SF2, and W for WAAS. N_x refers to the number of total-station recorded positions available from each path (row).
[b] Values represent average XTE_x (cm), SD_x (cm), and $RMSE_x$ (cm) for this row given N_x datapoints. Negative or positive XTE_x values represent cross-track error to the right or left of the reference line, respectively. $P2P_x$ values are not dependent upon N_x, however.
[c] XTE, SD, and RMSE refer to average values across all five rows with all N_x datapoints for this event. P2P refers to average of four $P2P_x$ values available.
[d] Total N refers to sum of N_x datapoints.

Table N.6. Summary signal-correction quality statistics for testing event 6 (March 28, 2006); tests R_{41}, D_{41}, and W_{41}.

Signal[a]	Row 1[b]	Row 2[b]	Row 3[b]	Row 4[b]	Row 5[b]	XTE[c]	N[d]	SD[c]	RMSE[c]	P2P[c]
XTE_R	-2	0	-5	-6	-5	-4				
N_R	26	30	36	46	50		188			
SD_R	5	4	4	3	5			5		
$RMSE_R$	5	4	6	6	7				6	
$P2P_R$	--	-2	-5	-1	1					-2
XTE_J										
N_J										
SD_J										
$RMSE_J$										
$P2P_J$										
XTE_D	60	66	57	63	54	59				
N_D	22	28	34	42	53		179			
SD_D	3	5	6	8	7			8		
$RMSE_D$	60	67	57	63	55				60	
$P2P_D$	--	6	-9	6	-9					-2
XTE_W		-13	-4	-10	-5	-8				
N_W		32	35	40	51		158			
SD_W		8	17	27	26			22		
$RMSE_W$		15	17	28	26				23	
$P2P_W$		--	9	-6	5					3

[a] Cross-track error by signal (XTE_x) refers to the correction signals evaluated during the test, marked by the subscript R for RTK, J for John Deere SF1, D for John Deere SF2, and W for WAAS. N_x refers to the number of total-station recorded positions available from each path (row).
[b] Values represent average XTE_x (cm), SD_x (cm), and $RMSE_x$ (cm) for this row given N_x datapoints. Negative or positive XTE_x values represent cross-track error to the right or left of the reference line, respectively. $P2P_x$ values are not dependent upon N_x, however.
[c] XTE, SD, and RMSE refer to average values across all five rows with all N_x datapoints for this event. P2P refers to average of four $P2P_x$ values available.
[d] Total N refers to sum of N_x datapoints.

Table N.7. Summary signal-correction quality statistics for testing event 7 (March 28, 2006); tests R_{42}, D_{42}, and W_{42}.

Signal[a]	Row 1[b]	Row 2[b]	Row 3[b]	Row 4[b]	Row 5[b]	XTE[c]	N[d]	SD[c]	RMSE[c]	P2P[c]
XTE_R	0	-1	-5	-3	-4	-3				
N_R	23	29	34	41	50		177			
SD_R	4	4	4	4	5			5		
$RMSE_R$	4	4	6	5	6				5	
$P2P_R$	--	-1	-4	2	-1					-1
XTE_J										
N_J										
SD_J										
$RMSE_J$										
$P2P_J$										
XTE_D	20	53	39	34	24	33				
N_D	25	28	35	42	52		182			
SD_D	11	7	7	7	8			13		
$RMSE_D$	22	53	39	34	25				35	
$P2P_D$	--	33	-14	-5	-10					1
XTE_W		-12	-1	1	-1	-2				
N_W		23	35	41	49		148			
SD_W		13	18	24	25			22		
$RMSE_W$		17	18	24	25				22	
$P2P_W$		--	11	2	-2					4

[a] Cross-track error by signal (XTE_x) refers to the correction signals evaluated during the test, marked by the subscript R for RTK, J for John Deere SF1, D for John Deere SF2, and W for WAAS. N_x refers to the number of total-station recorded positions available from each path (row).
[b] Values represent average XTE_x (cm), SD_x (cm), and $RMSE_x$ (cm) for this row given N_x datapoints. Negative or positive XTE_x values represent cross-track error to the right or left of the reference line, respectively. $P2P_x$ values are not dependent upon N_x, however.
[c] XTE, SD, and RMSE refer to average values across all five rows with all N_x datapoints for this event. P2P refers to average of four $P2P_x$ values available.
[d] Total N refers to sum of N_x datapoints.

Table N.8. Summary signal-correction quality statistics for testing event 8 (April 7, 2006); tests R_{51}, J_{51}, and D_{51}.

Signal[a]	Row 1[b]	Row 2[b]	Row 3[b]	Row 4[b]	Row 5[b]	XTE[c]	N[d]	SD[c]	RMSE[c]	P2P[c]
XTE_R	-2	-7	-7	-8	-8	-7				
N_R	34	34	46	56	73		243			
SD_R	3	4	4	4	4			4		
$RMSE_R$	4	8	8	8	9				8	
$P2P_R$	--	-5	0	-1	0					-2
XTE_J	0	6	-5	-7	-9	-4				
N_J	32	27	45	50	61		215			
SD_J	3	10	12	13	15			13		
$RMSE_J$	3	12	13	15	18				14	
$P2P_J$	--	6	-11	-2	-2					-2
XTE_D	9	27	27	22	28	24				
N_D	37	39	51	50	72		249			
SD_D	4	8	6	6	7			9		
$RMSE_D$	9	28	27	23	29				25	
$P2P_D$	--	18	0	-5	6					5
XTE_W										
N_W										
SD_W										
$RMSE_W$										
$P2P_W$										

[a] Cross-track error by signal (XTE_x) refers to the correction signals evaluated during the test, marked by the subscript R for RTK, J for John Deere SF1, D for John Deere SF2, and W for WAAS. N_x refers to the number of total-station recorded positions available from each path (row).
[b] Values represent average XTE_x (cm), SD_x (cm), and $RMSE_x$ (cm) for this row given N_x datapoints. Negative or positive XTE_x values represent cross-track error to the right or left of the reference line, respectively. $P2P_x$ values are not dependent upon N_x, however.
[c] XTE, SD, and RMSE refer to average values across all five rows with all N_x datapoints for this event. P2P refers to average of four $P2P_x$ values available.
[d] Total N refers to sum of N_x datapoints.

Table N.9. Summary signal-correction quality statistics for testing event 9 (April 7, 2006); tests R_{52}, J_{52}, and D_{52}.

Signal[a]	Row 1[b]	Row 2[b]	Row 3[b]	Row 4[b]	Row 5[b]	XTE[c]	N[d]	SD[c]	RMSE[c]	P2P[c]
XTE_R	-3	-8	-6	-7	-8	-7				
N_R	28	33	39	46	61		207			
SD_R	4	4	4	5	5			5		
$RMSE_R$	5	9	8	9	10				8	
$P2P_R$	--	-5	2	-1	-1					-1
XTE_J	-1	-30	-19	-23	-34	-23				
N_J	29	30	41	49	64		213			
SD_J	9	9	8	16	14			16		
$RMSE_J$	9	32	20	28	36				28	
$P2P_J$	--	-29	11	-4	-11					-8
XTE_D	42	44	50	50	50	48				
N_D	30	35	44	51	57		217			
SD_D	5	4	6	6	6			6		
$RMSE_D$	42	44	50	50	50				48	
$P2P_D$	--	2	6	0	0					2
XTE_W										
N_W										
SD_W										
$RMSE_W$										
$P2P_W$										

[a] Cross-track error by signal (XTE_x) refers to the correction signals evaluated during the test, marked by the subscript R for RTK, J for John Deere SF1, D for John Deere SF2, and W for WAAS. N_x refers to the number of total-station recorded positions available from each path (row).
[b] Values represent average XTE_x (cm), SD_x (cm), and $RMSE_x$ (cm) for this row given N_x datapoints. Negative or positive XTE_x values represent cross-track error to the right or left of the reference line, respectively. $P2P_x$ values are not dependent upon N_x, however.
[c] XTE, SD, and RMSE refer to average values across all five rows with all N_x datapoints for this event. P2P refers to average of four $P2P_x$ values available.
[d] Total N refers to sum of N_x datapoints.

Table N.10. Summary signal-correction quality statistics for testing event 10 (June 14, 2006); tests R_{61} and D_{61}.

Signal[a]	Row 1[b]	Row 2[b]	Row 3[b]	Row 4[b]	Row 5[b]	XTE[c]	N[d]	SD[c]	RMSE[c]	P2P[c]
XTE_R	0	-3	-4	-5	-5	-4				
N_R	22	29	32	34	33		150			
SD_R	5	6	4	5	6			5		
$RMSE_R$	4	7	6	7	8				7	
$P2P_R$	--	-3	-1	-1	0					-1
XTE_J										
N_J										
SD_J										
$RMSE_J$										
$P2P_J$										
XTE_D	43	46	37	34	38	39				
N_D	25	24	27	27	24		127			
SD_D	4	8	10	9	15			11		
$RMSE_D$	43	46	39	35	41				41	
$P2P_D$	--	3	-9	-3	4					-1
XTE_W										
N_W										
SD_W										
$RMSE_W$										
$P2P_W$										

[a] Cross-track error by signal (XTE_x) refers to the correction signals evaluated during the test, marked by the subscript R for RTK, J for John Deere SF1, D for John Deere SF2, and W for WAAS. N_x refers to the number of total-station recorded positions available from each path (row).
[b] Values represent average XTE_x (cm), SD_x (cm), and $RMSE_x$ (cm) for this row given N_x datapoints. Negative or positive XTE_x values represent cross-track error to the right or left of the reference line, respectively. $P2P_x$ values are not dependent upon N_x, however.
[c] XTE, SD, and RMSE refer to average values across all five rows with all N_x datapoints for this event. P2P refers to average of four $P2P_x$ values available.
[d] Total N refers to sum of N_x datapoints.

Table N.11. Summary signal-correction quality statistics for testing event 11 (June 14, 2006); tests R_{62}, J_{62}, and D_{62}.

Signal[a]	Row 1[b]	Row 2[b]	Row 3[b]	Row 4[b]	Row 5[b]	XTE[c]	N[d]	SD[c]	RMSE[c]	P2P[c]
XTE_R	-4	-5	-7	-7	-4	-5				
N_R	19	33	36	36	42		166			
SD_R	5	5	4	4	5			5		
$RMSE_R$	6	7	8	8	7				7	
$P2P_R$	--	-1	-2	0	3					0
XTE_J	-16	3	8	-2	-18	-5				
N_J	19	29	33	39	42		162			
SD_J	7	10	16	21	23			21		
$RMSE_J$	17	10	18	21	29				21	
$P2P_J$	--	19	5	-10	-16					0
XTE_D	11	-20	-11	-15	-21	-13				
N_D	20	28	34	36	39		157			
SD_D	6	5	10	12	12			14		
$RMSE_D$	12	20	14	19	23				19	
$P2P_D$	--	-31	9	-4	-6					-8
XTE_W										
N_W										
SD_W										
$RMSE_W$										
$P2P_W$										

[a] Cross-track error by signal (XTE_x) refers to the correction signals evaluated during the test, marked by the subscript R for RTK, J for John Deere SF1, D for John Deere SF2, and W for WAAS. N_x refers to the number of total-station recorded positions available from each path (row).
[b] Values represent average XTE_x (cm), SD_x (cm), and $RMSE_x$ (cm) for this row given N_x datapoints. Negative or positive XTE_x values represent cross-track error to the right or left of the reference line, respectively. $P2P_x$ values are not dependent upon N_x, however.
[c] XTE, SD, and RMSE refer to average values across all five rows with all N_x datapoints for this event. P2P refers to average of four $P2P_x$ values available.
[d] Total N refers to sum of N_x datapoints.

Table N.12. Summary signal-correction quality statistics for testing event 12 (June 16, 2006); tests R_{71}, J_{71}, and D_{71}.

Signal[a]	Row 1[b]	Row 2[b]	Row 3[b]	Row 4[b]	Row 5[b]	XTE[c]	N[d]	SD[c]	RMSE[c]	P2P[c]
XTE_R	-6	-4	-4	-6	-8	-6				
N_R	26	20	34	41	47		168			
SD_R	4	4	5	4	4			4		
$RMSE_R$	7	6	6	7	9				7	
$P2P_R$	--	2	0	-2	-2					0
XTE_J	118	95	89	94	99	98				
N_J	18	24	32	29	50		153			
SD_J	8	7	8	7	12			12		
$RMSE_J$	118	95	90	94	100				98	
$P2P_J$	--	-23	-6	5	5					-5
XTE_D	--	57	71	68	65	65				
N_D	--	28	31	37	50		146			
SD_D	--	5	5	6	8			8		
$RMSE_D$	--	57	71	69	65				66	
$P2P_D$	--	38	14	-3	-3					12
XTE_W										
N_W										
SD_W										
$RMSE_W$										
$P2P_W$										

[a] Cross-track error by signal (XTE_x) refers to the correction signals evaluated during the test, marked by the subscript R for RTK, J for John Deere SF1, D for John Deere SF2, and W for WAAS. N_x refers to the number of total-station recorded positions available from each path (row).
[b] Values represent average XTE_x (cm), SD_x (cm), and $RMSE_x$ (cm) for this row given N_x datapoints. Negative or positive XTE_x values represent cross-track error to the right or left of the reference line, respectively. $P2P_x$ values are not dependent upon N_x, however.
[c] XTE, SD, and RMSE refer to average values across all five rows with all N_x datapoints for this event. P2P refers to average of four $P2P_x$ values available.
[d] Total N refers to sum of N_x datapoints.

Table N.13. Summary signal-correction quality statistics for testing event 13 (June 16, 2006); tests R_{72}, J_{72}, and D_{72}.

Signal[a]	Row 1[b]	Row 2[b]	Row 3[b]	Row 4[b]	Row 5[b]	XTE[c]	N[d]	SD[c]	RMSE[c]	P2P[c]
XTE_R	-4	-5	-6	-7	-8	-6				
N_R	17	29	34	41	37		158			
SD_R	4	4	4	4	3			4		
$RMSE_R$	6	6	7	8	8				7	
$P2P_R$	--	-1	-1	-1	-1					-1
XTE_J	176	159	144	135	117	140				
N_J	24	32	37	46	57		196			
SD_J	8	8	13	10	18			24		
$RMSE_J$	176	160	144	136	118				142	
$P2P_J$	--	-17	-15	-9	-18					-15
XTE_D	5	40	55	62	49	46				
N_D	23	22	34	38	50		167			
SD_D	4	5	14	14	15			22		
$RMSE_D$	6	40	56	63	52				51	
$P2P_D$	--	35	15	7	-13					11
XTE_W										
N_W										
SD_W										
$RMSE_W$										
$P2P_W$										

[a] Cross-track error by signal (XTE_x) refers to the correction signals evaluated during the test, marked by the subscript R for RTK, J for John Deere SF1, D for John Deere SF2, and W for WAAS. N_x refers to the number of total-station recorded positions available from each path (row).
[b] Values represent average XTE_x (cm), SD_x (cm), and $RMSE_x$ (cm) for this row given N_x datapoints. Negative or positive XTE_x values represent cross-track error to the right or left of the reference line, respectively. $P2P_x$ values are not dependent upon N_x, however.
[c] XTE, SD, and RMSE refer to average values across all five rows with all N_x datapoints for this event. P2P refers to average of four $P2P_x$ values available.
[d] Total N refers to sum of N_x datapoints.

Table N.14. Box-and-whisker plot data (cm) for the 2006 season.

Testing Event [a]	Min	Q1	Med	Q3	Max	Testing Event [a]	Min	Q1	Med	Q3	Max
RTK						SF2					
R_{11}	-17	-7	-4	0	8	D_{21}	-10	11	20	27	47
R_{21}	-17	-8	-5	-2	6	D_{22}	0	19	26	34	48
R_{22}	-16	-8	-6	-3	4	D_{31}	17	40	48	54	79
R_{31}	-14	-5	-2	1	9	D_{32}	-25	16	38	45	59
R_{32}	-15	-6	-2	1	10	D_{41}	39	55	59	64	77
R_{41}	-16	-7	-4	-1	8	D_{42}	4	24	33	42	67
R_{42}	-14	-6	-3	1	9	D_{51}	2	18	24	30	44
R_{51}	-18	-10	-7	-4	3	D_{52}	33	43	48	52	62
R_{52}	-19	-10	-7	-4	5	D_{61}	9	34	41	46	59
R_{61}	-20	-7	-4	0	8	D_{62}	-50	-22	-13	-6	20
R_{62}	-19	-8	-6	-2	6	D_{71}	42	60	66	72	81
R_{71}	-18	-9	-6	-3	2	D_{72}	-3	36	53	63	77
R_{72}	-16	-9	-7	-4	4	Summary	-24	22	37	51	82
Summary	-18	-8	-5	-2	8						
						WAAS					
SF1						W_{11}	-21	1	10	20	48
J_{51}	-43	-14	-3	6	26	W_{21}	-91	-50	-37	-25	14
J_{52}	-62	-35	-23	-12	20	W_{22}	-84	-37	-15	2	48
J_{62}	-64	-16	-2	11	33	W_{31}	-95	-25	-2	16	105
J_{71}	73	89	97	106	128	W_{32}	-62	-16	-4	13	57
J_{72}	69	127	139	158	186	W_{41}	-55	-22	-13	7	44
Summary	-64	-15	5	101	186	W_{42}	-51	-20	-4	14	48
						Summary	-84	-28	-9	10	57

[a] Testing events are listed in Appendix I.

APPENDIX O

SUPPLEMENTAL 2007 XTE DATA

Table O.1. Summary signal-correction quality statistics for north-to-south testing event 1 (March 7, 2007); tests R_{S11}, J_{S11}, D_{S11}, and W_{S11}.

Signal[a]	Row 1[b]	Row 2[b]	Row 3[b]	Row 4[b]	Row 5[b]	XTE[c]	N[d]	SD[c]	RMSE[c]	P2P[c]
XTE_R	8	1	2	2	2	3				
N_R	65	67	70	72	66		340			
SD_R	6	5	6	8	8			7		
$RMSE_R$	10	5	6	8	8				8	
$P2P_R$	--	-7	1	0	0					-2
XTE_J	30	33	43	52	52	42				
N_J	68	78	71	70	59		346			
SD_J	11	7	7	10	8			13		
$RMSE_J$	32	34	44	53	53				44	
$P2P_J$	--	3	10	9	0					6
XTE_D	52	51	54	50	46	50				
N_D	61	58	72	54	51		292			
SD_D	4	4	7	9	6			6		
$RMSE_D$	52	51	54	51	47				51	
$P2P_D$	--	-1	3	-4	-4					-2
XTE_W	-59	-55	-50	-33	-43	-47				
N_W	47	66	70	70	65		318			
SD_W	16	16	17	21	15			20		
$RMSE_W$	62	57	53	39	46				51	
$P2P_W$	--	4	5	17	-10					4

[a] Cross-track error by signal (XTE_x) refers to the correction signals evaluated during the test, marked by the subscript R for RTK, J for John Deere SF1, D for John Deere SF2, and W for WAAS. N_x refers to the number of total-station recorded positions available from each path (row).
[b] Values represent average XTE_x (cm), SD_x (cm), and $RMSE_x$ (cm) for this row given N_x datapoints. Negative or positive XTE_x values represent cross-track error to the right or left of the reference line, respectively. $P2P_x$ values are not dependent upon N_x, however.
[c] XTE, SD, and RMSE refer to average values across all five rows with all N_x datapoints for this event. P2P refers to average of four $P2P_x$ values available.
[d] N refers to sum of N_x datapoints.

Table O.2. Summary signal-correction quality statistics for east-to-west testing event 1 (March 7, 2007); tests J_{W11}, D_{W11}, and W_{W11}.

Signal[a]	Row 1[b]	Row 2[b]	Row 3[b]	Row 4[b]	Row 5[b]	XTE[c]	N[d]	SD[c]	RMSE[c]	P2P[c]
XTE_R										
N_R										
SD_R										
$RMSE_R$										
$P2P_R$										
XTE_J	36	39	43	41	37	39				
N_J	34	34	26	30	19		143			
SD_J	7	9	12	16	13			12		
$RMSE_J$	37	40	45	44	39				41	
$P2P_J$	--	3	4	-2	-4					0
XTE_D	72	66	59	54	38	60				
N_D	29	31	31	27	14		132			
SD_D	6	10	12	15	13			15		
$RMSE_D$	72	66	60	56	40				62	
$P2P_D$	--	-6	-7	-5	-16					-8
XTE_W	90	135	131	149	144	131				
N_W	29	30	34	36	30		159			
SD_W	5	13	21	24	26			28		
$RMSE_W$	91	135	133	151	147				134	
$P2P_W$	--	45	-4	18	-5					14

[a] Cross-track error by signal (XTE_x) refers to the correction signals evaluated during the test, marked by the subscript R for RTK, J for John Deere SF1, D for John Deere SF2, and W for WAAS. N_x refers to the number of total-station recorded positions available from each path (row).
[b] Values represent average XTE_x (cm), SD_x (cm), and $RMSE_x$ (cm) for this row given N_x datapoints. Negative or positive XTE_x values represent cross-track error to the right or left of the reference line, respectively. $P2P_x$ values are not dependent upon N_x, however.
[c] XTE, SD, and RMSE refer to average values across all five rows with all N_x datapoints for this event. P2P refers to average of four $P2P_x$ values available.
[d] N refers to sum of N_x datapoints.

Table O.3. Summary signal-correction quality statistics for east-to-west testing event 2 (March 7, 2007); tests J_{W12}, D_{W12}, and W_{W12}.

Signal[a]	Row 1[b]	Row 2[b]	Row 3[b]	Row 4[b]	Row 5[b]	XTE[c]	N[d]	SD[c]	RMSE[c]	P2P[c]
XTE_R										
N_R										
SD_R										
$RMSE_R$										
$P2P_R$										
XTE_J	67	66	53	34	27	53				
N_J	36	35	31	25	19		146			
SD_J	14	11	13	21	18			21		
$RMSE_J$	68	67	54	39	32				57	
$P2P_J$	--	-1	-13	-19	-7					-10
XTE_D	126	106	70	50	25	82				
N_D	33	38	28	22	23		144			
SD_D	11	16	20	30	25			41		
$RMSE_D$	126	107	73	58	34				91	
$P2P_D$	--	-20	-36	-20	-25					-25
XTE_W	85	82	57	50	49	67				
N_W	35	35	32	28	23		153			
SD_W	5	8	22	15	19			22		
$RMSE_W$	86	83	61	52	52				70	
$P2P_W$	--	-3	-25	-7	-1					-9

[a] Cross-track error by signal (XTE_x) refers to the correction signals evaluated during the test, marked by the subscript R for RTK, J for John Deere SF1, D for John Deere SF2, and W for WAAS. N_x refers to the number of total-station recorded positions available from each path (row).
[b] Values represent average XTE_x (cm), SD_x (cm), and $RMSE_x$ (cm) for this row given N_x datapoints. Negative or positive XTE_x values represent cross-track error to the right or left of the reference line, respectively. $P2P_x$ values are not dependent upon N_x, however.
[c] XTE, SD, and RMSE refer to average values across all five rows with all N_x datapoints for this event. P2P refers to average of four $P2P_x$ values available.
[d] N refers to sum of N_x datapoints.

Table O.4. Summary signal-correction quality statistics for north-to-south testing event 2 (March 14, 2007); tests R_{S21}, J_{S21}, D_{S21}, and W_{S21}.

Signal[a]	Row 1[b]	Row 2[b]	Row 3[b]	Row 4[b]	Row 5[b]	XTE[c]	N[d]	SD[c]	RMSE[c]	P2P[c]
XTE_R	5	-2	-1	-2	-2	-1				
N_R	68	71	73	73	64		349			
SD_R	5	6	7	7	7			7		
$RMSE_R$	7	7	7	7	8				7	
$P2P_R$	--	-7	1	-1	0					-2
XTE_J	35	51	73	76	71	61				
N_J	65	70	65	71	65		336			
SD_J	9	4	6	6	11			17		
$RMSE_J$	36	51	73	76	76				64	
$P2P_J$	--	16	22	3	-5					9
XTE_D	-20	--	-22	-10	-3	-13				
N_D	57	--	78	75	73		283			
SD_D	5	--	5	7	9			10		
$RMSE_D$	21	--	22	12	9				17	
$P2P_D$	--	--	-2	12	7					4
XTE_W	6	-37	-8	-18	-11	-12				
N_W	67	47	71	68	69		322			
SD_W	23	14	18	17	20			23		
$RMSE_W$	24	40	20	25	22				26	
$P2P_W$	--	-43	29	-10	7					-4

[a] Cross-track error by signal (XTE_x) refers to the correction signals evaluated during the test, marked by the subscript R for RTK, J for John Deere SF1, D for John Deere SF2, and W for WAAS. N_x refers to the number of total-station recorded positions available from each path (row).
[b] Values represent average XTE_x (cm), SD_x (cm), and $RMSE_x$ (cm) for this row given N_x datapoints. Negative or positive XTE_x values represent cross-track error to the right or left of the reference line, respectively. $P2P_x$ values are not dependent upon N_x, however.
[c] XTE, SD, and RMSE refer to average values across all five rows with all N_x datapoints for this event. P2P refers to average of four $P2P_x$ values available.
[d] N refers to sum of N_x datapoints.

Table O.5. Summary signal-correction quality statistics for north-to-south testing event 3 (March 14, 2007); tests R_{S22}, J_{S22}, D_{S22}, and W_{S22}.

Signal[a]	Row 1[b]	Row 2[b]	Row 3[b]	Row 4[b]	Row 5[b]	XTE[c]	N[d]	SD[c]	RMSE[c]	P2P[c]
XTE_R	4	-2	-3	-3	-1	-1				
N_R	58	69	68	59	53		307			
SD_R	3	6	6	7	7			6		
$RMSE_R$	5	6	6	7	7				6	
$P2P_R$	--	-6	-1	0	2					-1
XTE_J	29	26	77	4	-40	17				
N_J	54	66	29	67	36		252			
SD_J	7	4	5	11	14			33		
$RMSE_J$	30	27	78	12	42				37	
$P2P_J$	--	-3	51	-73	-44					-17
XTE_D	26	34	31	36	35	32				
N_D	60	70	69	52	59		310			
SD_D	4	6	8	9	9			8		
$RMSE_D$	26	34	32	37	36				33	
$P2P_D$	--	8	-3	5	-1					2
XTE_W	--	37	12	6	-3	14				
N_W	--	64	71	65	53		253			
SD_W	--	10	9	15	16			19		
$RMSE_W$	--	38	15	16	16				24	
$P2P_W$	--	--	-25	-6	-9					-13

[a] Cross-track error by signal (XTE_x) refers to the correction signals evaluated during the test, marked by the subscript R for RTK, J for John Deere SF1, D for John Deere SF2, and W for WAAS. N_x refers to the number of total-station recorded positions available from each path (row).
[b] Values represent average XTE_x (cm), SD_x (cm), and $RMSE_x$ (cm) for this row given N_x datapoints. Negative or positive XTE_x values represent cross-track error to the right or left of the reference line, respectively. $P2P_x$ values are not dependent upon N_x, however.
[c] XTE, SD, and RMSE refer to average values across all five rows with all N_x datapoints for this event. P2P refers to average of four $P2P_x$ values available.
[d] N refers to sum of N_x datapoints.

Table O.6. Summary signal-correction quality statistics for east-to-west testing event 3 (March 14, 2007); tests R_{W21}, J_{W21}, D_{W21}, and W_{W21}.

Signal[a]	Row 1[b]	Row 2[b]	Row 3[b]	Row 4[b]	Row 5[b]	XTE[c]	N[d]	SD[c]	RMSE[c]	P2P[c]
XTE_R	16	17	12	9	9	13				
N_R	21	30	31	25	23		130			
SD_R	4	8	10	10	9			9		
$RMSE_R$	16	19	15	13	13				16	
$P2P_R$	--	1	-5	-3	0					-2
XTE_J	27	28	39	38	41	34				
N_J	29	30	32	23	24		138			
SD_J	4	10	8	18	12			12		
$RMSE_J$	28	30	39	42	42				36	
$P2P_J$	--	1	11	-1	3					4
XTE_D	--	8	24	52	51	32				
N_D	--	29	35	32	29		125			
SD_D	--	5	6	14	27			27		
$RMSE_D$	--	9	24	53	57				41	
$P2P_D$	--	--	16	28	-1					14
XTE_W	35	81	44	44	32	48				
N_W	22	29	31	27	31		140			
SD_W	21	36	31	47	30			38		
$RMSE_W$	41	89	54	64	43				61	
$P2P_W$	--	46	-37	0	-12					-1

[a] Cross-track error by signal (XTE_x) refers to the correction signals evaluated during the test, marked by the subscript R for RTK, J for John Deere SF1, D for John Deere SF2, and W for WAAS. N_x refers to the number of total-station recorded positions available from each path (row).
[b] Values represent average XTE_x (cm), SD_x (cm), and $RMSE_x$ (cm) for this row given N_x datapoints. Negative or positive XTE_x values represent cross-track error to the right or left of the reference line, respectively. $P2P_x$ values are not dependent upon N_x, however.
[c] XTE, SD, and RMSE refer to average values across all five rows with all N_x datapoints for this event. P2P refers to average of four $P2P_x$ values available.
[d] N refers to sum of N_x datapoints.

Table O.7. Summary signal-correction quality statistics for east-to-west testing event 4 (March 14, 2007); tests R_{W22}, J_{W22}, D_{W22}, and W_{W22}.

Signal[a]	Row 1[b]	Row 2[b]	Row 3[b]	Row 4[b]	Row 5[b]	XTE[c]	N[d]	SD[c]	RMSE[c]	P2P[c]
XTE_R	18	17	16	14	14	16				
N_R	25	37	33	26	33		154			
SD_R	7	6	8	7	7			7		
$RMSE_R$	19	18	18	16	15				17	
$P2P_R$	--	-1	-1	-2	0					-1
XTE_J	39	41	33	25	24	33				
N_J	34	30	36	29	29		158			
SD_J	7	6	8	9	8			10		
$RMSE_J$	40	42	34	26	25				34	
$P2P_J$	--	2	-8	-8	-1					-4
XTE_D	-206	-203	-112	-64	-50	-122				
N_D	24	30	24	32	32		142			
SD_D	27	6	10	14	16			69		
$RMSE_D$	208	203	113	65	52				140	
$P2P_D$	--	3	91	48	14					39
XTE_W	-62	-81	-66	-95	-31	-67				
N_W	28	35	36	25	27		151			
SD_W	38	51	29	30	48			45		
$RMSE_W$	73	95	72	100	56				81	
$P2P_W$	--	-19	15	-29	64					8

[a] Cross-track error by signal (XTE_x) refers to the correction signals evaluated during the test, marked by the subscript R for RTK, J for John Deere SF1, D for John Deere SF2, and W for WAAS. N_x refers to the number of total-station recorded positions available from each path (row).
[b] Values represent average XTE_x (cm), SD_x (cm), and $RMSE_x$ (cm) for this row given N_x datapoints. Negative or positive XTE_x values represent cross-track error to the right or left of the reference line, respectively. $P2P_x$ values are not dependent upon N_x, however.
[c] XTE, SD, and RMSE refer to average values across all five rows with all N_x datapoints for this event. P2P refers to average of four $P2P_x$ values available.
[d] N refers to sum of N_x datapoints.

Table O.8. Summary signal-correction quality statistics for north-to-south testing event 4 (April 13, 2007); tests R_{S31}, J_{S31}, D_{S31}, and W_{S31}.

Signal[a]	Row 1[b]	Row 2[b]	Row 3[b]	Row 4[b]	Row 5[b]	XTE[c]	N[d]	SD[c]	RMSE[c]	P2P[c]
XTE_R	4	-3	-1	0	-1	0				
N_R	63	67	63	62	65		320			
SD_R	5	6	6	6	6			6		
$RMSE_R$	6	6	7	6	6				6	
$P2P_R$	--	-7	2	1	-1					-1
XTE_J	21	44	60	56	49	46				
N_J	68	64	62	64	67		325			
SD_J	6	4	8	10	8			16		
$RMSE_J$	21	44	61	57	49				48	
$P2P_J$	--	23	16	-4	-7					7
XTE_D	8	71	57	52	40	46				
N_D	56	60	74	69	73		332			
SD_D	4	3	8	11	9			21		
$RMSE_D$	9	71	57	53	41				51	
$P2P_D$	--	63	-14	-5	-12					8
XTE_W	-10	-30	-21	-30	-63	-32				
N_W	41	61	68	63	64		297			
SD_W	18	26	21	9	24			27		
$RMSE_W$	20	40	30	31	67				42	
$P2P_W$	--	-20	9	-9	-33					-13

[a] Cross-track error by signal (XTE_x) refers to the correction signals evaluated during the test, marked by the subscript R for RTK, J for John Deere SF1, D for John Deere SF2, and W for WAAS. N_x refers to the number of total-station recorded positions available from each path (row).
[b] Values represent average XTE_x (cm), SD_x (cm), and $RMSE_x$ (cm) for this row given N_x datapoints. Negative or positive XTE_x values represent cross-track error to the right or left of the reference line, respectively. $P2P_x$ values are not dependent upon N_x, however.
[c] XTE, SD, and RMSE refer to average values across all five rows with all N_x datapoints for this event. P2P refers to average of four $P2P_x$ values available.
[d] N refers to sum of N_x datapoints.

Table O.9. Summary signal-correction quality statistics for north-to-south testing event 5 (April 13, 2007); tests R_{S32}, J_{S32}, D_{S32}, and W_{S32}.

Signal[a]	Row 1[b]	Row 2[b]	Row 3[b]	Row 4[b]	Row 5[b]	XTE[c]	N[d]	SD[c]	RMSE[c]	P2P[c]
XTE_R	6	-2	-1	1	-3	0				
N_R	48	66	69	71	63		317			
SD_R	6	6	7	7	7			7		
$RMSE_R$	8	7	7	7	8				7	
$P2P_R$	--	-8	1	2	-4					-2
XTE_J	5	46	59	43	34	38				
N_J	63	70	78	70	72		353			
SD_J	8	5	8	12	13			20		
$RMSE_J$	9	46	59	45	36				43	
$P2P_J$	--	41	13	-16	-9					7
XTE_D	-2	-57	-31	-7	3	-19				
N_D	70	65	70	57	59		321			
SD_D	20	6	6	13	10			26		
$RMSE_D$	20	58	32	14	10				32	
$P2P_D$	--	-55	26	24	10					1
XTE_W	--	6	0	1	-9	-1				
N_W	--	66	70	71	69		276			
SD_W	--	14	27	12	14			19		
$RMSE_W$	--	14	27	12	17				19	
$P2P_W$	--	--	-6	1	-10					-4

[a] Cross-track error by signal (XTE_x) refers to the correction signals evaluated during the test, marked by the subscript R for RTK, J for John Deere SF1, D for John Deere SF2, and W for WAAS. N_x refers to the number of total-station recorded positions available from each path (row).
[b] Values represent average XTE_x (cm), SD_x (cm), and $RMSE_x$ (cm) for this row given N_x datapoints. Negative or positive XTE_x values represent cross-track error to the right or left of the reference line, respectively. $P2P_x$ values are not dependent upon N_x, however.
[c] XTE, SD, and RMSE refer to average values across all five rows with all N_x datapoints for this event. P2P refers to average of four $P2P_x$ values available.
[d] N refers to sum of N_x datapoints.

Table O.10. Summary signal-correction quality statistics for east-to-west testing event 5 (April 13, 2007); tests R_{W31}, J_{W31}, D_{W31}, and W_{W31}.

Signal[a]	Row 1[b]	Row 2[b]	Row 3[b]	Row 4[b]	Row 5[b]	XTE[c]	N[d]	SD[c]	RMSE[c]	P2P[c]
XTE_R	11	17	18	14	9	14				
N_R	35	40	36	34	25		170			
SD_R	7	10	9	8	9			9		
$RMSE_R$	13	19	20	16	13				17	
$P2P_R$	--	6	1	-4	-5					0
XTE_J	29	29	27	23	16	26				
N_J	44	39	36	35	29		183			
SD_J	10	8	9	8	11			10		
$RMSE_J$	31	30	29	25	20				28	
$P2P_J$	--	0	-2	-4	-7					-3
XTE_D	46	48	36	30	25	37				
N_D	39	40	41	44	35		199			
SD_D	8	5	10	9	8			12		
$RMSE_D$	47	49	37	32	26				39	
$P2P_D$	--	2	-12	-6	-5					-5
XTE_W	-184	-155	-131	-79	-84	-130				
N_W	36	32	35	29	28		160			
SD_W	15	10	11	12	33			44		
$RMSE_W$	184	156	132	80	90				137	
$P2P_W$	--	29	24	52	-5					25

[a] Cross-track error by signal (XTE_x) refers to the correction signals evaluated during the test, marked by the subscript R for RTK, J for John Deere SF1, D for John Deere SF2, and W for WAAS. N_x refers to the number of total-station recorded positions available from each path (row).
[b] Values represent average XTE_x (cm), SD_x (cm), and $RMSE_x$ (cm) for this row given N_x datapoints. Negative or positive XTE_x values represent cross-track error to the right or left of the reference line, respectively. $P2P_x$ values are not dependent upon N_x, however.
[c] XTE, SD, and RMSE refer to average values across all five rows with all N_x datapoints for this event. P2P refers to average of four $P2P_x$ values available.
[d] N refers to sum of N_x datapoints.

Table O.11. Summary signal-correction quality statistics for east-to-west testing event 6 (April 13, 2007); tests R_{W32}, J_{W32}, D_{W32}, and W_{W32}.

Signal[a]	Row 1[b]	Row 2[b]	Row 3[b]	Row 4[b]	Row 5[b]	XTE[c]	N[d]	SD[c]	RMSE[c]	P2P[c]
XTE_R	16	18	15	13	11	15				
N_R	33	37	36	17	33		156			
SD_R	7	7	7	10	9			8		
$RMSE_R$	17	19	16	17	14				17	
$P2P_R$	--	2	-3	-2	-2					-1
XTE_J	-31	-12	-7	5	3	-8				
N_J	33	35	36	39	30		173			
SD_J	16	8	7	8	18			18		
$RMSE_J$	35	15	10	10	18				19	
$P2P_J$	--	19	5	12	-2					8
XTE_D	-40	-40	-43	-48	-41	-43				
N_D	38	27	32	33	34		164			
SD_D	8	6	8	8	10			10		
$RMSE_D$	41	41	44	49	42				44	
$P2P_D$	--	0	-3	-5	7					0
XTE_W	-68	40	31	19	-6	4				
N_W	34	33	38	33	32		170			
SD_W	20	29	9	23	35			46		
$RMSE_W$	71	49	32	30	35				46	
$P2P_W$	--	108	-9	-12	-25					16

[a] Cross-track error by signal (XTE_x) refers to the correction signals evaluated during the test, marked by the subscript R for RTK, J for John Deere SF1, D for John Deere SF2, and W for WAAS. N_x refers to the number of total-station recorded positions available from each path (row).
[b] Values represent average XTE_x (cm), SD_x (cm), and $RMSE_x$ (cm) for this row given N_x datapoints. Negative or positive XTE_x values represent cross-track error to the right or left of the reference line, respectively. $P2P_x$ values are not dependent upon N_x, however.
[c] XTE, SD, and RMSE refer to average values across all five rows with all N_x datapoints for this event. P2P refers to average of four $P2P_x$ values available.
[d] N refers to sum of N_x datapoints.

Table O.12. Summary signal-correction quality statistics for north-to-south testing event 6 (April 30, 2007); tests R_{S41}, J_{S41}, D_{S41}, and W_{S41}.

Signal[a]	Row 1[b]	Row 2[b]	Row 3[b]	Row 4[b]	Row 5[b]	XTE[c]	N[d]	SD[c]	RMSE[c]	P2P[c]
XTE_R	5	0	-1	0	-2	1				
N_R	65	68	66	62	61		322			
SD_R	6	6	4	5	7			6		
$RMSE_R$	8	6	4	5	8				6	
$P2P_R$	--	-5	-1	1	-2					-2
XTE_J	63	54	54	50	45	53				
N_J	56	66	71	71	65		329			
SD_J	6	6	6	8	7			9		
$RMSE_J$	63	55	54	51	45				54	
$P2P_J$	--	-9	0	-4	-5					-4
XTE_D	53	36	38	38	31	39				
N_D	62	72	61	72	58		325			
SD_D	6	6	4	7	6			9		
$RMSE_D$	53	37	38	38	38				40	
$P2P_D$	--	-17	2	0	-7					-6
XTE_W	-8	-33	-23	-27	-15	-21				
N_W	67	67	60	57	64		315			
SD_W	12	12	12	9	14			15		
$RMSE_W$	14	35	25	28	20				26	
$P2P_W$	--	-25	10	-4	12					-2

[a] Cross-track error by signal (XTE_x) refers to the correction signals evaluated during the test, marked by the subscript R for RTK, J for John Deere SF1, D for John Deere SF2, and W for WAAS. N_x refers to the number of total-station recorded positions available from each path (row).
[b] Values represent average XTE_x (cm), SD_x (cm), and $RMSE_x$ (cm) for this row given N_x datapoints. Negative or positive XTE_x values represent cross-track error to the right or left of the reference line, respectively. $P2P_x$ values are not dependent upon N_x, however.
[c] XTE, SD, and RMSE refer to average values across all five rows with all N_x datapoints for this event. P2P refers to average of four $P2P_x$ values available.
[d] N refers to sum of N_x datapoints.

Table O.13. Summary signal-correction quality statistics for east-to-west testing event 7 (April 30, 2007); test D_{W41}.

Signal[a]	Row 1[b]	Row 2[b]	Row 3[b]	Row 4[b]	Row 5[b]	XTE[c]	N[d]	SD[c]	RMSE[c]	P2P[c]
XTE_R										
N_R										
SD_R										
$RMSE_R$										
$P2P_R$										
XTE_J										
N_J										
SD_J										
$RMSE_J$										
$P2P_J$										
XTE_D	-12	-44	-11	-3	-26	-17				
N_D	35	26	34	35	26		156			
SD_D	9	22	23	25	31			26		
$RMSE_D$	15	49	25	24	40				31	
$P2P_D$	--	-32	33	8	-23					-4
XTE_W										
N_W										
SD_W										
$RMSE_W$										
$P2P_W$										

[a] Cross-track error by signal (XTE_x) refers to the correction signals evaluated during the test, marked by the subscript R for RTK, J for John Deere SF1, D for John Deere SF2, and W for WAAS. N_x refers to the number of total-station recorded positions available from each path (row).
[b] Values represent average XTE_x (cm), SD_x (cm), and $RMSE_x$ (cm) for this row given N_x datapoints. Negative or positive XTE_x values represent cross-track error to the right or left of the reference line, respectively. $P2P_x$ values are not dependent upon N_x, however.
[c] XTE, SD, and RMSE refer to average values across all five rows with all N_x datapoints for this event. P2P refers to average of four $P2P_x$ values available.
[d] N refers to sum of N_x datapoints.

Table O.14. Summary signal-correction quality statistics for north-to-south testing event 7 (June 5, 2007); tests R_{S51}, J_{S51}, D_{S51}, and W_{S51}.

Signal[a]	Row 1[b]	Row 2[b]	Row 3[b]	Row 4[b]	Row 5[b]	XTE[c]	N[d]	SD[c]	RMSE[c]	P2P[c]
XTE_R	-2	-8	-8	-7	-8	-6				
N_R	55	51	64	57	59		286			
SD_R	7	8	7	6	7			7		
$RMSE_R$	7	11	10	10	11				10	
$P2P_R$	--	-6	0	1	-1					-2
XTE_J	-14	-29	-26	-26	-29	-25				
N_J	55	60	58	58	50		281			
SD_J	7	7	5	6	8			9		
$RMSE_J$	15	30	26	26	30				26	
$P2P_J$	--	-15	3	0	-3					-4
XTE_D	-27	-47	-17	-9	-15	-23				
N_D	65	53	60	59	7		294			
SD_D	6	4	5	8	9			15		
$RMSE_D$	28	47	18	13	17				27	
$P2P_D$	--	-20	30	8	-6					3
XTE_W	-20	-44	-18	-20	-34	-27				
N_W	46	51	56	55	50		258			
SD_W	19	20	20	17	15			21		
$RMSE_W$	28	48	26	26	37				34	
$P2P_W$	--	-24	26	-2	-14					-4

[a] Cross-track error by signal (XTE_x) refers to the correction signals evaluated during the test, marked by the subscript R for RTK, J for John Deere SF1, D for John Deere SF2, and W for WAAS. N_x refers to the number of total-station recorded positions available from each path (row).
[b] Values represent average XTE_x (cm), SD_x (cm), and $RMSE_x$ (cm) for this row given N_x datapoints. Negative or positive XTE_x values represent cross-track error to the right or left of the reference line, respectively. $P2P_x$ values are not dependent upon N_x, however.
[c] XTE, SD, and RMSE refer to average values across all five rows with all N_x datapoints for this event. P2P refers to average of four $P2P_x$ values available.
[d] N refers to sum of N_x datapoints.

Table O.15. Summary signal-correction quality statistics for north-to-south testing event 8 (June 5, 2007); tests R_{S52}, J_{S52}, D_{S52}, and W_{S52}.

Signal[a]	Row 1[b]	Row 2[b]	Row 3[b]	Row 4[b]	Row 5[b]	XTE[c]	N[d]	SD[c]	RMSE[c]	P2P[c]
XTE_R	0	-13	-10	-8	-11	-9				
N_R	47	45	62	52	56		262			
SD_R	6	7	8	4	7			8		
$RMSE_R$	6	15	12	9	13				12	
$P2P_R$	--	-13	3	2	-3					-3
XTE_J	-66	-76	-52	-57	-69	-64				
N_J	48	65	66	61	52		292			
SD_J	6	4	8	11	7			12		
$RMSE_J$	67	76	53	58	69				65	
$P2P_J$	--	-10	24	-5	-12					-1
XTE_D	49	33	26	29	28	32				
N_D	50	65	65	59	55		294			
SD_D	7	13	10	8	11			13		
$RMSE_D$	49	36	28	30	30				35	
$P2P_D$	--	-16	-7	3	-1					-5
XTE_W	27	-5	-11	-7	2	-2				
N_W	20	54	55	57	56		242			
SD_W	10	15	12	15	15			17		
$RMSE_W$	29	16	17	17	15				18	
$P2P_W$	--	-32	-6	4	9					-6

[a] Cross-track error by signal (XTE_x) refers to the correction signals evaluated during the test, marked by the subscript R for RTK, J for John Deere SF1, D for John Deere SF2, and W for WAAS. N_x refers to the number of total-station recorded positions available from each path (row).
[b] Values represent average XTE_x (cm), SD_x (cm), and $RMSE_x$ (cm) for this row given N_x datapoints. Negative or positive XTE_x values represent cross-track error to the right or left of the reference line, respectively. $P2P_x$ values are not dependent upon N_x, however.
[c] XTE, SD, and RMSE refer to average values across all five rows with all N_x datapoints for this event. P2P refers to average of four $P2P_x$ values available.
[d] N refers to sum of N_x datapoints.

Table O.16. Summary signal-correction quality statistics for east-to-west testing event 8 (June 5, 2007); tests R_{W51}, J_{W51}, D_{W51}, and W_{W51}.

Signal[a]	Row 1[b]	Row 2[b]	Row 3[b]	Row 4[b]	Row 5[b]	XTE[c]	N[d]	SD[c]	RMSE[c]	P2P[c]
XTE_R	4	4	1	3	14	3				
N_R	37	37	36	29	7		146			
SD_R	8	6	9	15	21			11		
$RMSE_R$	9	7	9	15	24				11	
$P2P_R$	--	0	-3	-2	11					2
XTE_J	10	36	28	24	26	25				
N_J	39	40	38	32	21		170			
SD_J	10	7	8	17	22			15		
$RMSE_J$	14	36	29	29	34				29	
$P2P_J$	--	26	-8	-4	2					4
XTE_D	15	35	18	16	5	18				
N_D	44	30	30	29	24		157			
SD_D	10	8	10	16	12			14		
$RMSE_D$	18	36	21	22	12				23	
$P2P_D$	--	20	-17	-2	-11					-2
XTE_W	80	34	59	41	48	54				
N_W	32	33	28	18	9		120			
SD_W	12	9	16	25	5			23		
$RMSE_W$	84	35	61	48	49				59	
$P2P_W$	--	-46	25	-18	7					-8

[a] Cross-track error by signal (XTE_x) refers to the correction signals evaluated during the test, marked by the subscript R for RTK, J for John Deere SF1, D for John Deere SF2, and W for WAAS. N_x refers to the number of total-station recorded positions available from each path (row).
[b] Values represent average XTE_x (cm), SD_x (cm), and $RMSE_x$ (cm) for this row given N_x datapoints. Negative or positive XTE_x values represent cross-track error to the right or left of the reference line, respectively. $P2P_x$ values are not dependent upon N_x, however.
[c] XTE, SD, and RMSE refer to average values across all five rows with all N_x datapoints for this event. P2P refers to average of four $P2P_x$ values available.
[d] N refers to sum of N_x datapoints.

Table O.17. Summary signal-correction quality statistics for east-to-west testing event 9 (June 5, 2007); tests J_{W52}, D_{W52}, and W_{W52}.

Signal[a]	Row 1[b]	Row 2[b]	Row 3[b]	Row 4[b]	Row 5[b]	XTE[c]	N[d]	SD[c]	RMSE[c]	P2P[c]
XTE_R										
N_R										
SD_R										
$RMSE_R$										
$P2P_R$										
XTE_J	29	28	20	22	28	25				
N_J	34	42	40	31	30		177			
SD_J	8	8	7	20	12			12		
$RMSE_J$	30	29	21	30	30				28	
$P2P_J$	--	-1	-8	2	6					0
XTE_D	31	-1	-70	-53	-17	-20				
N_D	38	38	36	30	26		168			
SD_D	5	8	19	34	36			44		
$RMSE_D$	31	8	72	63	40				48	
$P2P_D$	--	-32	-69	17	36					-12
XTE_W	-98	-54	-80	-32	-40	-64				
N_W	29	23	26	14	31		123			
SD_W	16	20	26	21	26			33		
$RMSE_W$	99	57	84	38	48				72	
$P2P_W$	--	44	-26	48	-8					58

[a] Cross-track error by signal (XTE_x) refers to the correction signals evaluated during the test, marked by the subscript R for RTK, J for John Deere SF1, D for John Deere SF2, and W for WAAS. N_x refers to the number of total-station recorded positions available from each path (row).
[b] Values represent average XTE_x (cm), SD_x (cm), and $RMSE_x$ (cm) for this row given N_x datapoints. Negative or positive XTE_x values represent cross-track error to the right or left of the reference line, respectively. $P2P_x$ values are not dependent upon N_x, however.
[c] XTE, SD, and RMSE refer to average values across all five rows with all N_x datapoints for this event. P2P refers to average of four $P2P_x$ values available.
[d] N refers to sum of N_x datapoints.

Table O.18. Summary signal-correction quality statistics for north-to-south testing event 9 (July 10, 2007); tests R_{S61}, J_{S61}, D_{S61}, and W_{S61}.

Signal[a]	Row 1[b]	Row 2[b]	Row 3[b]	Row 4[b]	Row 5[b]	XTE[c]	N[d]	SD[c]	RMSE[c]	P2P[c]
XTE_R	-2	-2	-4	-3	-3	-3				
N_R	51	55	54	64	63		287			
SD_R	10	6	4	7	8			7		
$RMSE_R$	10	6	6	7	9				8	
$P2P_R$	--	0	-2	1	0					0
XTE_J	16	-5	0	-3	-9	-1				
N_J	46	60	64	63	56		289			
SD_J	6	6	5	7	9			10		
$RMSE_J$	16	8	5	8	12				10	
$P2P_J$	--	-21	5	-3	-6					-6
XTE_D	-15	-43	-28	-12	-8	-21				
N_D	54	65	63	62	62		306			
SD_D	6	5	4	6	12			15		
$RMSE_D$	16	43	28	13	14				26	
$P2P_D$	--	-28	15	16	4					2
XTE_W	12	-17	-21	-3	-7	-9				
N_W	34	63	57	47	59		260			
SD_W	12	11	12	17	15			17		
$RMSE_W$	16	20	24	17	16				19	
$P2P_W$	--	-29	-4	18	-4					-5

[a] Cross-track error by signal (XTE_x) refers to the correction signals evaluated during the test, marked by the subscript R for RTK, J for John Deere SF1, D for John Deere SF2, and W for WAAS. N_x refers to the number of total-station recorded positions available from each path (row).
[b] Values represent average XTE_x (cm), SD_x (cm), and $RMSE_x$ (cm) for this row given N_x datapoints. Negative or positive XTE_x values represent cross-track error to the right or left of the reference line, respectively. $P2P_x$ values are not dependent upon N_x, however.
[c] XTE, SD, and RMSE refer to average values across all five rows with all N_x datapoints for this event. P2P refers to average of four $P2P_x$ values available.
[d] N refers to sum of N_x datapoints.

Table O.19. Summary signal-correction quality statistics for north-to-south testing event 10 (July 10, 2007); tests J_{S62}, D_{S62}, and W_{S62}.

Signal[a]	Row 1[b]	Row 2[b]	Row 3[b]	Row 4[b]	Row 5[b]	XTE[c]	N[d]	SD[c]	RMSE[c]	P2P[c]
XTE_R										
N_R										
SD_R										
$RMSE_R$										
$P2P_R$										
XTE_J	--	-23	-18	-16	-8	-16				
N_J	--	60	59	64	58		241			
SD_J	--	9	7	9	7			10		
$RMSE_J$	--	25	19	19	11				19	
$P2P_J$	--	--	5	0	8					4
XTE_D	-27	-12	-13	-4	1	-10				
N_D	50	61	60	63	60		294			
SD_D	9	10	7	7	7			12		
$RMSE_D$	28	15	15	8	7				16	
$P2P_D$	--	15	-1	9	3					6
XTE_W	13	-18	-8	-22	-12	-10				
N_W	52	56	63	62	62		295			
SD_W	10	13	12	17	13			18		
$RMSE_W$	16	22	16	28	18				20	
$P2P_W$	--	-31	10	-14	10					-6

[a] Cross-track error by signal (XTE_x) refers to the correction signals evaluated during the test, marked by the subscript R for RTK, J for John Deere SF1, D for John Deere SF2, and W for WAAS. N_x refers to the number of total-station recorded positions available from each path (row).
[b] Values represent average XTE_x (cm), SD_x (cm), and $RMSE_x$ (cm) for this row given N_x datapoints. Negative or positive XTE_x values represent cross-track error to the right or left of the reference line, respectively. $P2P_x$ values are not dependent upon N_x, however.
[c] XTE, SD, and RMSE refer to average values across all five rows with all N_x datapoints for this event. P2P refers to average of four $P2P_x$ values available.
[d] N refers to sum of N_x datapoints.

Table O.20. Summary signal-correction quality statistics for east-to-west testing event 10 (July 10, 2007); tests R_{W61}, J_{W61}, D_{W61}, and W_{W61}.

Signal[a]	Row 1[b]	Row 2[b]	Row 3[b]	Row 4[b]	Row 5[b]	XTE[c]	N[d]	SD[c]	RMSE[c]	P2P[c]
XTE_R	-2	-3	-4	-4	-3	-3				
N_R	31	33	33	36	31		164			
SD_R	5	7	9	8	7			7		
$RMSE_R$	6	8	10	8	4				8	
$P2P_R$	--	-1	-1	0	1					0
XTE_J	51	20	15	4	6	20				
N_J	38	34	37	33	34		176			
SD_J	5	5	9	11	10			19		
$RMSE_J$	51	21	18	12	12				28	
$P2P_J$	--	-31	-5	-9	2					-11
XTE_D	30	19	-5	-20	-22	0				
N_D	35	36	35	39	36		181			
SD_D	17	6	7	12	13			24		
$RMSE_D$	34	20	9	23	25				24	
$P2P_D$	--	-11	-24	-15	-2					-13
XTE_W	65	55	24	51	37	50				
N_W	36	42	20	25	27		150			
SD_W	12	17	16	29	13			22		
$RMSE_W$	66	58	28	58	40				54	
$P2P_W$	--	-10	-31	27	-14					-7

[a] Cross-track error by signal (XTE_x) refers to the correction signals evaluated during the test, marked by the subscript R for RTK, J for John Deere SF1, D for John Deere SF2, and W for WAAS. N_x refers to the number of total-station recorded positions available from each path (row).
[b] Values represent average XTE_x (cm), SD_x (cm), and $RMSE_x$ (cm) for this row given N_x datapoints. Negative or positive XTE_x values represent cross-track error to the right or left of the reference line, respectively. $P2P_x$ values are not dependent upon N_x, however.
[c] XTE, SD, and RMSE refer to average values across all five rows with all N_x datapoints for this event. P2P refers to average of four $P2P_x$ values available.
[d] N refers to sum of N_x datapoints.

Table O.21. Summary signal-correction quality statistics for east-to-west testing event 11 (July 10, 2007); tests J_{W62}, D_{W62}, and W_{W62}.

Signal[a]	Row 1[b]	Row 2[b]	Row 3[b]	Row 4[b]	Row 5[b]	XTE[c]	N[d]	SD[c]	RMSE[c]	P2P[c]
XTE_R										
N_R										
SD_R										
$RMSE_R$										
$P2P_R$	--									
XTE_J	27	16	27	16	15	20				
N_J	38	40	37	37	30		182			
SD_J	6	8	8	6	10			9		
$RMSE_J$	28	18	28	18	18				22	
$P2P_J$	--	-11	11	-11	-1					-3
XTE_D	16	13	12	5	-9	8				
N_D	40	33	40	40	34		187			
SD_D	6	7	9	9	6			12		
$RMSE_D$	17	14	15	10	11				14	
$P2P_D$	--	-3	-1	-7	-14					-6
XTE_W	-3	21	4	15	8	9				
N_W	32	34	34	23	30		153			
SD_W	8	6	11	17	15			14		
$RMSE_W$	9	22	11	23	17				17	
$P2P_W$	--	24	-17	11	-7					3

[a] Cross-track error by signal (XTE_x) refers to the correction signals evaluated during the test, marked by the subscript R for RTK, J for John Deere SF1, D for John Deere SF2, and W for WAAS. N_x refers to the number of total-station recorded positions available from each path (row).
[b] Values represent average XTE_x (cm), SD_x (cm), and $RMSE_x$ (cm) for this row given N_x datapoints. Negative or positive XTE_x values represent cross-track error to the right or left of the reference line, respectively. $P2P_x$ values are not dependent upon N_x, however.
[c] XTE, SD, and RMSE refer to average values across all five rows with all N_x datapoints for this event. P2P refers to average of four $P2P_x$ values available.
[d] N refers to sum of N_x datapoints.

Table O.22. Summary signal-correction quality statistics for north-to-south testing event 11 (July 18, 2007); tests R_{S71}, J_{S71}, D_{S71}, and W_{S71}.

Signal[a]	Row 1[b]	Row 2[b]	Row 3[b]	Row 4[b]	Row 5[b]	XTE[c]	N[d]	SD[c]	RMSE[c]	P2P[c]
XTE_R	4	-2	0	1	-2	0				
N_R	56	61	61	58	46		282			
SD_R	5	6	6	7	7			6		
$RMSE_R$	6	6	6	7	7				6	
$P2P_R$	--	-6	2	1	-3					-2
XTE_J	-47	-36	-44	-37	-31	-39				
N_J	58	65	70	65	44		302			
SD_J	8	8	6	10	9			10		
$RMSE_J$	48	37	44	38	32				41	
$P2P_J$	--	11	-8	7	6					4
XTE_D	-22	-25	-15	-17	-11	-19				
N_D	60	69	68	67	43		307			
SD_D	5	5	7	8	7			8		
$RMSE_D$	23	26	16	19	13				20	
$P2P_D$	--	-3	10	-2	6					3
XTE_W	25	9	12	15	24	16				
N_W	34	61	63	60	40		258			
SD_W	8	15	8	10	13			13		
$RMSE_W$	26	18	14	18	28				20	
$P2P_W$	--	-16	3	3	9					0

[a] Cross-track error by signal (XTE_x) refers to the correction signals evaluated during the test, marked by the subscript R for RTK, J for John Deere SF1, D for John Deere SF2, and W for WAAS. N_x refers to the number of total-station recorded positions available from each path (row).
[b] Values represent average XTE_x (cm), SD_x (cm), and $RMSE_x$ (cm) for this row given N_x datapoints. Negative or positive XTE_x values represent cross-track error to the right or left of the reference line, respectively. $P2P_x$ values are not dependent upon N_x, however.
[c] XTE, SD, and RMSE refer to average values across all five rows with all N_x datapoints for this event. P2P refers to average of four $P2P_x$ values available.
[d] N refers to sum of N_x datapoints.

Table O.23. Summary signal-correction quality statistics for north-to-south testing event 12 (July 18, 2007); tests J_{S72}, D_{S72}, and W_{S72}.

Signal[a]	Row 1[b]	Row 2[b]	Row 3[b]	Row 4[b]	Row 5[b]	XTE[c]	N[d]	SD[c]	RMSE[c]	P2P[c]
XTE_R										
N_R										
SD_R										
$RMSE_R$										
$P2P_R$										
XTE_J	-12	-39	-49	-40	-36	-40				
N_J	12	66	68	63	42		251			
SD_J	5	4	6	7	10			10		
$RMSE_J$	13	39	50	40	37				41	
$P2P_J$	--	-27	-10	9	4					-6
XTE_D	9	20	5	-4	-3	6				
N_D	59	65	63	60	46		293			
SD_D	6	7	6	7	8			11		
$RMSE_D$	11	21	8	8	9				13	
$P2P_D$	--	11	-15	-9	1					-3
XTE_W	--	18	-9	-6	-9	-1				
N_W	--	51	56	53	37		197			
SD_W	--	15	9	13	11			17		
$RMSE_W$	--	24	12	14	14				17	
$P2P_W$	--	--	-27	3	-3					-9

[a] Cross-track error by signal (XTE_x) refers to the correction signals evaluated during the test, marked by the subscript R for RTK, J for John Deere SF1, D for John Deere SF2, and W for WAAS. N_x refers to the number of total-station recorded positions available from each path (row).
[b] Values represent average XTE_x (cm), SD_x (cm), and $RMSE_x$ (cm) for this row given N_x datapoints. Negative or positive XTE_x values represent cross-track error to the right or left of the reference line, respectively. $P2P_x$ values are not dependent upon N_x, however.
[c] XTE, SD, and RMSE refer to average values across all five rows with all N_x datapoints for this event. P2P refers to average of four $P2P_x$ values available.
[d] N refers to sum of N_x datapoints.

Table O.24. Summary signal-correction quality statistics for north-to-south testing event 13 (July 18, 2007); tests J_{S73}, D_{S73}, and W_{S73}.

Signal[a]	Row 1[b]	Row 2[b]	Row 3[b]	Row 4[b]	Row 5[b]	XTE[c]	N[d]	SD[c]	RMSE[c]	P2P[c]
XTE_R										
N_R										
SD_R										
$RMSE_R$										
$P2P_R$										
XTE_J	-41	-41	-44	-45	-47	-43				
N_J	62	63	64	61	37		287			
SD_J	5	11	5	9	7			8		
$RMSE_J$	42	42	44	46	48				44	
$P2P_J$	--	0	-3	-1	-2					-2
XTE_D	17	12	20	26	24	20				
N_D	60	62	65	61	38		286			
SD_D	12	4	6	8	8			10		
$RMSE_D$	21	13	21	28	26				22	
$P2P_D$	--	-5	8	6	-2					2
XTE_W	-94	-88	-76	-69	-71	-80				
N_W	57	68	67	61	42		295			
SD_W	15	13	14	15	14			17		
$RMSE_W$	95	89	78	70	72				82	
$P2P_W$	--	6	12	7	-2					6

[a] Cross-track error by signal (XTE_x) refers to the correction signals evaluated during the test, marked by the subscript R for RTK, J for John Deere SF1, D for John Deere SF2, and W for WAAS. N_x refers to the number of total-station recorded positions available from each path (row).
[b] Values represent average XTE_x (cm), SD_x (cm), and $RMSE_x$ (cm) for this row given N_x datapoints. Negative or positive XTE_x values represent cross-track error to the right or left of the reference line, respectively. $P2P_x$ values are not dependent upon N_x, however.
[c] XTE, SD, and RMSE refer to average values across all five rows with all N_x datapoints for this event. P2P refers to average of four $P2P_x$ values available.
[d] N refers to sum of N_x datapoints.

Table O.25. Summary signal-correction quality statistics for east-to-west testing event 12 (July 18, 2007); tests R_{W71}, J_{W71}, D_{W71}, and W_{W71}.

Signal[a]	Row 1[b]	Row 2[b]	Row 3[b]	Row 4[b]	Row 5[b]	XTE[c]	N[d]	SD[c]	RMSE[c]	P2P[c]
XTE_R	-3	-5	-6	-6	-13	-2				
N_R	36	39	25	22	21		175			
SD_R	7	9	13	13	12			14		
$RMSE_R$	7	10	14	14	17				14	
$P2P_R$	--	-2	-1	0	-7					-2
XTE_J	32	36	32	27	28	32				
N_J	39	36	28	14	13		130			
SD_J	10	8	11	12	7			10		
$RMSE_J$	33	37	34	29	28				34	
$P2P_J$	--	4	-4	-5	1					-1
XTE_D	12	16	12	7	8	12				
N_D	39	41	33	21	18		152			
SD_D	7	9	17	16	16			13		
$RMSE_D$	14	19	20	17	17				18	
$P2P_D$	--	4	-4	-5	1					-1
XTE_W	78	52	38	37	38	54				
N_W	32	29	21	11	15		108			
SD_W	18	25	20	30	26			28		
$RMSE_W$	81	57	43	47	46				61	
$P2P_W$	--	-26	-14	-1	1					-10

[a] Cross-track error by signal (XTE_x) refers to the correction signals evaluated during the test, marked by the subscript R for RTK, J for John Deere SF1, D for John Deere SF2, and W for WAAS. N_x refers to the number of total-station recorded positions available from each path (row).
[b] Values represent average XTE_x (cm), SD_x (cm), and $RMSE_x$ (cm) for this row given N_x datapoints. Negative or positive XTE_x values represent cross-track error to the right or left of the reference line, respectively. $P2P_x$ values are not dependent upon N_x, however.
[c] XTE, SD, and RMSE refer to average values across all five rows with all N_x datapoints for this event. P2P refers to average of four $P2P_x$ values available.
[d] N refers to sum of N_x datapoints.

Table O.26. Summary signal-correction quality statistics for east-to-west testing event 13 (July 18, 2007); tests J_{W72}, D_{W72}, and W_{W72}.

Signal[a]	Row 1[b]	Row 2[b]	Row 3[b]	Row 4[b]	Row 5[b]	XTE[c]	N[d]	SD[c]	RMSE[c]	P2P[c]
XTE_R										
N_R										
SD_R										
$RMSE_R$										
$P2P_R$										
XTE_J	61	81	77	73	68	72				
N_J	35	34	32	32	33		166			
SD_J	15	6	19	17	27			19		
$RMSE_J$	63	81	79	75	73				74	
$P2P_J$	--	20	-4	-4	-5					2
XTE_D	44	48	67	45	69	53				
N_D	34	43	21	32	25		155			
SD_D	7	8	25	13	19			17		
$RMSE_D$	45	49	71	47	72				55	
$P2P_D$	--	4	19	-22	24					6
XTE_W	39	74	60	55	60	58				
N_W	34	35	28	30	32		159			
SD_W	7	18	14	20	22			21		
$RMSE_W$	39	76	61	58	64				61	
$P2P_W$	--	35	-14	-5	5					5

[a] Cross-track error by signal (XTE_x) refers to the correction signals evaluated during the test, marked by the subscript R for RTK, J for John Deere SF1, D for John Deere SF2, and W for WAAS. N_x refers to the number of total-station recorded positions available from each path (row).
[b] Values represent average XTE_x (cm), SD_x (cm), and $RMSE_x$ (cm) for this row given N_x datapoints. Negative or positive XTE_x values represent cross-track error to the right or left of the reference line, respectively. $P2P_x$ values are not dependent upon N_x, however.
[c] XTE, SD, and RMSE refer to average values across all five rows with all N_x datapoints for this event. P2P refers to average of four $P2P_x$ values available.
[d] N refers to sum of N_x datapoints.

Table O.27. Summary signal-correction quality statistics for east-to-west testing event 14 (July 18, 2007); tests J_{W73}, D_{W73}, and W_{W73}.

Signal[a]	Row 1[b]	Row 2[b]	Row 3[b]	Row 4[b]	Row 5[b]	XTE[c]	N[d]	SD[c]	RMSE[c]	P2P[c]
XTE_R										
N_R										
SD_R										
$RMSE_R$										
$P2P_R$										
XTE_J	49	49	56	45	37	47				
N_J	39	37	26	29	30		161			
SD_J	7	12	15	6	10			12		
$RMSE_J$	49	51	58	45	38				49	
$P2P_J$	--	0	7	-11	-8					-3
XTE_D	-3	-5	-9	-12	-6	-7				
N_D	37	37	30	33	29		166			
SD_D	8	10	12	16	17			13		
$RMSE_D$	8	11	14	20	17				15	
$P2P_D$	--	-2	-4	-3	6					-1
XTE_W	37	25	26	25	20	27				
N_W	34	26	26	28	23		137			
SD_W	8	14	17	16	7			14		
$RMSE_W$	38	28	31	30	21				31	
$P2P_W$	--	-12	1	-1	-5					-4

[a] Cross-track error by signal (XTE_x) refers to the correction signals evaluated during the test, marked by the subscript R for RTK, J for John Deere SF1, D for John Deere SF2, and W for WAAS. N_x refers to the number of total-station recorded positions available from each path (row).
[b] Values represent average XTE_x (cm), SD_x (cm), and $RMSE_x$ (cm) for this row given N_x datapoints. Negative or positive XTE_x values represent cross-track error to the right or left of the reference line, respectively. $P2P_x$ values are not dependent upon N_x, however.
[c] XTE, SD, and RMSE refer to average values across all five rows with all N_x datapoints for this event. P2P refers to average of four $P2P_x$ values available.
[d] N refers to sum of N_x datapoints.

Table O.28. Summary signal-correction quality statistics for north-to-south testing event 14 (July 31, 2007); tests R_{S81}, J_{S81}, D_{S81}, and W_{S81}.

Signal[a]	Row 1[b]	Row 2[b]	Row 3[b]	Row 4[b]	Row 5[b]	XTE[c]	N[d]	SD[c]	RMSE[c]	P2P[c]
XTE_R	6	-1	-1	2	0	1				
N_R	51	55	62	60	55		283			
SD_R	4	5	7	7	7			7		
$RMSE_R$	7	5	7	7	7				7	
$P2P_R$	--	-7	0	3	-2					-2
XTE_J	52	33	40	38	41	41				
N_J	54	60	61	60	58		293			
SD_J	4	5	6	7	7			9		
$RMSE_J$	52	33	41	38	42				41	
$P2P_J$	--	-19	7	-2	3					-3
XTE_D	18	16	19	22	21	19				
N_D	55	60	61	57	55		288			
SD_D	6	4	7	6	7			6		
$RMSE_D$	19	16	20	23	22				20	
$P2P_D$	--	-2	3	3	-1					1
XTE_W	91	62	49	85	97	77				
N_W	50	61	53	57	58		279			
SD_W	7	6	9	11	18			21		
$RMSE_W$	91	62	50	85	99				80	
$P2P_W$	--	-29	-13	36	12					2

[a] Cross-track error by signal (XTE_x) refers to the correction signals evaluated during the test, marked by the subscript R for RTK, J for John Deere SF1, D for John Deere SF2, and W for WAAS. N_x refers to the number of total-station recorded positions available from each path (row).
[b] Values represent average XTE_x (cm), SD_x (cm), and $RMSE_x$ (cm) for this row given N_x datapoints. Negative or positive XTE_x values represent cross-track error to the right or left of the reference line, respectively. $P2P_x$ values are not dependent upon N_x, however.
[c] XTE, SD, and RMSE refer to average values across all five rows with all N_x datapoints for this event. P2P refers to average of four $P2P_x$ values available.
[d] N refers to sum of N_x datapoints.

Table O.29. Summary signal-correction quality statistics for north-to-south testing event 15 (July 31, 2007); tests R_{S82}, J_{S82}, D_{S82}, and W_{S82}.

Signal[a]	Row 1[b]	Row 2[b]	Row 3[b]	Row 4[b]	Row 5[b]	XTE[c]	N[d]	SD[c]	RMSE[c]	P2P[c]
XTE_R	3	-2	-2	1	0	0				
N_R	53	64	65	66	64		312			
SD_R	5	4	7	7	7			6		
$RMSE_R$	5	4	7	7	7				6	
$P2P_R$	--	-5	0	3	-1					-1
XTE_J	75	59	71	73	78	71				
N_J	57	62	68	64	62		313			
SD_J	5	4	6	8	10			9		
$RMSE_J$	75	59	71	74	78				72	
$P2P_J$	--	-16	12	2	5					1
XTE_D	-1	3	1	4	13	3				
N_D	59	62	67	65	47		300			
SD_D	8	5	7	8	10			9		
$RMSE_D$	8	6	7	9	17				10	
$P2P_D$	--	4	-2	3	9					4
XTE_W	0	-36	-24	-29	-33	-24				
N_W	60	59	58	66	51		294			
SD_W	19	13	9	15	19			20		
$RMSE_W$	18	39	26	32	38				31	
$P2P_W$	--	-36	12	-5	-4					-8

[a] Cross-track error by signal (XTE_x) refers to the correction signals evaluated during the test, marked by the subscript R for RTK, J for John Deere SF1, D for John Deere SF2, and W for WAAS. N_x refers to the number of total-station recorded positions available from each path (row).
[b] Values represent average XTE_x (cm), SD_x (cm), and $RMSE_x$ (cm) for this row given N_x datapoints. Negative or positive XTE_x values represent cross-track error to the right or left of the reference line, respectively. $P2P_x$ values are not dependent upon N_x, however.
[c] XTE, SD, and RMSE refer to average values across all five rows with all N_x datapoints for this event. P2P refers to average of four $P2P_x$ values available.
[d] N refers to sum of N_x datapoints.

Table O.30. Summary signal-correction quality statistics for north-to-south testing event 16 (July 31, 2007); tests R_{S83}, J_{S83}, D_{S83}, and W_{S83}.

Signal[a]	Row 1[b]	Row 2[b]	Row 3[b]	Row 4[b]	Row 5[b]	XTE[c]	N[d]	SD[c]	RMSE[c]	P2P[c]
XTE_R	2	-4	-3	1	1	0				
N_R	60	61	63	59	60		303			
SD_R	5	5	5	5	6			6		
$RMSE_R$	6	6	5	5	6				6	
$P2P_R$	--	-6	1	4	0					0
XTE_J	85	82	95	86	86	87				
N_J	59	60	51	59	60		289			
SD_J	7	10	12	12	12			11		
$RMSE_J$	86	83	96	87	87				88	
$P2P_J$	--	-3	13	-9	0					0
XTE_D	-7	-10	3	-2	-13	-6				
N_D	58	61	65	63	59		306			
SD_D	8	4	7	7	8			9		
$RMSE_D$	11	11	8	7	15				11	
$P2P_D$	--	-3	13	-5	-11					-2
XTE_W	46	24	38	57	55	44				
N_W	57	58	63	54	59		291			
SD_W	13	5	13	14	12			17		
$RMSE_W$	48	24	40	59	56				47	
$P2P_W$	--	-22	14	19	-2					2

[a] Cross-track error by signal (XTE_x) refers to the correction signals evaluated during the test, marked by the subscript R for RTK, J for John Deere SF1, D for John Deere SF2, and W for WAAS. N_x refers to the number of total-station recorded positions available from each path (row).
[b] Values represent average XTE_x (cm), SD_x (cm), and $RMSE_x$ (cm) for this row given N_x datapoints. Negative or positive XTE_x values represent cross-track error to the right or left of the reference line, respectively. $P2P_x$ values are not dependent upon N_x, however.
[c] XTE, SD, and RMSE refer to average values across all five rows with all N_x datapoints for this event. P2P refers to average of four $P2P_x$ values available.
[d] N refers to sum of N_x datapoints.

Table O.31. Summary signal-correction quality statistics for east-to-west testing event 15 (July 31, 2007); tests R_{W81}, J_{W81}, D_{W81}, and W_{W81}.

Signal[a]	Row 1[b]	Row 2[b]	Row 3[b]	Row 4[b]	Row 5[b]	XTE[c]	N[d]	SD[c]	RMSE[c]	P2P[c]
XTE_R	-3	-4	0	-6	-11	-5				
N_R	37	37	35	40	22		171			
SD_R	6	8	9	10	9			9		
$RMSE_R$	6	9	8	12	14				10	
$P2P_R$	--	-1	4	-6	-5					-2
XTE_J	18	14	18	12	11	15				
N_J	36	37	39	30	22		164			
SD_J	6	6	9	8	7			8		
$RMSE_J$	19	16	20	14	13				17	
$P2P_J$	--	-4	4	-6	-1					-2
XTE_D	-2	10	17	9	10	9				
N_D	36	37	34	38	27		172			
SD_D	6	6	9	11	8			10		
$RMSE_D$	6	12	19	15	12				13	
$P2P_D$	--	12	7	-8	1					3
XTE_W	67	88	87	102	103	89				
N_W	32	31	31	30	27		151			
SD_W	8	12	14	26	19			22		
$RMSE_W$	67	89	88	106	105				92	
$P2P_W$	--	21	-1	15	1					9

[a] Cross-track error by signal (XTE_x) refers to the correction signals evaluated during the test, marked by the subscript R for RTK, J for John Deere SF1, D for John Deere SF2, and W for WAAS. N_x refers to the number of total-station recorded positions available from each path (row).
[b] Values represent average XTE_x (cm), SD_x (cm), and $RMSE_x$ (cm) for this row given N_x datapoints. Negative or positive XTE_x values represent cross-track error to the right or left of the reference line, respectively. $P2P_x$ values are not dependent upon N_x, however.
[c] XTE, SD, and RMSE refer to average values across all five rows with all N_x datapoints for this event. P2P refers to average of four $P2P_x$ values available.
[d] N refers to sum of N_x datapoints.

Table O.32. Summary signal-correction quality statistics for east-to-west testing event 16 (July 31, 2007); tests R_{W82}, J_{W82}, D_{W82}, and W_{W82}.

Signal[a]	Row 1[b]	Row 2[b]	Row 3[b]	Row 4[b]	Row 5[b]	XTE[c]	N[d]	SD[c]	RMSE[c]	P2P[c]
XTE_R	-3	-1	-3	-8	-7	-4				
N_R	39	39	39	36	22		175			
SD_R	6	6	11	12	8			9		
$RMSE_R$	7	6	11	15	10				10	
$P2P_R$	--	2	-2	-5	1					-1
XTE_J	-31	0	4	-6	-7	-7				
N_J	36	41	41	31	33		182			
SD_J	11	7	10	23	19			19		
$RMSE_J$	33	7	11	23	20				20	
$P2P_J$	--	31	4	-10	-1					6
XTE_D	0	4	-3	-8	-10	-3				
N_D	36	38	40	35	26		175			
SD_D	8	5	10	11	8			10		
$RMSE_D$	8	7	10	14	13				10	
$P2P_D$	--	4	-7	-5	-2					-2
XTE_W	33	113	118	113	122	98				
N_W	34	34	30	28	25		151			
SD_W	11	11	29	12	20			39		
$RMSE_W$	35	113	122	114	123				105	
$P2P_W$	--	80	5	-5	9					22

[a] Cross-track error by signal (XTE_x) refers to the correction signals evaluated during the test, marked by the subscript R for RTK, J for John Deere SF1, D for John Deere SF2, and W for WAAS. N_x refers to the number of total-station recorded positions available from each path (row).
[b] Values represent average XTE_x (cm), SD_x (cm), and $RMSE_x$ (cm) for this row given N_x datapoints. Negative or positive XTE_x values represent cross-track error to the right or left of the reference line, respectively. $P2P_x$ values are not dependent upon N_x, however.
[c] XTE, SD, and RMSE refer to average values across all five rows with all N_x datapoints for this event. P2P refers to average of four $P2P_x$ values available.
[d] N refers to sum of N_x datapoints.

Table O.33. Summary signal-correction quality statistics for north-to-south testing event 17 (August 3, 2007); tests R_{S91}, J_{S91}, D_{S91}, and W_{S91}.

Signal[a]	Row 1[b]	Row 2[b]	Row 3[b]	Row 4[b]	Row 5[b]	XTE[c]	N[d]	SD[c]	RMSE[c]	P2P[c]
XTE_R	2	-7	-5	-7	-8	-5				
N_R	54	52	58	53	41		258			
SD_R	7	6	6	6	5			7		
$RMSE_R$	7	9	8	9	10				9	
$P2P_R$	--	-9	2	-2	-1					-2
XTE_J	-25	-15	3	4	20	-2				
N_J	48	43	51	46	47		235			
SD_J	7	14	16	23	19			23		
$RMSE_J$	26	20	17	23	27				23	
$P2P_J$	--	10	18	1	16					9
XTE_D	-2	-16	-21	-21	-33	-19				
N_D	45	42	46	49	51		233			
SD_D	5	19	17	19	21			20		
$RMSE_D$	5	24	27	28	39				28	
$P2P_D$	--	-14	-5	0	-12					-8
XTE_W	-56	-45	-77	-58	-53	-59				
N_W	20	45	54	57	55		231			
SD_W	12	27	20	20	24			25		
$RMSE_W$	57	52	80	61	58				64	
$P2P_W$	--	11	-32	19	5					1

[a] Cross-track error by signal (XTE_x) refers to the correction signals evaluated during the test, marked by the subscript R for RTK, J for John Deere SF1, D for John Deere SF2, and W for WAAS. N_x refers to the number of total-station recorded positions available from each path (row).
[b] Values represent average XTE_x (cm), SD_x (cm), and $RMSE_x$ (cm) for this row given N_x datapoints. Negative or positive XTE_x values represent cross-track error to the right or left of the reference line, respectively. $P2P_x$ values are not dependent upon N_x, however.
[c] XTE, SD, and RMSE refer to average values across all five rows with all N_x datapoints for this event. P2P refers to average of four $P2P_x$ values available.
[d] N refers to sum of N_x datapoints.

Table O.34. Summary signal-correction quality statistics for east-to-west testing event 17 (August 3, 2007); tests R_{W91}, J_{W91}, D_{W91}, and W_{W91}.

Signal[a]	Row 1[b]	Row 2[b]	Row 3[b]	Row 4[b]	Row 5[b]	XTE[c]	N[d]	SD[c]	RMSE[c]	P2P[c]
XTE_R	35	28	23	29	32	29				
N_R	31	33	31	13	26		134			
SD_R	12	13	24	38	17			20		
$RMSE_R$	37	30	32	47	36				35	
$P2P_R$	--	-7	-5	6	3					-1
XTE_J	-54	-47	-42	-41	-33	-43				
N_J	19	32	30	25	21		127			
SD_J	14	11	16	13	14			15		
$RMSE_J$	56	48	45	43	36				46	
$P2P_J$	--	7	5	1	8					5
XTE_D	120	-74	44	82	17	37				
N_D	27	32	37	35	25		156			
SD_D	14	17	32	40	18			71		
$RMSE_D$	121	76	55	91	25				80	
$P2P_D$	--	-194	118	38	-65					-26
XTE_W	11	5	-5	35	22	13				
N_W	33	27	23	20	24		127			
SD_W	8	15	15	13	19			19		
$RMSE_W$	13	15	15	37	28				22	
$P2P_W$	--	-6	-10	40	-13					3

[a] Cross-track error by signal (XTE_x) refers to the correction signals evaluated during the test, marked by the subscript R for RTK, J for John Deere SF1, D for John Deere SF2, and W for WAAS. N_x refers to the number of total-station recorded positions available from each path (row).
[b] Values represent average XTE_x (cm), SD_x (cm), and $RMSE_x$ (cm) for this row given N_x datapoints. Negative or positive XTE_x values represent cross-track error to the right or left of the reference line, respectively. $P2P_x$ values are not dependent upon N_x, however.
[c] XTE, SD, and RMSE refer to average values across all five rows with all N_x datapoints for this event. P2P refers to average of four $P2P_x$ values available.
[d] N refers to sum of N_x datapoints.

Table O.35. Summary signal-correction quality statistics for north-to-south testing event 18 (August 23, 2007); tests R_{S101}, J_{S101}, D_{S101}, and W_{S101}.

Signal[a]	Row 1[b]	Row 2[b]	Row 3[b]	Row 4[b]	Row 5[b]	XTE[c]	N[d]	SD[c]	RMSE[c]	P2P[c]
XTE_R	3	-4	-3	-3	-6	-3				
N_R	44	51	45	62	58		260			
SD_R	6	6	7	6	7			7		
$RMSE_R$	6	7	7	7	9				7	
$P2P_R$	--	-7	1	0	-3					-2
XTE_J	-56	--	-51	-52	-59	-54				
N_J	55	--	69	64	56		244			
SD_J	4	--	6	6	9			7		
$RMSE_J$	56	-	51	52	60				55	
$P2P_J$	--	--	5	-1	-7					-1
XTE_D	-8	-40	-50	-42	-38	-41				
N_D	13	52	58	62	60		245			
SD_D	2	9	7	7	9			12		
$RMSE_D$	8	41	50	43	39				42	
$P2P_D$	--	-32	-10	8	4					-8
XTE_W	112	95	95	112	129	109				
N_W	51	55	63	61	63		293			
SD_W	5	6	7	13	13			16		
$RMSE_W$	113	95	95	113	129				110	
$P2P_W$	--	-17	0	17	17					4

[a] Cross-track error by signal (XTE_x) refers to the correction signals evaluated during the test, marked by the subscript R for RTK, J for John Deere SF1, D for John Deere SF2, and W for WAAS. N_x refers to the number of total-station recorded positions available from each path (row).
[b] Values represent average XTE_x (cm), SD_x (cm), and $RMSE_x$ (cm) for this row given N_x datapoints. Negative or positive XTE_x values represent cross-track error to the right or left of the reference line, respectively. $P2P_x$ values are not dependent upon N_x, however.
[c] XTE, SD, and RMSE refer to average values across all five rows with all N_x datapoints for this event. P2P refers to average of four $P2P_x$ values available.
[d] N refers to sum of N_x datapoints.

Table O.36. Summary signal-correction quality statistics for north-to-south testing event 19 (August 23, 2007); tests R_{S102}, J_{S102}, D_{S102}, and W_{S102}.

Signal[a]	Row 1[b]	Row 2[b]	Row 3[b]	Row 4[b]	Row 5[b]	XTE[c]	N[d]	SD[c]	RMSE[c]	P2P[c]
XTE_R	21	1	-3	-6	-10	0				
N_R	55	56	67	66	61		305			
SD_R	6	19	8	9	12			15		
$RMSE_R$	22	18	8	10	15				15	
$P2P_R$	--	-20	-4	-3	-4					-8
XTE_J	41	53	44	28	20	37				
N_J	54	57	59	61	51		282			
SD_J	9	6	9	7	10			14		
$RMSE_J$	42	53	45	28	22				40	
$P2P_J$	--	12	-9	-16	-8					-5
XTE_D	36	15	8	16	14	18				
N_D	61	63	66	68	62		320			
SD_D	7	12	7	8	10			13		
$RMSE_D$	37	19	10	18	18				22	
$P2P_D$	--	-21	-7	8	-2					-6
XTE_W	23	19	17	18	20	19				
N_W	25	53	49	63	60		250			
SD_W	35	19	20	11	15			19		
$RMSE_W$	41	27	26	21	25				27	
$P2P_W$	--	-4	-2	1	2					-1

[a] Cross-track error by signal (XTE_x) refers to the correction signals evaluated during the test, marked by the subscript R for RTK, J for John Deere SF1, D for John Deere SF2, and W for WAAS. N_x refers to the number of total-station recorded positions available from each path (row).
[b] Values represent average XTE_x (cm), SD_x (cm), and $RMSE_x$ (cm) for this row given N_x datapoints. Negative or positive XTE_x values represent cross-track error to the right or left of the reference line, respectively. $P2P_x$ values are not dependent upon N_x, however.
[c] XTE, SD, and RMSE refer to average values across all five rows with all N_x datapoints for this event. P2P refers to average of four $P2P_x$ values available.
[d] N refers to sum of N_x datapoints.

Table O.37. Summary signal-correction quality statistics for north-to-south testing event 20 (August 23, 2007); tests R_{S103}, J_{S103}, D_{S103}, and W_{S103}.

Signal[a]	Row 1[b]	Row 2[b]	Row 3[b]	Row 4[b]	Row 5[b]	XTE[c]	N[d]	SD[c]	RMSE[c]	P2P[c]
XTE_R	-3	-4	-6	-6	-4	-5				
N_R	46	55	57	50	46		254			
SD_R	3	6	5	6	6			6		
$RMSE_R$	4	8	8	8	7				7	
$P2P_R$	--	-1	-2	0	2					0
XTE_J	-27	-20	-18	-20	-37	-24				
N_J	43	53	52	54	52		254			
SD_J	6	5	7	8	7			10		
$RMSE_J$	27	21	19	22	38				26	
$P2P_J$	--	7	2	-2	-17					-2
XTE_D	-24	-24	-12	-12	-12	-17				
N_D	52	55	55	54	54		270			
SD_D	6	2	9	9	10			10		
$RMSE_D$	25	25	14	15	16				20	
$P2P_D$	--	0	12	0	0					3
XTE_W	-133	-222	-228	-235	-209	-206				
N_W	53	57	57	59	51		277			
SD_W	17	12	23	24	19			42		
$RMSE_W$	134	222	229	237	210				211	
$P2P_W$	--	-89	-6	-7	26					-19

[a] Cross-track error by signal (XTE_x) refers to the correction signals evaluated during the test, marked by the subscript R for RTK, J for John Deere SF1, D for John Deere SF2, and W for WAAS. N_x refers to the number of total-station recorded positions available from each path (row).
[b] Values represent average XTE_x (cm), SD_x (cm), and $RMSE_x$ (cm) for this row given N_x datapoints. Negative or positive XTE_x values represent cross-track error to the right or left of the reference line, respectively. $P2P_x$ values are not dependent upon N_x, however.
[c] XTE, SD, and RMSE refer to average values across all five rows with all N_x datapoints for this event. P2P refers to average of four $P2P_x$ values available.
[d] N refers to sum of N_x datapoints.

Table O.38. Summary signal-correction quality statistics for east-to-west testing event 18 (August 3, 2007); tests R_{W101}, J_{W101}, D_{W101}, and W_{W101}.

Signal[a]	Row 1[b]	Row 2[b]	Row 3[b]	Row 4[b]	Row 5[b]	XTE[c]	N[d]	SD[c]	RMSE[c]	P2P[c]
XTE_R	-1	-5	-5	-4	-1	-3				
N_R	44	33	35	31	18		161			
SD_R	10	8	8	11	13			10		
$RMSE_R$	10	9	9	11	12				10	
$P2P_R$	--	-4	0	1	3					0
XTE_J	-54	-41	-42	-49	-41	-46				
N_J	40	39	38	36	33		186			
SD_J	8	9	9	11	19			13		
$RMSE_J$	55	42	43	50	45				47	
$P2P_J$	--	13	-1	-7	8					3
XTE_D	9	-34	-77	-100	-86	-55				
N_D	39	41	34	34	35		183			
SD_D	6	10	10	17	19			42		
$RMSE_D$	11	36	77	101	88				69	
$P2P_D$	--	-43	-43	-23	14					-24
XTE_W	33	65	50	46	81	55				
N_W	27	25	34	29	28		143			
SD_W	15	12	16	20	9			22		
$RMSE_W$	37	66	52	50	81				59	
$P2P_W$	--	32	-15	-4	35					12

[a] Cross-track error by signal (XTE_x) refers to the correction signals evaluated during the test, marked by the subscript R for RTK, J for John Deere SF1, D for John Deere SF2, and W for WAAS. N_x refers to the number of total-station recorded positions available from each path (row).
[b] Values represent average XTE_x (cm), SD_x (cm), and $RMSE_x$ (cm) for this row given N_x datapoints. Negative or positive XTE_x values represent cross-track error to the right or left of the reference line, respectively. $P2P_x$ values are not dependent upon N_x, however.
[c] XTE, SD, and RMSE refer to average values across all five rows with all N_x datapoints for this event. P2P refers to average of four $P2P_x$ values available.
[d] N refers to sum of N_x datapoints.

Table O.39. Summary signal-correction quality statistics for east-to-west testing event 19 (August 3, 2007); tests R_{W102}, J_{W102}, D_{W102}, and W_{W102}.

Signal[a]	Row 1[b]	Row 2[b]	Row 3[b]	Row 4[b]	Row 5[b]	XTE[c]	N[d]	SD[c]	RMSE[c]	P2P[c]
XTE_R	2	2	-2	-2	-6	-1				
N_R	36	39	38	36	32		181			
SD_R	6	6	10	11	12			10		
$RMSE_R$	6	7	10	11	14				10	
$P2P_R$	--	0	-4	0	-4					-2
XTE_J	--	0	-15	-20	-19	-14				
N_J	--	28	36	37	33		134			
SD_J	--	7	9	14	14			14		
$RMSE_J$	--	7	17	24	24				20	
$P2P_J$	--	--	-15	-5	1					-6
XTE_D	-3	-20	-14	-12	-7	-11				
N_D	36	40	38	38	32		184			
SD_D	5	7	10	12	18			12		
$RMSE_D$	5	21	17	16	16				17	
$P2P_D$	--	-17	6	2	5					-1
XTE_W	52	81	86	77	68	73				
N_W	33	28	31	38	30		160			
SD_W	15	9	12	10	17			18		
$RMSE_W$	54	82	87	78	70				75	
$P2P_W$	--	29	5	-9	-9					4

[a] Cross-track error by signal (XTE_x) refers to the correction signals evaluated during the test, marked by the subscript R for RTK, J for John Deere SF1, D for John Deere SF2, and W for WAAS. N_x refers to the number of total-station recorded positions available from each path (row).
[b] Values represent average XTE_x (cm), SD_x (cm), and $RMSE_x$ (cm) for this row given N_x datapoints. Negative or positive XTE_x values represent cross-track error to the right or left of the reference line, respectively. $P2P_x$ values are not dependent upon N_x, however.
[c] XTE, SD, and RMSE refer to average values across all five rows with all N_x datapoints for this event. P2P refers to average of four $P2P_x$ values available.
[d] N refers to sum of N_x datapoints.

Table O.40. Summary signal-correction quality statistics for east-to-west testing event 20 (August 3, 2007); tests R_{W103}, J_{W103}, D_{W103}, and W_{W103}.

Signal[a]	Row 1[b]	Row 2[b]	Row 3[b]	Row 4[b]	Row 5[b]	XTE[c]	N[d]	SD[c]	RMSE[c]	P2P[c]
XTE_R	0	0	-2	-5	-3	-2				
N_R	37	34	35	26	23		155			
SD_R	7	8	16	18	13			13		
$RMSE_R$	7	8	16	19	13				13	
$P2P_R$	--	0	-2	-3	2					-1
XTE_J	2	-10	3	4	7	1				
N_J	35	30	35	27	20		147			
SD_J	6	12	12	18	15			13		
$RMSE_J$	6	15	12	18	16				14	
$P2P_J$	--	-12	13	1	3					1
XTE_D	2	16	15	11	9	11				
N_D	39	37	38	22	22		158			
SD_D	7	10	10	15	14			12		
$RMSE_D$	8	19	18	18	16				16	
$P2P_D$	--	14	-1	-4	-2					2
XTE_W	35	-30	-83	-110	-134	-59				
N_W	33	30	23	29	26		141			
SD_W	12	12	25	25	42			67		
$RMSE_W$	37	33	87	112	140				89	
$P2P_W$	--	-65	-53	-27	-24					-42

[a] Cross-track error by signal (XTE_x) refers to the correction signals evaluated during the test, marked by the subscript R for RTK, J for John Deere SF1, D for John Deere SF2, and W for WAAS. N_x refers to the number of total-station recorded positions available from each path (row).
[b] Values represent average XTE_x (cm), SD_x (cm), and $RMSE_x$ (cm) for this row given N_x datapoints. Negative or positive XTE_x values represent cross-track error to the right or left of the reference line, respectively. $P2P_x$ values are not dependent upon N_x, however.
[c] XTE, SD, and RMSE refer to average values across all five rows with all N_x datapoints for this event. P2P refers to average of four $P2P_x$ values available.
[d] N refers to sum of N_x datapoints.

Table O.41. Box-and-whisker plot data for the 2007 season (RTK correction).

Testing Event [a]	Min	Q1	Med	Q3	Max	Testing Event [a]	Min	Q1	Med	Q3	Max
southward						westward					
R_{S11}	-15	-2	3	8	21	R_{W21}	-9	6	14	19	33
R_{S21}	-19	-6	-1	4	18	R_{W22}	-3	11	16	21	29
R_{S22}	-20	-6	0	4	11	R_{W31}	-11	8	14	21	36
R_{S31}	-17	-4	0	4	12	R_{W32}	-9	11	15	20	35
R_{S32}	-22	-5	0	5	21	R_{W51}	-26	-3	4	10	34
R_{S41}	-18	-4	0	4	16	R_{W61}	-20	-8	-3	2	16
R_{S51}	-22	-12	-6	-2	12	R_{W71}	-39	-11	-5	3	12
R_{S52}	-30	-14	-9	-3	12	R_{W81}	-29	-11	-4	2	14
R_{S61}	-22	-8	-2	2	17	R_{W82}	-32	-11	-4	2	16
R_{S71}	-17	-4	0	5	15	R_{W91}	-29	17	31	44	72
R_{S81}	-17	-3	1	6	18	R_{W101}	-33	-10	-3	5	14
R_{S82}	-17	-4	0	4	15	R_{W102}	-27	-8	1	6	19
R_{S83}	-14	-5	-1	4	14	R_{W103}	-40	-8	-1	7	32
R_{S91}	-22	-10	-5	0	13	Summary	-33	-5	4	13	42
R_{S101}	-21	-8	-3	1	14						
R_{S102}	-41	-10	-2	12	38						
R_{S103}	-18	-8	-4	-1	10						
Summary	-22	-7	-1	3	19						

[a] Testing events are listed in Appendix J.

Table O.42. Box-and-whisker plot data for the 2007 season (SF1 correction).

Testing Event [a]	Min	Q1	Med	Q3	Max	Testing Event [a]	Min	Q1	Med	Q3	Max
southward						westward					
J_{S11}	12	32	43	52	73	J_{W11}	7	32	40	47	66
J_{S21}	17	49	67	75	95	J_{W12}	-9	40	58	69	90
J_{S22}	-52	2	23	30	86	J_{W21}	-2	26	33	43	59
J_{S31}	11	39	48	58	81	J_{W22}	4	26	34	40	53
J_{S32}	-9	29	44	52	87	J_{W31}	-1	20	26	33	49
J_{S41}	29	47	53	58	77	J_{W32}	-53	-17	-7	3	27
J_{S51}	-49	-31	-25	-19	-1	J_{W51}	-21	14	27	36	54
J_{S52}	-102	-73	-66	-54	-31	J_{W52}	-9	20	26	32	51
J_{S61}	-26	-7	-1	4	24	J_{W61}	-25	8	17	29	61
J_{S62}	-45	-23	-16	-10	10	J_{W62}	-6	14	21	27	42
J_{S71}	-62	-46	-41	-33	-15	J_{W71}	1	28	34	39	50
J_{S72}	-65	-47	-40	-35	-6	J_{W72}	20	62	78	85	100
J_{S73}	-64	-49	-43	-38	-23	J_{W73}	11	40	48	55	78
J_{S81}	18	34	41	47	64	J_{W81}	-7	10	15	20	34
J_{S82}	46	65	72	78	94	J_{W82}	-56	-18	-2	6	21
J_{S83}	58	78	87	94	117	J_{W91}	-83	-52	-43	-34	-10
J_{S91}	-56	-22	-5	18	50	J_{W101}	-81	-54	-44	-37	-17
J_{S101}	-85	-59	-53	-49	-37	J_{W102}	-55	-22	-14	-4	13
J_{S102}	0	27	38	49	70	J_{W103}	-37	-6	2	10	29
J_{S103}	-50	-28	-23	-17	-4	Summary	-57	1	22	38	94
Summary	-102	-31	21	52	117						

[a] Testing events are listed in Appendix J.

Table O.43. Box-and-whisker plot data for the 2007 season (SF2 correction).

Testing Event [a]	Min	Q1	Med	Q3	Max	Testing Event [a]	Min	Q1	Med	Q3	Max
southward						westward					
D_{S11}	34	47	51	55	66	D_{W11}	14	54	64	72	83
D_{S21}	-44	-21	-15	-6	15	D_{W12}	-24	59	87	116	145
D_{S22}	10	26	31	38	53	D_{W21}	-67	13	29	55	77
D_{S31}	-2	36	51	63	79	D_{W22}	-239	-200	-106	-58	-30
D_{S32}	-71	-36	-20	2	30	D_{W31}	5	28	37	47	65
D_{S41}	19	33	38	44	61	D_{W32}	-64	-49	-42	-38	13
D_{S51}	-54	-30	-21	-13	7	D_{W41}	-87	-31	-14	4	21
D_{S52}	-2	23	32	41	63	D_{W51}	-24	7	19	27	50
D_{S61}	-53	-32	-20	-10	14	D_{W52}	-134	-62	-5	14	42
D_{S62}	-41	-18	-9	-2	21	D_{W61}	-57	-17	-5	20	58
D_{S71}	-36	-25	-19	-14	3	D_{W62}	-22	0	10	16	37
D_{S72}	-22	-2	6	14	34	D_{W71}	-25	6	14	21	37
D_{S73}	-6	13	19	26	45	D_{W72}	10	43	50	58	97
D_{S81}	2	15	19	23	34	D_{W73}	-46	-13	-4	3	14
D_{S82}	-18	-2	3	9	26	D_{W81}	-16	1	9	15	33
D_{S83}	-29	-12	-6	1	16	D_{W82}	-31	-10	-2	4	23
D_{S91}	-78	-33	-14	-4	13	D_{W91}	-111	-7	44	100	144
D_{S101}	-72	-48	-42	-36	-5	D_{W101}	-166	-86	-70	-28	20
D_{S102}	-15	9	16	26	48	D_{W102}	-46	-20	-11	-4	22
D_{S103}	-44	-25	-17	-10	9	D_{W103}	-26	3	12	20	30
Summary	-78	-16	3	27	79	Summary	-84	-13	7	27	95

[a] Testing events are listed in Appendix J.

Table O.44. Box-and-whisker plot data for the 2007 season (WAAS correction).

Testing Event [a]	Min	Q1	Med	Q3	Max	Testing Event [a]	Min	Q1	Med	Q3	Max
southward						westward					
W_{S11}	-105	-61	-50	-33	10	W_{W11}	56	112	138	151	175
W_{S21}	-76	-28	-13	5	38	W_{W12}	9	54	72	85	95
W_{S22}	-45	3	12	27	47	W_{W21}	-72	18	44	74	138
W_{S31}	-98	-49	-31	-17	35	W_{W22}	-172	-99	-69	-38	41
W_{S32}	-40	-11	-4	10	73	W_{W31}	-205	-162	-136	-91	-1
W_{S41}	-59	-32	-21	-10	18	W_{W32}	-104	-22	17	35	85
W_{S51}	-85	-41	-28	-14	28	W_{W51}	-8	37	52	71	98
W_{S52}	-54	-15	-6	10	44	W_{W52}	-143	-96	-55	-32	-17
W_{S61}	-50	-22	-10	1	36	W_{W61}	-16	36	52	64	110
W_{S62}	-53	-21	-12	2	29	W_{W62}	-31	-1	10	21	38
W_{S71}	-13	7	16	24	51	W_{W71}	-30	39	60	70	115
W_{S72}	-39	-11	-2	4	43	W_{W72}	-5	40	62	73	103
W_{S73}	-111	-94	-79	-70	-32	W_{W73}	-17	19	30	37	56
W_{S81}	11	59	80	92	135	W_{W81}	37	71	92	103	147
W_{S82}	-77	-37	-25	-12	20	W_{W82}	14	68	115	125	145
W_{S83}	-5	28	47	57	81	W_{W91}	-30	2	12	22	52
W_{S91}	-119	-77	-60	-44	7	W_{W101}	-2	41	57	70	94
W_{S101}	71	96	106	119	153	W_{W102}	18	63	76	85	112
W_{S102}	-31	6	20	29	69	W_{W103}	-202	-99	-74	-15	67
W_{S103}	-307	-236	-219	-189	-97	Summary	-112	10	44	77	175
Summary	-119	-33	-10	16	102						

[a] Testing events are listed in Appendix J.

APPENDIX P

SDI PRODUCT SPECIFICATIONS AND LABORATORY DATA

P.1 DRIPLINE PRODUCT SPECIFICATIONS

The dripline product evaluated for this study was Netafim® DripNET PC™ pressure-compensating product (Netafim USA, 2010). Manufacturer emitter data are presented in figure P.1-1. Manufacturer product performance, as a function of flow rate versus operating pressure, is presented in figure P.1-2.

Figure P.1-1. Dripline emitter data provided by manufacturer.

DRIPPER DATA

Dripper GPH	Exponent (x)	Constant (k)	Kd 636	Kd 875	Cv
0.26	0.0	0.26	0.40	0.25	0.025

Figure P.1-2. Dripline product performance provided by manufacturer.

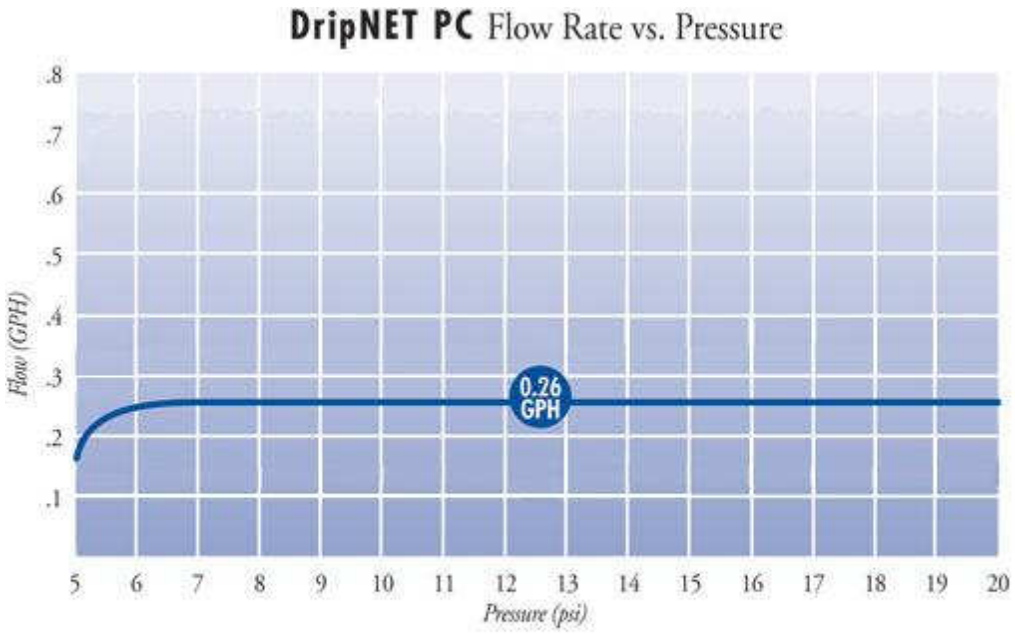

P.2 HORIZONTAL (0% SLOPE) TESTS

A section of new Netafim® DripNET PC™ dripline with 20 contiguous emitters was selected for testing. To establish a baseline measurement, the dripline was conditioned for up to one hour at an operating pressure of 83 kPa; after this conditioning period, emitter discharge was recorded for a five-minute period. Three replications occurred in this manner, and the five-minute emitter discharge values are recorded in Table P.2.

Table P.2. Five-minute emitter discharge (mL) from horizontal dripline, 83 kPa test.

	Rep 1	Rep 2	Rep 3
	89	91	91
	91	94	92
	84	86	85
	94	96	92
	86	88	89
	86	87	86
	85	85	85
	92	93	95
	88	90	90
	83	84	85
	84	86	87
	81	82	84
	85	88	88
	90	92	91
	91	94	95
	89	90	91
	92	91	94
	88	89	89
	87	88	88
	89	89	91
Cumul.	1754	1783	1788
Mean	88	89	89
SD	3.4	3.6	3.4
CV, %	3.9	4.1	3.8

P.3 COMPARISON OF SLOPE (0% VS. 6% RISE)

The section of new Netafim® DripNET PC™ dripline with 20 contiguous emitters used to generate data for Table P.2 was selected for re-testing. The dripline was oriented horizontally (0% slope) and conditioned for up to one hour at an operating pressure of 117 kPa; after this conditioning period, emitter discharge was recorded for a five-minute period. The dripline was then oriented on a slope (6% rise) and conditioned for up to one hour at an average operating pressure of 117 kPa; after this conditioning period, emitter discharge was recorded for a five-minute period. One replication for each slope occurred, and the five-minute emitter discharge values are recorded in Table P.3.

Table P.3. Five-minute emitter discharge (mL) from dripline on two slopes, 117 kPa test.

	0% slope	6% slope
	88	89
	93	92
	85	87
	92	94
	86	88
	85	87
	85	84
	91	92
	90	91
	84	83
	85	86
	81	84
	86	88
	90	92
	92	89
	89	88
	90	83
	86	86
	86	86
	85	85
Cumul.	1749	1754
Mean	87	88
SD	3.2	3.2
CV, %	3.7	3.7

P.4 OPERATING-PRESSURE TESTS, SIX-PERCENT SLOPE RISE

A section of new Netafim® DripNET PC™ dripline with 20 contiguous emitters was selected for testing. The dripline was oriented on a slope (6% rise) and conditioned for at least 15 minutes at an initial minimum operating pressure of 48 kPa; after this conditioning period, emitter discharge was recorded for a five-minute period. While discharge continued, the operating pressure was increased to the next desired level, re-conditioned for at least 15 minutes, and another five-minute data collection occurred. This method was continued for the next two operating pressures chosen. Three replications occurred in this manner, and the five-minute emitter discharge values are recorded in Tables P.4-1 and P.4-2.

Table P.4-1. Five-minute emitter discharge (mL) across 48-kPa and 83-kPa operating pressures, six-percent slope rise.

	48 kPa, R1	48 kPa, R2	48 kPa, R3	83 kPa, R1	83 kPa, R2	83 kPa, R3
	85	85	84	85	84	84
	87	88	88	89	87	88
	93	93	93	94	92	93
	82	83	85	86	82	84
	85	87	86	88	85	85
	86	85	86	86	84	85
	95	94	93	95	91	95
	85	86	86	84	84	85
	90	88	90	90	87	89
	93	92	92	90	91	91
	85	86	86	86	87	86
	86	84	84	85	83	82
	84	88	87	83	84	85
	91	91	90	89	89	85
	91	90	90	88	88	88
	85	90	89	85	86	87
	91	94	95	89	92	92
	79	82	83	78	81	81
	87	89	90	85	88	90
	82	83	85	81	82	85
Cumulative	1742	1758	1762	1736	1727	1740
Mean	87	88	88	87	86	87
SD	4.2	3.7	3.4	4.0	3.4	3.7
CV, %	4.8	4.2	3.9	4.6	4.0	4.3

Table P.4-2. Five-minute emitter discharge (mL) across 117-kPa and 138-kPa operating pressures, six-percent slope rise.

	117 kPa, R1	117 kPa, R2	117 kPa, R3	138 kPa, R1	138 kPa, R2	138 kPa, R3
	83	82	82	82	82	81
	88	87	87	89	88	88
	93	92	91	92	91	91
	85	84	84	85	85	85
	86	85	85	86	85	84
	85	85	84	84	85	84
	95	93	93	95	93	93
	85	85	82	84	85	84
	90	88	88	90	88	88
	92	90	89	91	90	90
	88	86	85	86	85	86
	86	82	83	85	83	82
	84	86	84	86	86	83
	91	90	89	90	90	89
	90	90	89	90	90	89
	85	88	84	86	87	85
	88	94	93	89	93	93
	79	81	83	83	83	83
	85	90	91	87	80	91
	82	86	85	83	87	87
Cumulative	1740	1744	1731	1743	1736	1736
Mean	87	87	87	87	87	87
SD	4.0	3.7	3.6	3.5	3.6	3.6
CV, %	4.6	4.2	4.1	4.0	4.1	4.2

P.5 EMITTER DISCHARGE VERSUS SDI TESTING APPARATUS ESTIMATES

A section of new Netafim® DripNET PC™ dripline with 100 contiguous emitters was selected for testing. The dripline was oriented horizontally and conditioned for at least 15 minutes at an initial minimum operating pressure of 48 kPa; after this conditioning period, emitter discharge was recorded for a five-minute period; in addition, the mass of the supply vessel from the SDI-testing apparatus was recorded at the beginning and ending of the five-minute period. While discharge continued, the operating pressure was increased to the next desired level, re-conditioned for at least 15 minutes, and another five-minute data collection occurred. This method was continued for the next two operating pressures chosen. Three replications occurred in this manner, and the five-minute emitter discharge values and apparatus discharge equivalent values are recorded in the Tables P.5-1 to P.5-12.

Table P.5-1. Five-minute emitter discharge (mL) versus apparatus estimate (kg); 48-kPa operating pressure, replication #1.

48 kPa, Rep1										
	89	91	85	79	85	83	81	85	87	89
	86	86	83	88	93	82	84	80	86	87
	85	90	81	85	85	85	85	90	86	88
	91	84	83	83	75	82	83	82	83	93
	87	89	85	92	84	80	80	91	90	87
	92	86	87	84	88	87	86	86	82	91
	88	82	78	84	84	82	80	81	88	86
	89	92	86	83	82	83	82	88	89	86
	76	75	85	78	84	86	83	89	85	85
	88	80	94	81	81	82	86	81	90	81
Emitter mean	85									
Emitter SD	4.0									
Emitter CV, %	4.7									
Cumulative output	8505									

Start – finish mass, kg: 20.00 – 11.34 = 8.66 kg; estimable to 87 mL / emitter

Table P.5-2. Five-minute emitter discharge (mL) versus apparatus estimate (kg); 48-kpa operating pressure, replication #2.

48 kPa, Rep2										
	87	88	85	82	.	85	81	86	89	90
	88	87	83	90	95	77	86	83	84	86
	82	91	.	85	87	86	86	90	86	90
	90	85	86	83	75	83	86	88	85	92
	84	92	82	91	86	80	.	93	87	90
	90	87	86	84	89	87	87	85	85	90
	90	86	80	84	83	84	80	83	88	85
	77	94	86	82	84	87	83	88	88	92
	83	81	82	81	85	87	84	88	83	88
	88	80	96	83	85	84	87	82	90	80
Emitter mean	86									
Emitter SD	3.9									
Emitter CV, %	4.5									
Cumulative output	8538									

Start – finish mass, kg: 19.00 – 10.40 = 8.60 kg; estimable to 86 mL / emitter

Table P.5-3. Five-minute emitter discharge (mL) versus apparatus estimate (kg); 48-kpa operating pressure, replication #3.

48 kPa, Rep3										
	88	90	88	82	86	84	82	86	88	90
	89	87	66	90	95	82	84	82	85	84
	87	93	.	86	90	89	85	90	87	91
	90	87	87	83	80	85	86	87	85	91
	86	94	80	92	88	68	79	92	90	88
	93	88	87	87	90	88	87	85	89	91
	93	86	82	88	88	85	83	84	88	88
	90	95	87	84	85	86	84	88	86	93
	86	80	83	80	83	86	84	85	81	88
	95	81	88	83	86	84	88	81	88	80
Emitter mean	86									
Emitter SD	4.6									
Emitter CV, %	5.3									
Cumulative output	8614									

Start – finish mass, kg: 23.00 – 14.46 = 8.54 kg; estimable to 85 mL / emitter

Table P.5-4. Five-minute emitter discharge (mL) versus apparatus estimate (kg); 83-kPa operating pressure, replication #1.

83 kPa, Rep1										
	86	85	87	81	86	80	82	82	83	86
	87	85	.	88	93	81	.	80	.	83
	87	91	82	84	90	84	81	83	87	86
	87	91	85	81	82	84	81	86	82	90
	90	92	86	89	.	.	75	90	88	83
	92	86	90	86	90	88	88	85	89	88
	88	86	81	82	82	85	83	85	88	83
	91	94	85	84	84	85	81	88	90	91
	82	82	85	77	81	85	83	87	90	90
	83	82	90	82	87	84	86	82	90	79
Emitter mean	85									
Emitter SD	3.7									
Emitter CV, %	4.4									
Cumulative output	8117									

Start – finish mass, kg: 23.00 – 14.26 = 8.74 kg; estimable to 87 mL / emitter

Table P.5-5. Five-minute emitter discharge (mL) versus apparatus estimate (kg); 83-kPa operating pressure, replication #2.

83 kPa, Rep2										
	93	91	88	83	89	86	82	85	90	94
	91	89	86	91	98	79	87	81	90	87
	89	92	.	86	88	89	84	91	94	92
	89	87	88	85	78	85	83	88	89	92
	85	94	85	95	89	77	82	94	89	89
	92	88	.	87	93	85	83	85	86	90
	93	86	81	87	86	84	81	82	87	85
	90	94	87	76	86	85	82	87	89	91
	84	.	83	81	84	87	85	87	78	88
	94	79	87	82	88	84	88	80	90	79
Emitter mean	87									
Emitter SD	4.5									
Emitter CV, %	5.1									
Cumulative output	8424									

Start – finish mass, kg: 22.00 – 13.40 = 8.60 kg; estimable to 86 mL / emitter

Table P.5-6. Five-minute emitter discharge (mL) versus apparatus estimate (kg); 83-kPa operating pressure, replication #3.

83 kPa, Rep3										
	79	94	85	87	91	82	82	85	88	92
	95	93	90	94	99	78	.	80	85	85
	90	97	80	90	91	84	80	84	90	90
	92	89	90	86	83	77	80	82	89	93
	87	91	91	99	89	.	77	91	89	85
	92	87	85	86	90	87	85	85	86	90
	93	85	80	86	85	83	82	84	85	87
	79	93	84	82	.	87	81	88	89	92
	85	77	84	83	84	83	79	85	85	89
	93	81	88	82	87	80	85	82	89	90
Emitter mean	86									
Emitter SD	4.9									
Emitter CV, %	5.7									
Cumulative output	8389									

Start – finish mass, kg: 22.00 – 13.54 = 8.46 kg; estimable to 85 mL / emitter

Table P.5-7. Five-minute emitter discharge (mL) versus apparatus estimate (kg); 117-kPa operating pressure, replication #1.

117 kPa, Rep1										
	98	89	90	82	88	87	83	85	92	96
	91	87	85	91	94	78	76	81	81	88
	84	90	82	89	86	89	83	92	88	91
	84	87	87	77	81	89	89	90	83	93
	76	87	89	91	85	79	81	92	90	90
	88	83	79	87	90	86	88	87	89	93
	96	86	81	84	.	82	82	83	89	85
	88	91	.	78	81	90	80	91	93	96
	.	.	85	83	84	86	81	86	85	89
	90	83	90	83	92	82	87	82	89	78
Emitter mean	86									
Emitter SD	4.8									
Emitter CV, %	5.5									
Cumulative output	8297									

Start – finish mass, kg: 21.00 – 12.38 = 8.62 kg; estimable to 86 mL / emitter

Table P.5-8. Five-minute emitter discharge (mL) versus apparatus estimate (kg); 117-kPa operating pressure, replication #2.

117 kPa, Rep2										
	97	87	90	84	90	87	85	86	89	96
	89	87	88	91	96	83	84	82	87	88
	86	92	76	87	87	86	82	92	92	90
	86	84	86	77	78	87	85	89	86	93
	86	90	90	91	78	.	80	92	90	89
	90	86	75	87	90	86	87	80	87	89
	96	88	81	86	81	78	78	79	87	82
	94	95	88	85	83	79	82	86	91	91
	81	85	83	84	86	83	81	.	84	81
	92	81	91	81	90	80	85	82	90	.
Emitter mean	86									
Emitter SD	4.8									
Emitter CV, %	5.6									
Cumulative output	8360									

Start – finish mass, kg: 19.00 – 10.38 = 8.62 kg; estimable to 86 mL / emitter

Table P.5-9. Five-minute emitter discharge (mL) versus apparatus estimate (kg); 117-kPa operating pressure, replication #3.

117 kPa, Rep3										
	.	92	89	86	.	85	83	85	88	95
	91	90	90	93	99	86	88	80	89	84
	86	93	84	87	89	88	80	90	91	89
	88	87	88	86	83	87	82	87	85	93
	87	93	91	91	88	.	81	90	90	88
	90	86	87	86	90	81	85	81	86	89
	94	86	81	86	85	84	79	80	87	82
	90	92	87	85	85	85	83	87	91	92
	82	62	82	83	85	87	82	84	85	88
	91	80	87	81	88	82	86	82	89	76
Emitter mean	86									
Emitter SD	4.7									
Emitter CV, %	5.5									
Cumulative output	8379									

Start – finish mass, kg: 20.02 – 11.38 = 8.64 kg; estimable to 86 mL / emitter

Table P.5-10. Five-minute emitter discharge (mL) versus apparatus estimate (kg); 138-kPa operating pressure, replication #1.

138 kPa, Rep1										
	99	90	88	85	85	89	90	90	94	98
	92	89	89	94	97	90	92	87	93	87
	89	93	75	85	89	92	86	96	97	95
	87	87	90	87	80	93	90	94	90	97
	.	94	92	96	89	.	86	97	94	93
	90	84	87	85	90	86	89	79	88	90
	94	85	81	85	85	87	77	85	90	88
	78	91	86	87	84	81	86	83	92	93
	77	83	87	84	86	88	79	86	87	88
	89	80	87	82	90	83	86	81	90	80
Emitter mean	88									
Emitter SD	5.1									
Emitter CV, %	5.8									
Cumulative output	8630									

Start – finish mass, kg: 23.00 – 14.30 = 8.70 kg; estimable to 87 mL / emitter

Table P.5-11. Five-minute emitter discharge (mL) versus apparatus estimate (kg); 138-kPa operating pressure, replication #2.

138 kPa, Rep2										
	.	90	92	85	92	85	85	85	90	94
	93	91	90	81	95	85	88	77	88	84
	89	95	85	89	89	85	75	89	92	91
	85	89	90	86	86	85	82	87	85	91
	84	93	92	95	89	.	77	86	88	89
	91	81	87	87	91	84	85	87	88	88
	96	87	82	85	84	75	83	80	90	84
	92	86	86	86	86	87	83	85	91	90
	85	81	86	86	87	89	81	86	87	85
	90	80	86	82	90	83	88	82	90	80
Emitter mean	87									
Emitter SD	4.3									
Emitter CV, %	4.9									
Cumulative output	8499									

Start – finish mass, kg: 23.00 – 14.36 = 8.64 kg; estimable to 86 mL / emitter

Table P.5-12. Five-minute emitter discharge (mL) versus apparatus estimate (kg); 138-kPa operating pressure, replication #3.

138 kPa, Rep3										
	.	90	92	85	92	85	85	85	90	94
	93	91	90	81	95	85	88	77	88	84
	89	95	85	89	89	85	75	89	92	91
	85	89	90	86	86	85	82	87	85	91
	84	93	92	95	89	.	77	86	88	89
	91	81	87	87	91	84	85	87	88	88
	96	87	82	85	84	75	83	80	90	84
	92	86	86	86	86	87	83	85	91	90
	85	81	86	86	87	89	81	86	87	85
	90	80	86	82	90	83	88	82	90	80
Emitter mean	86									
Emitter SD	3.8									
Emitter CV, %	4.4									
Cumulative output	8438									

Start – finish mass, kg: 21.02 – 12.36 = 8.66 kg; estimable to 87 mL / emitter

Table P.5-13.Emitter exponent calculations as referenced in ASAE S553 (2008).

					Sums
Operating Pressure (kPa), p	48	83	117	138	386
Mean Emitter Discharge (L h^{-1})[a], q	1.028	1.032	1.032	1.044	4.136
Log (p)	1.681	1.919	2.068	2.140	7.808
Log (q)	0.012	0.014	0.014	0.019	0.058
[Log (p)] x [Log (q)]	0.020	0.026	0.028	0.040	0.115
$[Log\ (p)]^2$	2.827	3.683	4.277	4.579	15.366

[a] Mean emitter discharge refers to average discharge from three replications of 100 contiguous emitters.

$$\text{Emitter exponent} = \frac{\sum[Log\ (p) \times Log\ (q)] - \frac{1}{n}[\sum Log\ (p)][\sum Log\ (q)]}{\sum[Log\ (p)]^2 - \frac{1}{n}[\sum Log\ (p)]^2}$$

where n=number of pressure levels tested; therefore, emitter exponent =

$$\frac{0.115 - \frac{1}{4} \times 7.808 \times 0.058}{15.366 - \frac{1}{4} \times 7.808^2}$$

equals 0.011.

APPENDIX Q

SDI FIELD DATA

Q.1. TEST SITE LOCATION

The SDI study was conducted at the Tennessee Valley Research and Extension Center (TVREC), Belle Mina, Alabama. The test plot was referred to by station personnel as Field 52, located in the southwest corner of the property, as is indicated in Figure Q.1.

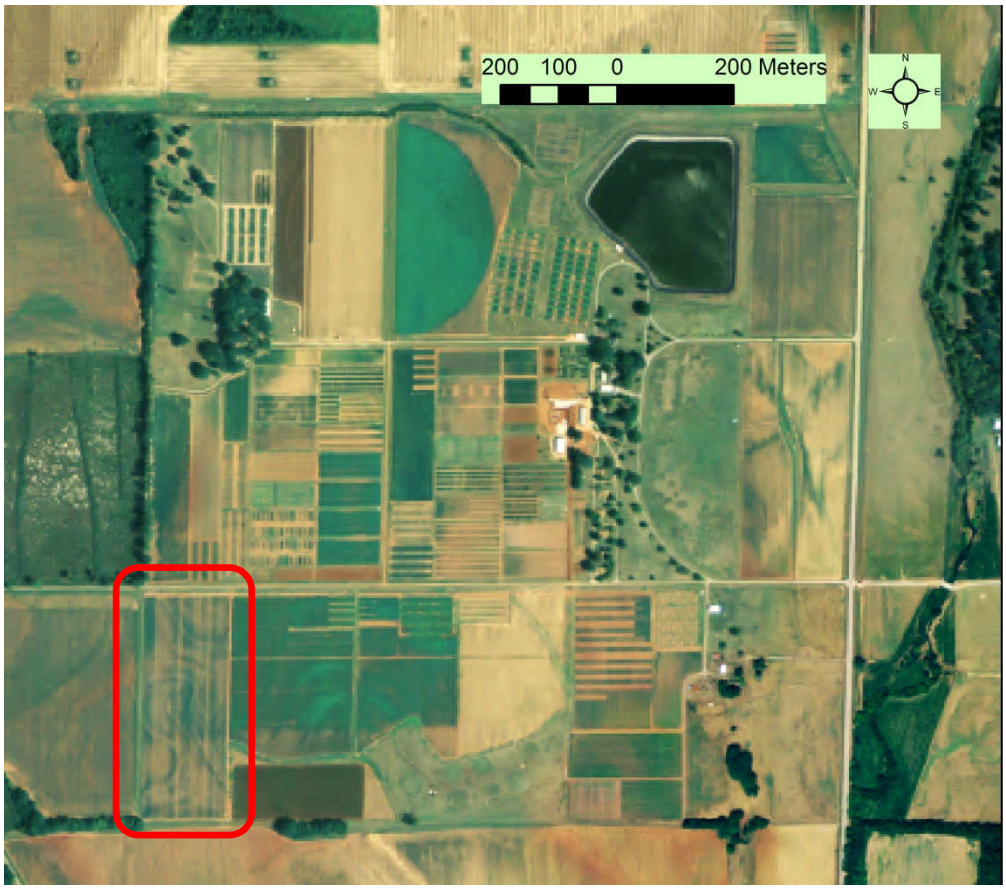

Figure Q.1. Aerial imagery of Tennessee Valley Research and Extension Center (TVREC), Belle Mina, Alabama (2006 data; imagery courtesy of Aerial Photography Field Office, United States Department of Agriculture).

Q.2 ATTRIBUTES OF TEST SITE

Field 52 is equipped with a subsurface-drip irrigation (SDI) system, optimized for the seasonal growth of cotton. Long-term interdisciplinary research concerns the overall lint-yield production under optimal-watering and drought-stress conditions; therefore, the SDI system was designed such that the watering "zones" corresponded with the treatment plots within the randomized-complete block design established in 2003. Because the irrigation treatments have been unaltered since 2003, the system zones that correspond to optimal watering treatment have been used more often than the non-supplemented zones.

The treatment plots are approx. 380m in length and 6m in width. SDI laterals were horizontally centered in each treatment plot at 2.03-m spacing and at a depth of 0.3m. For each irrigation-treatment plot, the three center-most laterals were targeted for this study. Treatment plots relating to supplemental irrigation usage are illustrated in Figure Q.2-1.

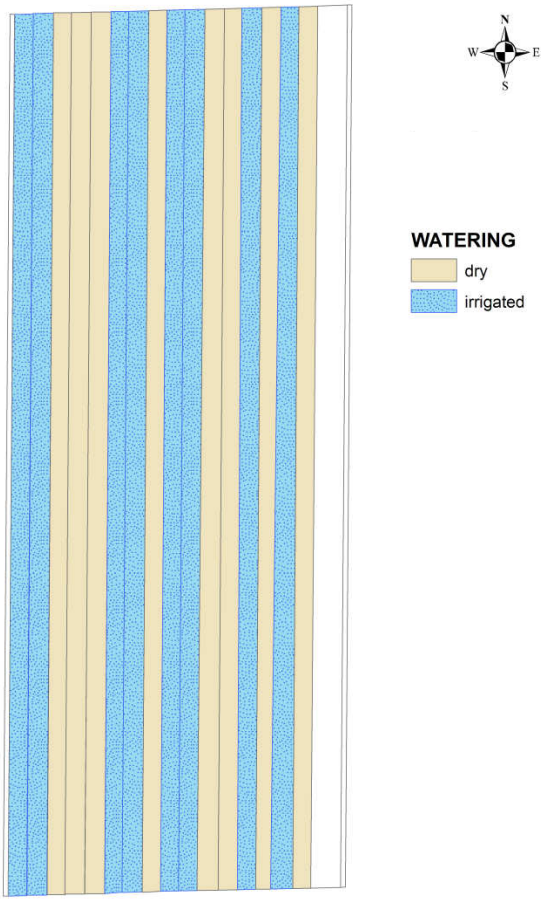

Figure Q.2-1. Irrigation treatment assignment for Field 52.

Topographic data were collected with a survey-grade GPS receiver, sub-inch accuracy. The data were converted to a digital elevation model (DEM) in ArcGIS V.9 software. From the DEM, a slope-classification map was produced for Field 52. Three categories of slope classification were determined: 0 - 2%, 2 - 4%, and greater than 4% rise. With the slope map and the irrigation treatment map, dripline-sampling locations were then derived as a 3x2 randomized complete block design with three replications (18 total sampling locations), illustrated in Figure Q.2-2. Sampling locations with site-number designations are represented in Figure Q.2-3.

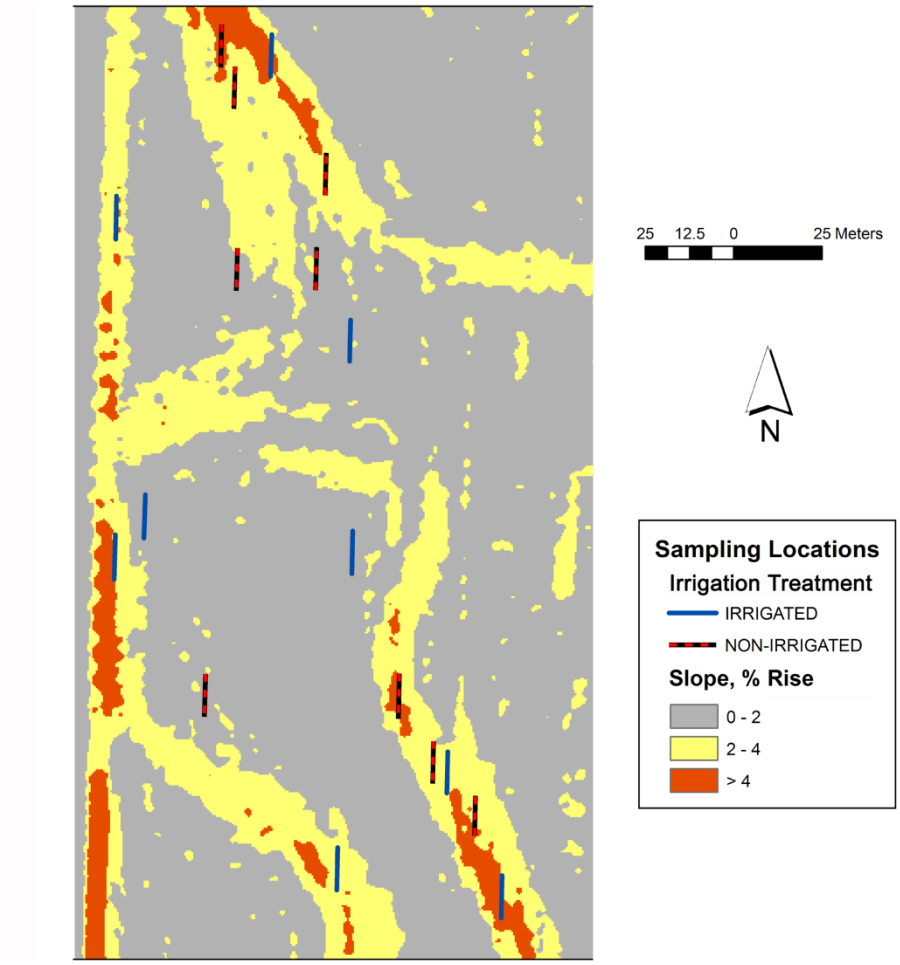

Figure Q.2-2. Sampling locations for Field 52, based on irrigation treatment (system use frequency) and surface slope attributes.

Figure Q.2-3. Dripline-sampling locations in Field 52.

Q.3 FIELD DATA

The following tables represent SDI test-sample discharges for each target operating pressure at each sampling location. In addition, actual dripline slope is presented, calculated by measuring difference in elevation of each end of the 12.2-m portion of drip tape with a survey-grade GPS receiver with centimeter accuracy.

Table Q.3-1. SDI-apparatus sample-discharge values for Sites 1-4.

Site 1					1.3% slope
	48 kpa----------	19.52 kg	-	17.78 kg	= 1.74 kg
	83 kpa----------	16.48 kg	-	14.76 kg	= 1.72 kg
	117 kpa----------	13.58 kg	-	11.88 kg	= 1.70 kg
	138 kpa----------	11.26 kg	-	9.54 kg	= 1.72 kg
Site 2					1.2% slope
	48 kpa----------	18.36 kg	-	16.72 kg	= 1.64 kg
	83 kpa----------	15.80 kg	-	14.06 kg	= 1.74 kg
	117 kpa----------	12.98 kg	-	11.00 kg	= 1.98 kg
	138 kpa----------	10.08 kg	-	7.94 kg	= 2.14 kg
Site 3					0.8% slope
	48 kpa----------	19.76 kg	-	18.04 kg	= 1.72 kg
	83 kpa----------	17.04 kg	-	15.28 kg	= 1.76 kg
	117 kpa----------	14.22 kg	-	12.48 kg	= 1.74 kg
	138 kpa----------	11.82 kg	-	10.04 kg	= 1.78 kg
Site 4					1.7% slope
	48 kpa----------	20.72 kg	-	19.00 kg	= 1.72 kg
	83 kpa----------	17.78 kg	-	16.00 kg	= 1.78 kg
	117 kpa----------	15.12 kg	-	13.32 kg	= 1.80 kg
	138 kpa----------	12.68 kg	-	10.88 kg	= 1.80 kg

Table Q.3-2. SDI-apparatus sample-discharge values for Sites 5-8.

Site 5					0.3% slope
	48 kpa----------20.90 kg	-	19.36 kg	=	1.54 kg
	83 kpa----------18.06 kg	-	16.40 kg	=	1.66 kg
	117 kpa----------15.84 kg	-	14.12 kg	=	1.72 kg
	138 kpa----------13.82 kg	-	12.08 kg	=	1.74 kg
Site 6					0.6% slope
	48 kpa----------19.84 kg	-	18.30 kg	=	1.54 kg
	83 kpa----------17.70 kg	-	16.06 kg	=	1.74 kg
	117 kpa----------15.16 kg	-	13.44 kg	=	1.72 kg
	138 kpa----------12.80 kg	-	11.04 kg	=	1.76 kg
Site 7					0.4% slope
	48 kpa----------19.26 kg	-	17.54 kg	=	1.72 kg
	83 kpa----------16.50 kg	-	14.80 kg	=	1.70 kg
	117 kpa----------14.00 kg	-	12.30 kg	=	1.70 kg
	138 kpa----------11.58 kg	-	9.88 kg	=	1.70 kg
Site 8					1.8% slope
	48 kpa----------14.94 kg	-	13.36 kg	=	1.58 kg
	83 kpa----------12.42 kg	-	10.78 kg	=	1.64 kg
	117 kpa----------10.02 kg	-	8.26 kg	=	1.76 kg
	138 kpa---------- 7.20 kg	-	5.46 kg	=	1.74 kg

Table Q.3-3. SDI-apparatus sample-discharge values for Sites 9-12.

Site 9				1.9% slope
48 kpa----------19.18 kg	-	18.36 kg	=	0.82 kg
83 kpa----------17.76 kg	-	16.88 kg	=	0.88 kg
117 kpa----------16.38 kg	-	15.46 kg	=	0.92 kg
138 kpa----------15.16 kg	-	14.20 kg	=	0.96 kg
Site 10				0.5% slope
48 kpa----------18.42 kg	-	16.80 kg	=	1.62 kg
83 kpa----------15.94 kg	-	14.18 kg	=	1.76 kg
117 kpa----------13.34 kg	-	11.56 kg	=	1.78 kg
138 kpa----------10.84 kg	-	9.04 kg	=	1.80 kg
Site 11				0.4% slope
48 kpa----------20.10 kg	-	18.24 kg	=	1.86 kg
83 kpa----------17.46 kg	-	15.56 kg	=	1.90 kg
117 kpa----------14.78 kg	-	12.86 kg	=	1.92 kg
138 kpa----------12.04 kg	-	10.12 kg	=	1.92 kg
Site 12				0.5% slope
48 kpa----------21.04 kg	-	19.58 kg	=	1.46 kg
83 kpa----------18.90 kg	-	17.22 kg	=	1.68 kg
117 kpa----------16.48 kg	-	14.74 kg	=	1.74 kg
138 kpa----------14.20 kg	-	12.42 kg	=	1.78 kg

Table Q.3-4. SDI-apparatus sample-discharge values for Sites 13-16.

Site 13				1.3% slope
48 kpa----------18.36 kg	-	16.70 kg	=	1.66 kg
83 kpa----------16.02 kg	-	14.32 kg	=	1.70 kg
117 kpa----------13.54 kg	-	11.86 kg	=	1.68 kg
138 kpa----------11.32 kg	-	9.64 kg	=	1.68 kg
Site 14				0.7% slope
48 kpa----------20.86 kg	-	19.22 kg	=	1.64 kg
83 kpa----------18.52 kg	-	16.90 kg	=	1.62 kg
117 kpa----------16.16 kg	-	14.44 kg	=	1.72 kg
138 kpa----------13.78 kg	-	12.08 kg	=	1.70 kg
Site 15				0.7% slope
48 kpa----------17.78 kg	-	16.04 kg	=	1.74 kg
83 kpa----------15.42 kg	-	13.62 kg	=	1.80 kg
117 kpa----------12.96 kg	-	11.22 kg	=	1.74 kg
138 kpa----------10.36 kg	-	8.62 kg	=	1.74 kg
Site 16				0.8% slope
48 kpa----------19.40 kg	-	17.62 kg	=	1.78 kg
83 kpa----------16.74 kg	-	14.86 kg	=	1.88 kg
117 kpa----------13.02 kg	-	11.26 kg	=	1.76 kg
138 kpa----------10.74 kg	-	8.98 kg	=	1.76 kg

Table Q.3-5. SDI-apparatus sample-discharge values for Sites 17 and 18.

Site 17				1.1% slope
48 kpa----------18.78 kg	-	16.98 kg	=	1.80 kg
83 kpa----------16.14 kg	-	14.32 kg	=	1.82 kg
117 kpa----------13.38 kg	-	11.70 kg	=	1.68 kg
138 kpa----------11.20 kg	-	9.38 kg	=	1.82 kg
Site 18				1.9% slope
48 kpa----------19.34 kg	-	17.80 kg	=	1.54 kg
83 kpa----------16.80 kg	-	15.08 kg	=	1.72 kg
117 kpa----------14.16 kg	-	12.42 kg	=	1.74 kg
138 kpa----------11.68 kg	-	9.96 kg	=	1.72 kg